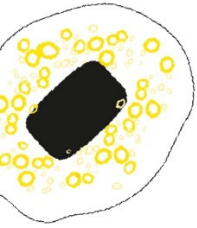


UNIVERSITY OF TWENTE.

EEMCS - Radio Systems



**Electromagnetic Field Exposure assessment of 5G NR Cell-free Massive
MIMO overlapping with Legacy Cellular Technologies**

Thesis Report

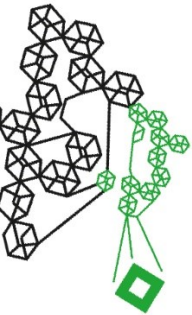
Electrical Engineering MSc Thesis

Luis Diego R. Siles Cárdenas

Supervisor:
dr. Yang Miao

Committee chair:
prof.dr.ir. A.B.J. Kokkeler
dr. Suzan Bayhan
dr. Shanshan Wang

Enschede – Netherlands
August - 2023



Acknowledgements

My thanks to everyone who contributed and supported me during the creation of this thesis.

Contents

Contents.....	iii
List of Tables.....	v
List of Figures	vi
List of Annexes.....	ix
Abstract.....	x
1 Introduction.....	1
1.1 Background.....	1
1.1.1 EMF guidelines and regulation.....	2
1.1.2 ICNIRP	3
1.1.3 BioInitiative Reports	3
1.1.4 Health Council of The Netherlands report	4
1.1.5 Local entity in The Netherlands in charge of EMF measurements.....	4
1.1.6 Software Methods for EMF assessments and RF Propagation.....	5
1.2 Literature Review.....	6
1.2.1 Cell-free Massive MIMO	6
1.2.2 EMF Exposure Study from User Equipments in 5G.....	7
1.2.3 EMF Exposure Case studies	8
1.3 Research Question.....	9
2 Methodology	10
2.1 Problem Description.....	10
2.2 Flowchart of Research Procedure Steps.....	11
2.2.1 Scenario Definition	12
2.2.2 Link Budget Definition.....	12
2.2.3 Simulation Environment Setup.....	14
2.2.4 Simulation Procedures.....	16
2.2.5 EMF Definition.....	16
2.2.6 EMF Extrapolation from PDSCH Data.....	17
3 Simulation Setup	20
3.1 Network Replication.....	20
3.2 mmWave Cell-free Massive MIMO Topology.....	21
3.3 Computational Zones	22
3.4 Simulation Parameters.....	23
3.4.1 Transmit Power.....	23
3.4.2 BS Antenna Configuration	23
3.4.3 mmWave Frequency	23

3.4.4	User Density	24
3.4.5	Number of Base Stations	24
3.4.6	Sub-Carrier Spacing and Bandwidth.....	24
3.5	Simulation’s Propagation Models	24
3.5.1	Small scale Fading Propagation modeling	24
3.5.2	GSM and UMTS Propagation Model - Okumura-Hata	25
3.5.3	LTE Propagation Model - COST 231 Hata	26
3.5.4	5G NR Propagation Model - 3GPP 38.901	27
4	Results and Analysis.....	30
4.1	EMF validation simulation	30
4.2	EMF exposure assessment of Legacy Cellular Technologies and Cell-free Massive MIMO.....	32
4.3	Cell-free Massive MIMO analysis	35
4.3.1	Cell-free study location 1	37
4.3.2	Cell-free study location 2	39
4.3.3	Cell-free study location 3	41
4.3.4	Cell-free study location 4	43
4.3.5	Cell-free study location 5	45
4.3.6	Overall Cell-free Massive MIMO assessment - Location 1 to 5	47
4.4	Monte Carlo Simulations.....	48
4.4.1	Dense Urban vs Urban CDF	49
4.4.2	Topology 2 vs Topology 1 Simulations	50
4.4.3	240 kHz vs 120 kHz Subcarrier spacing simulations - 40 dBm	51
4.4.4	240 kHz vs 120 kHz Subcarrier spacing simulations – 60 dBm.....	52
4.4.5	400 MHz vs 100 MHz Channel Bandwidth simulation	53
4.5	BLER and RSRQ Results	54
4.6	Throughput simulation results	56
5	Conclusion Recommendations and Future Work	58
5.1	Conclusion	58
5.2	Recommendations	60
5.3	Future work.....	60
	References	61
	Annexes	65

List of Tables

Table 1 Exposure limits for radio-frequency fields for the general public by country.....	2
Table 2. Neurological studies results report summary [11].	4
Table 3. Summary of Agentschap Telecom measurement protocols.	5
Table 4. Summary Cell-free Massive MIMO.....	6
Table 5. Analysis on Cell-free massive MIMO Summary.....	7
Table 6. EMF exposure case studies summary.....	8
Table 7. Considered components in the simulation environment.....	12
Table 8. Attributes considered for the calculation of the Link budget.	13
Table 9. User type definition.	15
Table 10. Mobility and density Atoll configurations.....	15
Table 11. Considered configuration parameters.....	19
Table 12. COST 231 values for different environments.	26
Table 13. COST 231 Parameters Validity Ranges.	26
Table 14. 3GPP 38.901 UMi for NLOS and LOS Pathloss equations [27].	28
Table 15. Details for the 5 Cell-free Massive MIMO specific scenario studies.	36
Table 16. Location 1 mmWave Cell-free MIMO configuration.	37
Table 17. Location 2 mmWave Cell-free Massive MIMO configuration.	39
Table 18. Location 3 mmWave Cell-free Massive MIMO configuration.	41
Table 19. Location 4 mmWave Cell-free Massive MIMO configuration.	43
Table 20. Location 5 mmWave Cell-free MIMO configuration.	45
Table 21. Summary of the EMF findings in relation to the considered parameters.	59
Table 22. Cell-free study location 1 data.	70
Table 23. Cell-free study location 2 data.	71
Table 24. Cell-free study location 3 data.	71
Table 25. Cell-free study location 4 data.	72
Table 26. Cell-free study location 5 data.	72
Table 27. Electric field level calibration with Agentschap Measurements.....	76

List of Figures

Figure 1. ICNIRP EMF Reference levels – Left: 1998 Release [5] Right: 2020 Release [6].	3
Figure 2. Shooting and Bouncing Rays	5
Figure 3. Image Theory.....	6
Figure 4. Procedure flowchart.	11
Figure 5. EMF determination challenges.	17
Figure 6. Enschede’s BSs map locations.	20
Figure 7. Topology 1 mmWave deployment with 28 BSs.....	21
Figure 8. Topology 2 mmWave deployment with 7 BSs.....	21
Figure 9. Computational Zone 1.....	22
Figure 10. Computational Zone 2.....	23
Figure 11. Okumura Hata configuration in the simulation software Atoll.	25
Figure 12. Cost-231 Hata configuration in the simulation software Atoll.....	27
Figure 13. 3GPP 38.901 Propagation Model properties in Atoll.	28
Figure 14. Top: Antenneregister Map with the considered BSs and measurements in Enschede. Bottom: Replication of Enschede’s network on the simulation software Atoll.	30
Figure 15. EMF verification of the replicated network vs Agentschap Telecom measurements.	31
Figure 16. EMF value example in the simulation software Atoll.....	31
Figure 17. Atoll EMF reports CDF.....	32
Figure 18. Atoll EMF reports area percentage histogram.....	32
Figure 19. Former vs Upgraded Network E. Field Increase & Required E. field Increase to reach ICNIRP limits.....	34
Figure 20. Simulation scenario layout applicable to section 4.3.....	35
Figure 21. Cell-free MIMO study Location 1.	37
Figure 22. Cell-free MIMO study Location 1 E. field vs Distance.	38
Figure 23. Cell-free Massive MIMO study Location 2.	39
Figure 24. Cell-free Massive MIMO study Location 2 E. field vs Distance.	40
Figure 25. Cell-free study Location 3.	41
Figure 26. Cell-free Massive MIMO study Location 3 E. field vs Distance.	42
Figure 27. Cell-free study Location 4.	43
Figure 28. Cell-free Massive MIMO study Location 4 E. field vs Distance.	44
Figure 29. Cell-free MIMO study Location 5.	45
Figure 30. Cell-free MIMO study Location 5 E. field vs Distance.	46
Figure 31. Overall Cell-free mmWave E. field levels.	47
Figure 32. Outdoor coverage test results of a mmWave beamforming prototype [39].	48
Figure 33. Dense Urban vs Urban Monte Carlo simulations’ CDF.....	49
Figure 34. Dense Urban vs Urban Average Increased and decreased E. field levels.	49
Figure 35. Topology 2 vs Topology 1 Monte Carlo simulations’ CDF and E. field Increase.	50

Figure 36. 240 kHz vs 120 kHz SCS - 40 dBm Monte Carlo simulations' CDF and E. field Increase.....	51
Figure 37. 240 kHz vs 120 kHz SCS - 60 dBm Monte Carlo simulations' CDF and E. field Increase.....	52
Figure 38. 400 vs 100 MHz Channel BW Monte Carlo simulations' CDF and E. field Decrease.	53
Figure 39. BLER CDF plots for 4.4.1.....	54
Figure 40. RSRQ CDF plots for 4.4.1.....	55
Figure 41. User Throughput prediction in the mmWave portion of the network.....	56
Figure 42. Downlink and Uplink Throughputs per User CDF.....	57
Figure 43. E. field measurement from the latest released measurement reports using the older guidelines.....	65
Figure 44. mmWave Antenna beam pattern.....	65
Figure 45. Beamforming patterns.	66
Figure 46. Snapshot of the simulation data showing some of the user throughputs.....	73
Figure 47. EMF Atoll simulation generated report display range applicable on section 4.2.	73
Figure 48. Broadband service properties.....	75
Figure 49. Atoll Simulation algorithm.	77
Figure 50. mmWave Transmitter configuration example.	78
Figure 51. Sample 1 for measurement location 1.....	79
Figure 52. Sample 2 for measurement location 1.....	79
Figure 53. Sample 3 for measurement location 1.....	80
Figure 54. Sample 4 for measurement location 1.....	80
Figure 55. Sample 5 for measurement location 1.....	81
Figure 56. Sample 6 for measurement location 1.....	81
Figure 57. Sample 7 for measurement location 1.....	82
Figure 58. Sample 8 for measurement location 1.....	82
Figure 59. Sample 9 for measurement location 1.....	83
Figure 60. Sample 10 for measurement location 1.....	83
Figure 61. LTE Simulation data location 1.....	84
Figure 62. GSM Simulation data location 1.....	84
Figure 63. LTE Simulation data location 2.....	84
Figure 64. GSM Simulation data location 2.....	85
Figure 65. LTE Simulation data location 3.....	85
Figure 66. GSM Simulation data location 3.....	85
Figure 67. LTE Simulation data location 4.....	85
Figure 68. GSM Simulation data location 4.....	86
Figure 69. LTE Simulation data location 4.....	86
Figure 70. GSM Simulation data location 5.....	86
Figure 71. Uncalibrated Atoll EMF report example.....	87

Figure 72. BLER & RSRQ CDF for the Cross Marker simulation from 4.4.1 (128x128, 60 dBm, Dense Urban).	87
Figure 73. BLER & RSRQ CDF for the Dotted Marker simulation from 4.4.1 (4x4, 60 dBm, Dense Urban).	88
Figure 74. BLER & RSRQ CDF for the Square Marker simulation from 4.4.1 (128x128, 40 dBm, Dense Urban).	88
Figure 75. BLER & RSRQ CDF for the Dashed Marker simulation from 4.4.1 (4x4, 40 dBm, Dense Urban).	88
Figure 76. BLER & RSRQ CDF for the “x” Cross Marker simulation from 4.4.1 (128x128, 60 dBm, Urban).	89
Figure 77. BLER & RSRQ CDF for the Diamond Marker simulation from 4.4.1 (4x4, 60 dBm, Urban).	89
Figure 78. BLER & RSRQ CDF for the Circle Marker simulation from 4.4.1 (128x128, 40 dBm, Urban).	89
Figure 79. BLER & RSRQ CDF for the Line Marker simulation from 4.4.1 (4x4, 40 dBm, Urban).	90
Figure 80. Statistical simulation summary example.	90

List of Annexes

Annex A: Agentschap Telecom sample measurement	65
Annex B: mmWave Antenna Pattern and beamforming pattern.....	65
Annex C: Electric field equation 1 derivation.....	66
Annex D: Electric field equation 2 derivation.....	66
Annex E: MatLab scripts calculating Electric fields	67
Annex F: Haversine implementation to calculate exact distances from users to the serving antennas in the software Atoll on Java.....	68
Annex G: Cell-free studies data tables.....	70
Annex H: Throughput simulation data.....	73
Annex I: Atoll EMF simulation generated report ranges applicable on section 4.2.....	73
Annex J: User densities estimation.....	73
Annex K: Base Station quantity estimations.....	74
Annex L: Broadband service properties in Atoll.....	75
Annex M: Electric field level calibration with Agentschap Measurements.....	76
Annex N: Atoll simulation algorithm	77
Annex O: mmWave transmitter configuration	78
Annex P: Figures for the taken samples for Measurement location 1	79
Annex Q: LTE and GSM simulations from section 4.3.....	84
Annex R: Uncalibrated Atoll EMF report example.....	87
Annex S: BLER and RSRQ simulation plots.....	87
Annex T: Statistical simulation summary example	90

Abstract

This research investigates the overall EMF (Electromagnetic Field) exposure in a simulation environment when a substantial number of mmWave BSs (Base Stations) is introduced into an established network, specifically in Enschede, The Netherlands. It acknowledges applicable EMF exposure regulations as well as independent research groups regarding EMF exposure. The simulation replicates thirty-eight BSs from the existing mobile network to calibrate the simulation environment and align with Agentschap Telecom EMF measurements. An additional twenty-eight introduced BSs simulate a technological upgrade adopting Cell-free Massive MIMO with mmWave frequencies. ICNIRP (International Commission on Non-Ionizing Radiation Protection) guidelines are used as a reference. Multiple simulations explore various network configurations, including User Density, BS Quantity, BS Antenna Configuration, SCS (Sub-Carrier Spacing), Channel Bandwidth, and Transmit Power, to analyze their impact on EMF exposure. Notable changes in the electric field are observed, particularly in BS Antenna Configurations, with different behaviors based on User Density. There is a 3 dB increase in the electric field by using a 120 kHz SCS configuration. The introduction of the mmWave Cell-free Massive MIMO BSs projects an increase in the electric field level of 9 dB in the considered region.

1 Introduction

1.1 Background

The prospects of future networks adopting Cell-free Massive MIMO are favorable due to many potential advantages in terms of capacity and Quality of Service (QoS). The Massive MIMO (Multiple Input Multiple Output) technology in 5G networks allows for increased network capacity, ensuring optimal performance even while handling a large number of connected devices. Additionally, utilizing mmWave frequencies (>26.5 GHz) enables faster data transmission rates.

The Cell-free Massive MIMO scheme takes this a step further by aiming to equalize the QoS for users through multiple APs (Access Points) surrounding them. In the Netherlands, although there are currently no laws specific to mmWave frequencies, there is a growing interest in their utilization, especially in the 20 - 40 GHz range and the n257 band starting at 26.5 GHz.

The Ministry of Economic Affairs and Climate has sought advice from the Health Council of the Netherlands concerning 5G and health, including the use of mmWaves. However, the Health Council concluded that making definitive statements about mmWave frequencies is challenging due to medical and ethical reasons, and more research is required.

The focus of this research is to provide insights into the EMF exposure significance when using multiple BS antennas due to the innovative Cell-free scheme while operating in the mmWave frequencies. This insight can prove valuable for future network designs and optimizations, which focus on minimizing EMF exposure for the population, either due to regulatory requirements or precautionary compliance. By examining various parameters and their combinations, this thesis aims to identify the trade-offs that decision-makers may encounter, empowering them to make informed choices that align with their specific circumstances.

This thesis can also predict the expected E. (Electric) field levels that Agentschap Telecom may encounter from the introduction of a substantial number of mmWave BS antennas, considering the already existing GSM, 3G and 4G “Legacy” technologies in Enschede's network. This valuable insight could motivate the reallocation of resources from routine measurements that consistently fall below regulation levels. While this study is specific to Enschede, the findings can have relevance to other larger cities in the Netherlands where BSs' deployments are more extensive.

1.1.1 EMF guidelines and regulation

Table 1 presents a comprehensive overview of the EMF exposure limitations, as currently listed by the World Health Organization [1], which exhibit a prevailing homogenic pattern across countries, albeit with a few exceptions for some of the countries in this list:

		Electric field (V/m)		Power density (W/m ²)	
		900 MHz	1800 MHz	900 MHz	1800 MHz
Australia	2017	41.1	58.1	4.5	9
Austria	2017	41.25	58.34	4.5	9
Bahrain	2017	41	58	4.5	9
Brazil	2017	41.25	58.34	4.5	9
Bulgaria	2017	6.14	6.14	0.1	0.1
Canada	2017	32.1	40.07	2.74	4.4
Finland	2017	41.4	58.55	4.5	9
France	2017	41	58	4.5	9
Germany	2017	41.25	58	4.5	9
Greece	2017	31.9/34.5	45.1/48.8	2.7/3.15	5.4/6.3
Israel	2017	[13.0]	[18.0]	[0.45]	[0.9]
Italy	2017	6/20	6/20	0.1/1.0	0.1/1.0
Japan	2017	47.55	61.4	6	10
Malaysia	2017	41.25	58.34	4.5	9
Netherlands	2017	41.25	58.34	4.5	9
Republic of Korea	2017	41.25	58.34	4.5	9
Russian Federation	2017			1	1
Saudi Arabia	2017	41.25	58.34	4.5	9
South Africa	2017	[41.0]	[58.0]	[4.5]	[9.0]
Sweden	2017	[41.25]	[58.33]	[4.5]	[9]
Switzerland	2017	4/41.25	6/58.34		
Türkiye	2017	3/10.23/41.0	3/14.5/58	0.27	0.55
United Kingdom	2017	[41.25]	[58.34]	[4.5]	[9.0]
United States of America	2017	47.6	61.4	6	10

Table 1 Exposure limits for radio-frequency fields for the general public by country.

The reason for the high resemblance in limitations is due to the fact that most governments have based their limitations on the ICNIRP guidelines.

In some countries like Bulgaria, there have been efforts to develop their own precautionary reference levels. This country has a limit of 6,14 V/m as seen in Table 1. The difference may lie on the fact that there may be a closer relationship between Biomedical physics and Radio Systems. Efforts such as measurements on BSs were realized on National conferences dedicated to Biomedical physics and Engineering in Bulgaria, examples of this are [2] and [3]. Bulgaria has also developed specific limitations stipulated in laws [4].

Another exception in Table 1. with lower conditional limits is Italy. This country has a 6 V/m limitation for the general public, in specific places such as parks and schools where developing children may be present, and 20 V/m everywhere else.

1.1.2 ICNIRP

ICNIRP (International Commission on Non-Ionizing Radiation Protection) is a private German organization which collaborates with the World Health Organization (WHO). ICNIRP developed guidelines [5] in 1998 for the protection in terms of EMF exposure. These guidelines cite SAR (Specific Absorption Rate) calculations and reference EMF levels based on changes in temperature in exposed tissues, and set thresholds against adverse health effects.

ICNIRP released an updated version of their guidelines in [6] in the year 2020. One of the relevant changes was the addition of an exposure area averaging approach to attempt to account for smaller beam diameters of directive antennas.

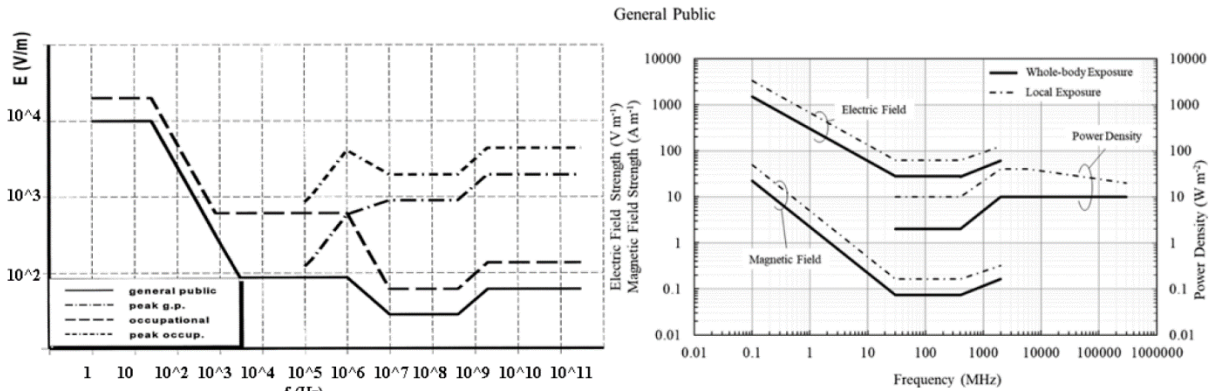


Figure 1. ICNIRP EMF Reference levels – Left: 1998 Release [5] Right: 2020 Release [6].

In Fig. 1 the reference levels' limitations released by ICNIRP in the years 1998 and 2020 are displayed. On the left of Fig. 1 the solid line represents the limits in V/m at different frequencies for the general public. On the right of Fig. 1 the dashed-dotted and solid lines represent the whole-body and local exposure limits in W/m^2 for the general public. The claim is that the updated guidelines provide protection and account for upcoming technological developments that use higher frequencies. This feature is related to what ICNIRP calls basic restrictions.

However, to facilitate the demonstration of compliance, they also have referential levels, which use quantities that are more easily assessed than the basic restrictions. Most countries utilize the referential EMF levels because of their practicality and they are assumed to be conservative levels. The new reference levels are given in terms of Power Density, and set to $10 W/m^2$ for the relevant frequencies of 5G NR (New Radio) and mmWave communication. If transformed to V/m, assuming free space conditions, the level is 61,4 V/m which happens to be the same as in 1998. In this context the revised guidelines would essentially be the same for the higher frequency spectrum.

1.1.3 BioInitiative Reports

The BioInitiative reports found in [7] have been prepared by 29 authors from ten countries, ten holding medical degrees (MDs), 21 PhDs, and three MsC, MA or MPHs. Among the authors are three former presidents of the Bioelectromagnetics Society, and five full members of BEMS. This group states that existing public safety limits from entities such as FCC and ICNIRP do not sufficiently protect the public's health against chronic exposures.

In general, engineers measure the average intensity of radiation over several minutes and its thermal heating effects, biologists focus on the variability of radiation’s intensity, non-thermal and long-term effects from EMF exposure. This group has conducted hundreds of biological studies, one example is shown in Table 2.

Percent comparison in Neurological Studies		
	RF (Radio Frequency) radiation	ELF - EMF
Number of Studies	391	311
Reported Effect	74%	91%
Reported no significant Effect	26%	9%

Table 2. Neurological studies results report summary [8].

Table 2 shows the amount of studies realized under two kinds of radiation, Radio Frequency radiation and ELF (Extremely Low Frequency) radiation studies and whether or not they reported significant biological effects. Radio Frequency radiation is referred to the spectrum between 3 kHz and 300 GHz, and ELF radiation referred to the spectrum between 3 Hz and 30 Hz. The BioInitiative group conclusion found in [9] and recommendation cite a precautionary action level for chronic exposure to pulsed radiofrequency radiation (RFR). This is considered to be within the range of 0.3 nanowatts to 0.6 nanowatts per square centimeter or its equivalent reference level of 0.11 to 0.15 V/m. This level is deemed reasonable as a precautionary measure to address potential health concerns associated with long-term exposure to pulsed Radio Frequency Radiation.

1.1.4 Health Council of The Netherlands report

The Health Council of The Netherlands (Gezondheidsraad) conducted studies regarding 5G deployments in the year 2020 and the following conclusions were drawn from it: For the frequencies between 700 – 5000 MHz an increased level of oxidative stress is possible. For the frequencies of 20 – 40 GHz: A statement is yet not possible [10]. Regarding mmWave, the advice is to wait before commissioning 26 GHz, because practically nothing is known about the effects of exposure to frequencies in these bands [11].

On a final note, the Health Council advises to use ICNIRP guidelines, but states that at the same time adverse health effects cannot be ruled out, even if exposure is below these limits. For this reason, the council recommends applying the ALARA principle (As Low As Reasonably Achievable) [11].

1.1.5 Local entity in The Netherlands in charge of EMF measurements

Agentschap Telecom is in charge of verifying that the EMF exposure is compliant with the limitations from the regulation. Apart from following ICNIRP guidelines, this entity has its own set of protocols found in [12], some of them are shown in Table 3.

Measurement Equipment	Measurement registers levels below 5% of ICNIRP limits	Measurement registers levels above 5% of ICNIRP limits	Additional precautions
EMF Meter: Narda NBM 550	A measurement of 6 minutes is conducted.	A measurement of 30 minutes is conducted.	Abort measurement if foreign sources are in the vicinity.
Software:NBM TS			
Wooden tripod			
Measuring laptop			

Table 3. Summary of Agentschap Telecom measurement protocols.

Table 3 shows the equipment used for the measurements along some of the protocols related to them. If measurements register EMF levels that are only 5% of the ICNIRP limitations, measurements will be realized only for the duration of 6 minutes, this to save time and cover more measurement locations on the saved time. Although it is stated that the latest ICNIRP guidelines are being applied, the latest measurement reports that are publicly available show that the 1998 guidelines are being used during measurements and can be found in Annex A. However there is no real discrepancy, as it was noted previously in section 1.1.2, that when it comes specifically to reference levels, the 1998 and 2020 guidelines would end up essentially being the same in the way they are utilized in most countries, including The Netherlands.

This research will utilize EMF measurements performed by Agentschap Telecom to calibrate the ray tracing software, which will be discussed in more detail in section 4.1.

1.1.6 Software Methods for EMF assessments and RF Propagation

Path loss can be estimated using theoretical and empirical models based on range, but these models lack accuracy in capturing temporal and spatial information. In contrast, ray tracing models are tailored to 3D environments, making them suitable for scenarios like urban environments.

Ray Tracing employs discrete rays that represent wavefronts as they propagate from a transmitter through a scenario. These rays interact with the scenario's geometry, undergoing reflections, diffractions, and transmissions. The rays reaching a receiver illustrate potential signal paths. By superimposing the contributions of all these waves, one can calculate the electric field, received power, and other electromagnetic quantities at the receiver point. Two main methods exist referenced in [13] and [14]:

Shooting-and-Bouncing Rays (SBR): This approach involves shooting rays in various directions, typically at fixed angular intervals. The rays interact with surfaces, splitting into additional paths through reflections, transmissions, and diffractions from wedges.

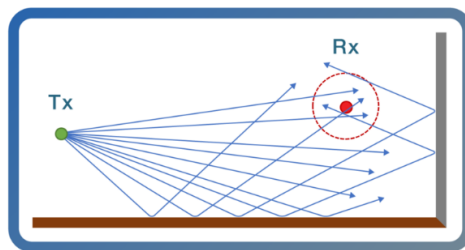


Figure 2. Shooting and Bouncing Rays

Image Theory: This method identifies all possible paths between a predefined transmitter-receiver pair using image-based techniques. It determines ray-tracing interactions and repeats the process for subsequent pairs of points in the calculation.

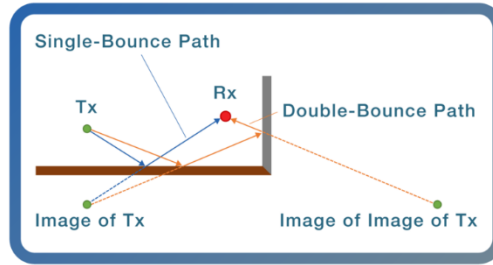


Figure 3. Image Theory.

The Shooting-and-Bouncing Rays (SBR) method is efficient for identifying ray-tracing paths in complex scenes. However, as the rays propagate, they gradually disperse and may not interact with smaller objects, leading to potential errors in path length and phase calculations. On the other hand, Image Theory provides more precise results, but it requires repeating the calculations for each transmitter-receiver pair, making it computationally demanding, especially in scenes with numerous facets and many transmit-receive pairs.

1.2 Literature Review

In this section the researched scholarly works and papers are referenced and summarized. As well as synthesizing the state of the art knowledge, identifying possible gaps and key findings.

1.2.1 Cell-free Massive MIMO

The next generation of 5G networks addresses the growing demand for high-speed data by introducing cell-free configurations that can resolve issues like interference. One such solution is massive MIMO with a cell-free topology. In this configuration, multiple access points (APs) are uniformly distributed to serve a limited number of User Equipments. Data provided in the works of [15] is summarized in Table 4.

Goal	Methodology	System Architecture and Operation	Channel Estimation and Management	Duplexing Techniques	Diversity	Tested Algorithms			
						Distributed	Centralized	Perfect Scheme	Regular Scheme
Find an optimal scalability scheme	Numerical analysis to achieve maximum optimization in transmission.	Scalability upgrade	Standard Channel Estimation	TDD	Macro-diversity	LP-MMSE	P-MMSE	P-MMSE-TOT	MR-TOT
		AP+CPUs operate as single cell	Dynamic Cooperation Clustering			L-MMSE	P-MMSE-TOT and MMSE	MR-TOT and LP-MMSE-TOT	LP-MMSE_TOT

Table 4. Summary Cell-free Massive MIMO.

Conventional MIMO technology, which relies on FDD (Frequency Division Duplex) operation, is limited in scalability. In FDD, the available spectrum is divided into separate frequency bands for UL (Uplink) and DL (Downlink). As the number of users or BS antennas increase, the divided and fixed spectrum for UL and DL limits the flexibility to adaptively allocate resources depending on different traffic demands, making it less scalable. However,

the use of the TDD (Time Division Duplex) method offers improved radiated energy efficiency and higher throughput. TDD facilitates the introduction of more antennas due to its mitigated interference, and at the same time aiding in the implementation of spatial multiplexing due to the increased number of antennas. With more antennas, the energy can be concentrated more precisely in smaller regions, resulting in improved beamforming and focused transmission which could play a role in specific EMF exposure scenarios.

In the past Cell-free Massive MIMO faced scalability challenges also due to its network-centric approach. However, a shift towards a user-centric technique has been adopted, where each user equipment (UE) is served by a subset of access points (APs) that divide the network into multiple cooperation clusters, and where the APs and CPUs (Centralized Processing Units) operate as a single cell. To achieve scalability, a new framework has been developed known as Dynamic cooperation clustering (DCC) which enables the system to efficiently handle scalability while ensuring effective cooperation among APs and UEs.

As for scalability purposes, the Classical MR (Maximum Ratio) Combining and LP-MMSE (Linear Precoding based on Minimum Mean Square Error) are preferred. MR Combining is a receiver-side technique that weighs the received signals from multiple antennas based on their channel gains to maximize the received signal power at the receiver. LP-MMSE is a transmitter-side technique that computes a precoding matrix of data symbols to minimize the MSE (Mean Square Error) between the transmitted and received signals at the intended receivers. In [1], it was concluded that Performance loss depends on the limited number of APs and the algorithm used for cluster formation. If the performance can be affected by the limited number of APs, to make up for this loss it is possible that some configurations would opt to increase the power, which could in turn increase the EMF exposure in specific scenarios that will be put to test in this research.

1.2.2 EMF Exposure Study from User Equipments in 5G

Goal	Methodology	Operation Frequencies [GHz]	Antenna type	Number of elements	Element separation distance	Phone chasis dimensions [mm ²]	Patch element dimensions [mm]	Substrate thickness [mm]	Permittivity [F/m]	Total Injected power [dBm]	Peak Power Density @ 1mm [V/m]	Peak Power Density @ 70mm [V/m]
EMF exposure for the design of UEs assesment	Measurements with a probe are realized. Results are expressed in Max. Allowed PD and PD vs dist.	15	Patch array	8x1	$\lambda/2$	140x78 mm ²	4.6x5.7	0.8	3.55	23	~1942	~123
		28					3.1x4		2.2			~238

Table 5. Analysis on Cell-free massive MIMO Summary.

The works in [16] studied and measured the Power Density radiated from UEs at different distances on the mmWave frequencies of 15 and 28 GHz as shown in Table 5, which summarizes the technical details and some of the test results from [2]. At close range distances of about 1 mm, the peak power density measurements obtained is approximately 1942 V/m as shown in Table 5, which is much higher than EMF levels for the general public limit of 61.4 V/m from ICNIRP [9]. A maximum allowed Power Density with different number of antenna elements at 50 mm away is also cited. With 4 and 8 antenna elements, a maximum allowed PD (Power Density) of 12 and 15 dBm respectively, in order to meet the PD regulation limitations of 10 [W/m²] or 61.4 [V/m]. In [16], it is advised to conduct new

measurements as the devices are meant to be used closer than 50mm away from users. It is also noted that measurements are difficult due to the disrupting influence of the probe itself, which could jeopardize the accuracy of the measurements.

1.2.3 EMF Exposure Case studies

The following case studies shown in Table 6 are from the works in [17], [18], [19], [20] and share some similarities in terms of configuration and overall results.

	Site location	Frequency [GHz]	Channel BW [MHz]	Scenario	Methodology	Measurement Antenna	Spectrum Analyzer/ Software	Measurement Time lengths [min]	EMF Level [V/m]
1	Malasya - Urban [17]	29,5	N/A. Possibly 100 MHz or 200 MHz	Outdoor LOS - Distance = 22 [m] - Tests: UE Off; VoiceCall; VideoCall;Videostream; 100%UL; 100%DL	Measure SS-RSRP -> Sum for each Channel -> Sum all channels for E_avg	Omni Directional QOM-SL 26-40 GHz	R&S TSMA6 scanner/R&S ROMES4	1,6 and 30 [min]	Max=5.7 Avrg=2.02
2	Tokyo - Urban [18]	28.2-28.3	100	Outdoor LOS - Distance = 11.6 [m] Tests: UE Off;UE On with Data Tx;UE On to Off	Measure SS-RSRP -> Total E field strenght is computed in the post processing	Double-ridged Horn antenna (DRH50; RFspin)	Anritsu MS2090A	1 [min]	Max=0.08 Avrg=0.04
3	Italy - Urban [19]	27.15 - 27.25	100	Outdoor LOS - Distance = 91 [m] - Tests: TA - No DL Traffic; TB - DL Traffic (for 5 to 30s);TC - DL Traffic (for 1 h)	DL Traffic is generated and injected -> Measure the channel power directly through a self made Algorithm	Horn antenna (Anritsu 2000-2003-R) 26-40 GHz	Anritsu MS2090A/Self made algorithm MWave	5-30 [s]; 1[h]	TA = 0.014 TB = 0.071 TC = 0.052 (Average Exposures)
4	Italy - Urban [20]	902 MHz to 2140 MHz	5 to 20	Ray trace Simulation over Fuorigrotta area ~ 650 m ²	Uses a Elevation model map (DEM),along a vector file for position,height of buildings and characterization of antennas to output EMF levels	NA	NA	NA	Some zones above 20

Table 6. EMF exposure case studies summary.

The first three studies were realized using mmWave operation frequencies and are all outdoor LOS scenarios, while the fourth is a simulation study on non-mmWave frequencies. The first case study does not specify the Channel Bandwidth used, but they do provide the number of Sub-Carriers used of 1584, which would correspond to the compatible channel bandwidths of 100 or 200 MHz. The first two cases use the measurements from the SS-RSRP (Synchronization Signal Reference Signal Received Power), being the always ON signal in 5G NR, as a reference to calculate the Electric field. The third case has its own algorithm to use the received power as a parameter to calculate the E. field and at the same time attempt to gain an insight on the role of the different DL traffic conditions being generated. The first case study uses an omni directional antenna while the second and third use horn antennas and use spectrum analyzers that share similar capabilities for the relevant purposes. These also attempted to apply time lengths from the ICNIRP guidelines and IEEE.

All of the study cases resulted in E. field values well below the limitation of 61.4 [V/m] cited in the guidelines of ICNIRP. Some of the EMF studies in Table 6 share setup similarities. The first 3 studies use a single BS (Base Station) and UE, however some of their configurations and measurement methodologies are different, which resulted in different EMF levels. Table 6 shows EMF results that are comparable to one another, such as the maximum and average levels from study 2 and tests TB and TC from study 3. Study 1 differentiates from 2 and 3 in EMF levels possibly due to their assessment based on multiple channels at the same time and a higher channel bandwidth configuration. Although the channel bandwidth is not explicitly referenced in [3], the provided information of using 1584

Sub-Carriers, makes a higher Channel Bandwidth configuration a possibility. Study 4 differentiates the most in terms of EMF levels since it makes an EMF assessment based on a simulation of multiple BSs and access technologies present in the specific area of Fuorigrotta, Naples-Italy [6]. The results from this case study pointed at some areas already exceeding the 20 [V/m] pre-5G deployments, which is the limit for the general public in Italy in regular areas, while 6 [V/m] is the limitation for areas concurred by populations deemed as sensitive such as schools, daycare centers or playgrounds.

Based on the findings of section 1.2.1, the number of Access Points (APs) or BSs can significantly impact performance and resulting EMF levels. Section 1.2.2 highlights that mmWave User Equipment (UEs) could be a crucial EMF source, but assessing it remains challenging, even in controlled laboratory conditions. EMF assessments in section 1.2.3 indicate varying EMF levels across different case studies due to distinct configurations and methodologies used. Hence, understanding the relationship between configurations and resulting EMF levels becomes important when considering network technological upgrades. Additionally, conducting assessments across multiple technologies, such as in case study 4, significantly influences the resulting EMF levels.

Building upon the insights from the previous sections, the impact of various configurations on EMF levels in a Cell-free Massive MIMO deployment has been established. In light of these findings, it becomes crucial to investigate the relationship between configuration parameters and resulting EMF exposure while considering network technological upgrades. This leads us to the central research question of this study

1.3 Research Question

In a Cell-free Massive MIMO deployment in Enschede that accounts for the already present GSM, 3G, 4G, and 5G technologies, to what extent do variant parameters:

- User Density
- Base Station Quantity
- Base Station Antenna Configuration
- Channel Bandwidth
- Sub-Carrier Spacing
- Transmit Power

influence the EMF exposure, while achieving optimal Block Error Rate, Reference Signal Received Quality, Throughput performance, and EMF general public regulation compliance?

2 Methodology

This chapter includes the problem description and a flowchart outlining the simulation procedure, followed by a by a comprehensive explanation of each step within the process.

2.1 Problem Description

A ray tracing software is used, where mobile technologies are considered, along a Cell-free Massive MIMO mmWave deployment. The chosen place is Enschede, thirty eight BSs from its RAN (Radio Access Network) will be replicated within the simulation software. This means to include a number of BSs which include GSM (Global System for Mobile communication), 3G UMTS (Universal Mobile Telecommunications System), 4G LTE (Long Term Evolution) and 5G technologies belonging to current operators in the city. This information is leveraged from the governmental antenna registry from The Netherlands, which includes information for the coordinates of the BSs, along with the number of antennas, technologies, radiation power, azimuth and height.

This resource also includes EMF measurements realized by Agentschap Telecom. All of the available measurements are used as reference to normalize the simulation replicated scenario. One of the EMF simulations involves calibrating the scenario to get the same values as the ones provided in the publicly available measurements, to ensure that results found from network additions would represent EMF levels close to what would be measured in real life. Additionally, the clutter zones data from the city is also included to account for the different types of zones in the map which are constrained by different environment conditions.

The related EMF exposure is assessed in two ways. One directly through the simulation software EMF exposure simulation feature, and also through realizing independent calculations using user specific data from Monte Carlo simulations with the software.

2.2 Flowchart of Research Procedure Steps

Figure 4 shows the flowchart for the different steps considered in this thesis, where the main steps are labeled with a letter in parenthesis and further described in the subsequent subsections.

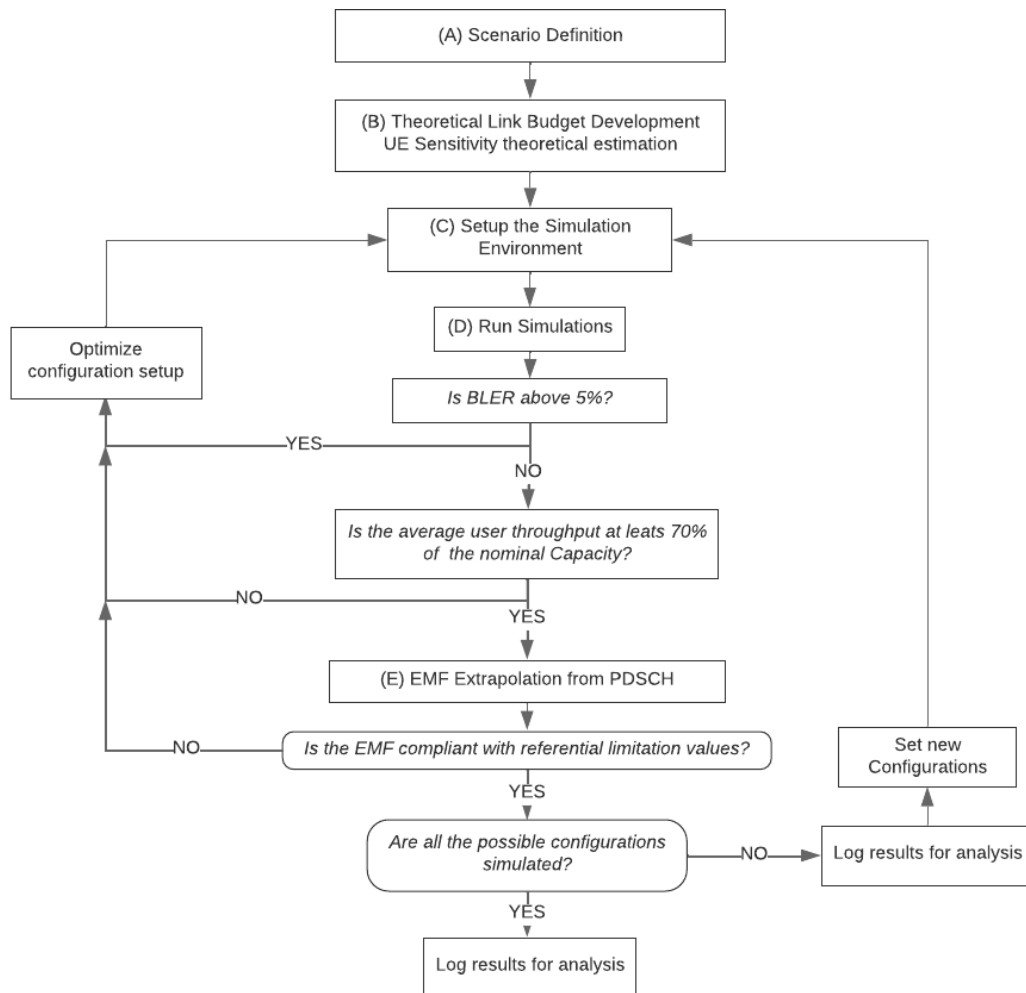


Figure 4. Procedure flowchart.

2.2.1 Scenario Definition

In step “(A)” from Fig. 4 a place is chosen, the currently present and to introduce technologies are defined for the simulation environment.

Place	Technologies	Propagation models	Bands	Frequency [MHz]
Enschede - The Netherlands	GSM	Okumura-Hata	E-GSM-900/E-UTRA 8	925
	3G			
	4G	Cost-Hata	n1 / E-UTRA 1	2.110
			n7 / E-UTRA 7	2.620
			n20 / E-UTRA 20	791
			n38	2.600
			n50	1.500
	5G	3GPP:38.901	n3 / E-UTRA 3	1.805
			n28 / E-UTRA 28	758
n257			28.000	

Table 7. Considered components in the simulation environment.

The network in Enschede, which includes its existing and considered technologies of GSM, 3G, 4G and 5G in the bands n3 and n28, will be referred to as the “former network” throughout the document. The introduced technology is 5G using the frequency band n257 as shown in Table 7.

2.2.2 Link Budget Definition

In step (B) from Fig. 4, a portion of Enschede’s mobile network is to be replicated, this is done for two reasons. Firstly to have a scenario representative of a real network deployment, and secondly to use measurements from [21] to calibrate the simulation scenario. Obtaining the same approximate values as in the measurements normalizes the simulation environment to provide meaningful results from additions on the network. Meaning the mmWave introduced antennas.

A link budget calculator is developed to theoretically calculate the needed separation between the mmWave BSs which should allow a successful connectivity for the given parameters.

(f_c)	Center f [GHz]	28,00
(RB_{Nr})	Max number of RBs (Resource Blocks)	132,08
(Δf)	Subcarrier spacing [kHz]	120
(SC_{QTY})	Subcarrier Quantity	1585
(NF)	Noise figure [dB]	4
$(SINR)$	Target SINR(Signal-to-Interference-plus-Noise Ratio)[dB]	-2
(L_c)	Cable loss [dB]	2
(G_A)	BS Antenna Gain [dB]	18
(H_A)	BS Antenna Height [m]	25
(P_t)	BS Transmit Power [dBm]	23
(L_B)	Body loss [dB]	3
(F_s)	Slow fading margin [dB]	7
(L_{flg})	Foliage Loss [dB]	8,5
(L_{rain})	Rain/Ice margin [dB]	1
(I_M)	Interference margin [dB]	2
(d)	Distance [m]	148
(BW_{ch})	Channel BW (Bandwidth) [MHz]	200
(BW_{RB})	One RB BW [kHz]	1440
(BW_{mx})	Max. Channel BW [MHz]	190,2
(GB)	Min. Guard Band [kHz]	4900
$(PL_{UMa_{LOS}})$	LOS (Line of Sight) Path Loss UMa (Urban Macro) [dB]	104,69
$(PL_{UMi_{LOS}})$	Path Loss UMi (Urban Micro) [dB]	106,92
(LB_{UMa})	Link Budget UMa [dBm]	-89,19
(LB_{UMi})	Link Budget UMi [dBm]	-91,42
(N_T)	Thermal Noise [dBm]	-91,21
$(R\chi_S)$	Receiver sensitivity:	-89,21
	Radio Channel Status:	PASS

Table 8. Attributes considered for the calculation of the Link budget.

The values shown in Table 8 in the orange fields are parameters that depend on other values from the same table, the blue fields are parameters set according to the scenario. For example the distance of 148 meters is determined to be the threshold distance right before the sensitivity becomes bigger than the link budget and the connection fails.

The chosen Tx Power of the BS is set to a low value of 23 dBm as a conservative measure for tests that would reduce the maximum transmitting power.

Note that in this case one of the main purposes of this assessment is to determine the approximate distances for an optimal operation, in order to take it into account when placing the BSs for the hypothetical mmWave cell-free network. The equations found in [22] and [23] used in this calculator are the following:

$$BW_{RB_1} = 12 * \Delta f \quad (1)$$

$$RB_{Nr} = \frac{BW_{ch} * 10^3 - 2 * GB}{BW_{RB_1}} \quad (2)$$

$$SC_{Qty} = RB_{Nr} * 12 \quad (3)$$

$$BW_{mx} = \frac{\Delta f * SC_{Qty}}{10^3} \quad (4)$$

$$PL_{UMa_{LOS}} = 28 + 22 * \log_{10}(d) + 20 \log_{10}(f_c) \quad (5)$$

$$PL_{UMi_{LOS}} = 32,4 + 21 * \log_{10}(d) + 20 \log_{10}(f_c) \quad (6)$$

$$LB = P_t + G_A - L_c - NF - L_b - PL - F_s - L_{fltg} - L_{rain} - I_M \quad (7)$$

$$N_T = -174 + 10 \log(BW_{mx}) \quad (8)$$

$$Rx_S = NF + N_T + SINR \quad (9)$$

For which acronyms used in expressions (1) through (9) are available in Table 8.

2.2.3 Simulation Environment Setup

In Fig. 4, step (C) defines the simulation setup and considerations for the ray tracing software. The ray tracing software used is Atoll, which is a radio planning and optimization software tool used in the telecommunications industry. It is widely employed by network operators, equipment vendors, and radio planning engineers for tasks such as network design, coverage prediction, capacity analysis, interference analysis, and optimization of wireless communication networks.

Atoll provides features and functionalities to assist in the planning and optimization of various wireless technologies, including GSM, UMTS, LTE, and 5G NR. The software offers capabilities for creating network models, importing terrain data, simulating radio propagation, designing antenna systems, generating coverage maps, performing traffic analysis, evaluating network performance as well as EMF exposure assessment. A few research efforts employing the radio planning software Atoll for LTE and 5G NR include references [24], [25] and [26]. The EMF exposure considerations by the simulation software is discussed in section 2.2.5, and the algorithm used in simulations can be found in Annex N.

An initial setup for the simulation is carried out next, where the following tasks are involved:

- Importing a DEM file for the terrain: A Digital Elevation Map for the chosen area is used to account for the differences in altitude from buildings and vegetation.
- Importing a map with clutter zones: This map allows the delimitation of the different zones that belong to buildings, Trees, grassland, water bodies and cropland. This allows for a better definition of the environment, which also helps with the relevant losses involved for clutter zones such as buildings.
- Placement of BSs and Antennas: A portion of Enschede's mobile network is replicated and all the involved BSs are placed. These coordinates are available in the rijksdriehoekscoördinaten system in the governmental antenna registry which needs to be transformed to a coordinate compatible with the simulation software. The antenna technology, quantity, transmit power, azimuth and height information can also be found. There are about 800 antennas that need to be placed manually in the simulation environment in order to replicate the relevant portion for Enschede's mobile network.
- Configuration for the various variables: In this step all the frequencies have to be set for each antenna. Not all of the frequencies are available in the simulation software

by default, the missing ones need to be added with their correct corresponding values for them to work, such as the ARFCN (Absolute Radio Frequency Channel Number) and compatible carriers.

- Antenna types are defined. The antenna type used for the network to replicate is the ideal 3GPP antenna for simplicity, and a more directive antenna pattern is used for the mmWave BSs. A fixed beamforming is used for the mmWave network and the antenna patterns can be found in Annex B.
- Computational zones are created. Computational zones are polygons to delimit an area of interest. These zones can be manually drawn or defined through a specific set of coordinates. Computational zones can be defined in the city's map to save computational resources and are defined in section 3.3.
- User types, traffic maps using user types, as well as user density and mobility are also defined to be used in the simulations:

User type	Service	Terminal	Requests/hour	Duration(sec)	UL Volume (Kbytes)	DL Volume (Kbytes)
mmWave_User	Broadband	5G Smartphone	0,25	30	1000	500000
Business_User	Broadband	5G Smartphone	0,05	65	10.000	50.000
	Internet	5G Smartphone	0,01	200	5.000	20.000
	Voice Call	5G Smartphone	0,2	240		
Standard_User	Internet	4G Smartphone	0,1	70	2.000	15.000
	Voice Call	4G Smartphone	0,2	240		

Table 9. User type definition.

Environment	User Profile	Mobility	Density (Subscribers/km ²)
Urban	mmWave_User	Pedestrian	1.000
	mmWave_User	50 km/h	500
	Business User	Pedestrian	400
	Standard User	Pedestrian	400
Dense Urban	mmWave_User	Pedestrian	7.000
	mmWave_User	50 km/h	5.000
	Business User	Pedestrian	800
	Standard User	Pedestrian	800

Table 10. Mobility and density Atoll configurations.

Note that the attributes in Table 9 and 10 are set this way by design, in order to get the desired amount of active users in the Monte Carlo simulations for the estimations calculated in Annex J. A nominal throughput example for the service of Broadband can be found in Annex L and the Monte Carlo algorithm used by Atoll in Annex N.

- A calibration for the simulation environment is carried out using measurements realized by Agentschap Telecom which are visible in Antenneregister [21] before placing the additional mmWave BSs for the Cell-free Massive MIMO network. This is elaborated on in Section 4.1.

2.2.4 Simulation Procedures

In step (D) from Fig. 4, multiple simulations are conducted which are elaborated on in sections 4.2, 4.3 and 4.4. For Monte Carlo simulations, BLER and user Throughput data is available. Simulations are made sure to comply with a BLER lower than 5%, which is a more strict BLER target than the typical one for eMBB (Enhanced Mobile Broadband) in 5G NR [27]. For throughput, a 70% or above of the nominal throughput for the considered service, which is a target defined for this design. This process is intended for determining compliance with optimal performance levels while using various different configurations

2.2.5 EMF Definition

The EMF definition relevant to sections 4.1 and 4.2 are obtained by conduction EMF simulations directly on the simulation software. The EMF definition relevant to sections 4.3 and 4.4 are performed to the EMF extrapolation from PDSCH (Physical Downlink Shared Channel) discussed in section 2.2.6.

The simulation software Atoll has proprietary rights over the implementation specifics of some of its tools such as EMF exposure simulations. However, in [28] it is stated that EMF exposure, is regarded as the cumulative electromagnetic field measured at a specific location. Atoll acknowledges that while the acceptable level of EMF exposure may vary depending on the jurisdiction, it typically ranges within a few V/m. To evaluate EMF exposure, Atoll incorporates an internal propagation model tailored specifically for this purpose. The analysis can be performed in two dimensions for open areas like parks or roads or in three dimensions for buildings. In the case of buildings, there is an option to assess EMF exposure only at the front façade, where the exposure tends to be the highest.

The internal propagation model employs distinct propagation classes, which are derived from input files. These classes are categorized as either opaque or transparent. Opaque classes cause diffraction losses at the object's edges but do not allow the signal to pass through entirely. Transparent classes enable signal passage, though some losses may occur. These classes are characterized by the following parameters [28]:

- Penetration loss (dB): Represents the loss experienced when the signal enters the object.
- Linear loss (dB/m): Denotes a linear loss applied for every meter within the object.
- Distribution of measurement points: Field strength measurements are taken at a set of points and can be displayed on a single pixel of the map in the considered area.

Atoll uses default propagation classes, including:

- Open: Suitable for obstacle-free areas, such as open spaces or water bodies. Open areas are transparent, with no diffraction loss.
- Vegetation: Designed for regions covered with vegetation, like parks, which can be considered transparent with some degree of diffraction loss.

- Building: Intended for opaque objects like buildings, where the signal undergoes both transmission loss and diffraction loss.

2.2.6 EMF Extrapolation from PDSCH Data

Works in [17] and [18] from section 1.2.3 had to use the SS-RSRP signal to extrapolate the related E. field, because it was the most accessible signal to measure but there can be some issues if performed that way. The synchronization signal power level reported by the SS-RSRP parameter, is different than the one used for Data transmission, such as the PDSCH signal. Consider the following scenarios:

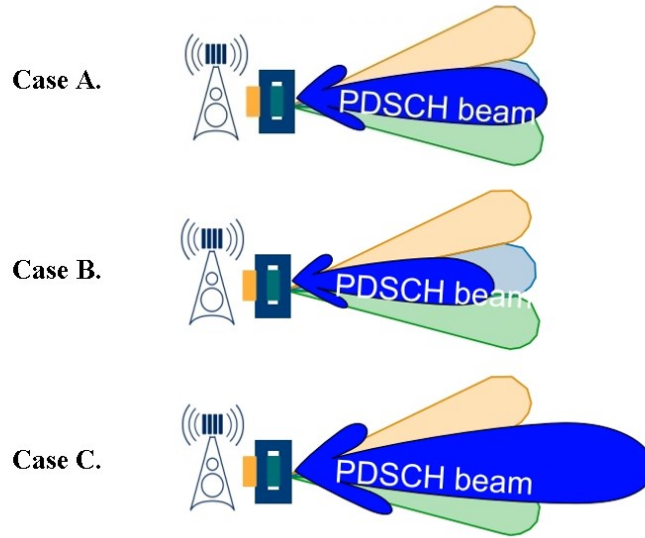


Figure 5. EMF determination challenges.

In Case A of Fig. 5, there are 3 light colored beams which correspond to synchronization signals reported by the SS-RSRP, and one blue beam corresponding to the PDSCH. If the E. field was evaluated using either of the synchronization or PDSCH beams in Case A, there would be no major discrepancy between them. On the other hand, the E. field estimation using the SS-RSRP beams from Case B and C in Fig. 5 would result in an overestimation and underestimation respectively, of the actual received field during Data transmission.

Since the PDSCH level for each user is available through the simulator, it will be the parameter used to estimate the E. field level, in step (E) from Fig. 4. This is a similar approach to the one used in [19], where the received power was measured directly as downlink traffic was injected in the system.

To extrapolate the E. field level the approach used in [17] and [18] of section 1.2.3 can be used, namely:

$$E_{field} = E_{SSB} = \frac{1}{20} 10^{\frac{P+AF}{20}} \quad (10)$$

Equation (10) gives the E. field for each Synchronization Signal Block (SSB), where P is the Power level of the SS-RSRP in dBm, and AF is the antenna factor. A derivation of this equation can be found in Annex C.

$$E_{asmt} = E_{SSB} * \sqrt{F_{extBeam} * F_{BW} * F_{PR} * F_{TDC}}. \quad (11)$$

In Equation (11) from [17],

- E_{asmt} is the maximum E. field, E_{SSB} is the SSB field calculated in (10).
- $F_{extBeam}$ is the spectrum measurement between no UE and UE in dBm.
- F_{BW} is the Sub-Carrier quantity.
- F_{PR} is the power reduction factor where if equal to 1 the system operates at maximum power.
- F_{TDC} is the technology duty cycle factor used to quantify how often the system is actively operating .

Alternatively, an equation derived from the Friis transmission equation can be used if distances are to be accounted in the extrapolation of the E. field with the following equation:

$$E_{field} = \sqrt{\left(\left(30 * 10^{-3} * 10^{\frac{P_r}{10}} \right) * \left(3 * \frac{10^8}{(4 * \pi * d * f)} \right) * \frac{(4 * \pi * d)^2}{G_t} \right)} \quad (12)$$

Where P_r is the received power in dBm, in this case, the power of the PDSCH beam, d is the distance in meters, f is the frequency in Hz and G_t is the gain in dB of the Transmitting antenna. A derivation for this equation can be found in Annex D and the MatLab script can be found in Annex E.

The simulation reports do not provide distances from the Users to the BSs directly, the only direct way to know the distance is to use a ruler tool within the software, but this is not viable when there are thousands of samples. However simulations do provide the serving Transmitter and the exact coordinates of the user on the map. Using the haversine equation [29], a script written in java was developed specific to this case to calculate the distances to the serving cells and can be found in Annex F:

$$a = \sin^2\left(\frac{(x_1 - x_2)}{2}\right) + \cos x_1 * \cos x_2 * \sin^2(y_1 - y_2) \quad (13)$$

$$c = 2 * \operatorname{atan}\left(\frac{\sqrt{a}}{\sqrt{1 - a}}\right) \quad (14)$$

$$d = R * c \quad (15)$$

Where x_1 and x_2 correspond to the latitude values , y_1 and y_2 correspond to the longitude values of the two points, and R is the radius of the Earth. Since the Earth is not completely round a correction factor was applied to the formula. The ruler tool was used to determine the correction factor and confirm that the distances are coherent with the calculated

ones through the script. The serving cells have to be indexed as well with their corresponding coordinates to be introduced in the algorithm.

To estimate the E. field of a GSM transmission the following equation from [30] can be used:

$$S = \frac{PG}{4\pi r^2} * 100 \quad (16)$$

Where S is power density, $\mu\text{W}/\text{cm}^2$; P is the transmission power of the BS in Watts; G is the gain, where the typical GSM BS antenna gain of 12 dB is assumed, and r is the distance between the BS and considered point in meters. The power density is to be converted to V/m by the following equation [31]:

$$P_D = \frac{E^2}{Z_0} \quad (18)$$

Where P_D is the power density in W/m^2 ; E is the electric field in V/m and Z_0 is the impedance which is assumed to be 377 $[\Omega]$ in free space.

The methodology uses ICNIRP general referential values in [6] to assess whether or not E. field levels are compliant or not. Since levels found in the already present network in Enschede go above the referential levels from the BioInitiative group in [9], these were not directly used as means of determining compliance but serve as an additional perspective for the results.

The simulations are carried out with fixed settings for the former mobile network of Enschede mentioned in 2.2.1. All the possible combinations for the mmWave portion of the network are done in terms of the following parameters:

User Density	BS Antenna Configuration	BS Quantity	Sub-carrier Spacing	Tx Power	Channel BW
Urban	4x4	7	120 [kHz]	40 [dBm]	100 [MHz]
Dense Urban	128x128	28	240 [kHz]	60 [dBm]	400 [MHz]

Table 11. Considered configuration parameters.

The reasoning for the use of these parameters is elaborated on in the next chapter.

3 Simulation Setup

This chapter presents the simulation environment and outlines the considerations taken into account, along with the rationale behind the selection of parameters used in the simulations.

3.1 Network Replication

To replicate Enschede's mobile network, Antenneregister [21] is used to deploy 38 BSs. There are around 800 different types of antennas distributed on all of these BSs.

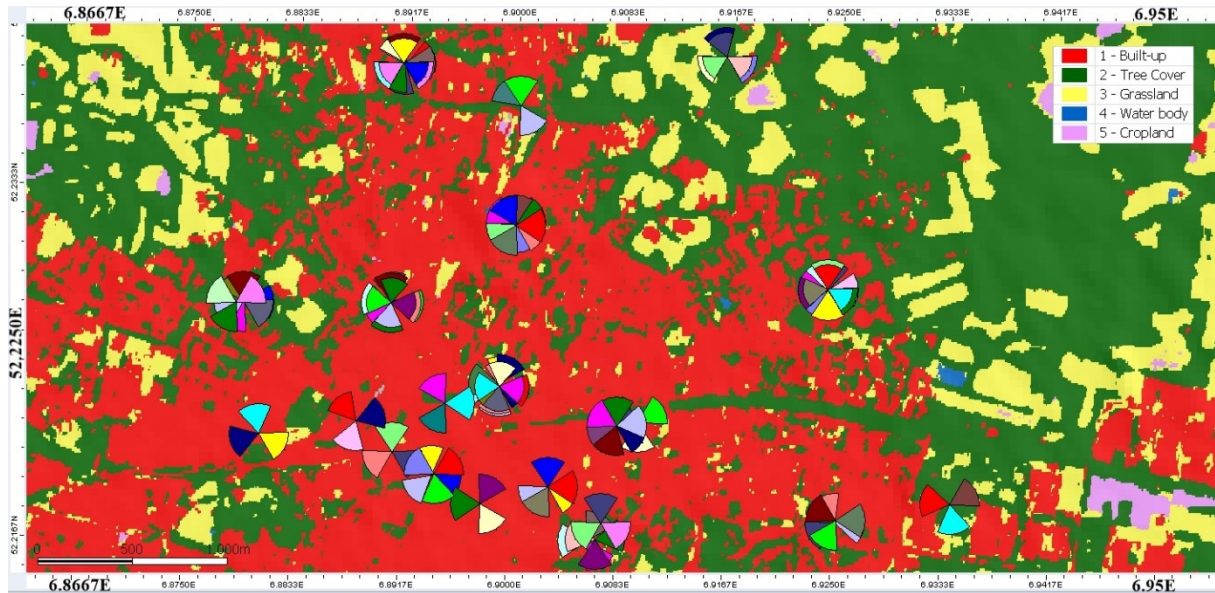


Figure 6. Enschede's BSs map locations.

The replication of the network was realized for the mid to northern area of Enschede and it includes the access technologies of 3G UMTS, 4G LTE, GSM, and 5G NR registered antennas which may not be fully operational at this point in time in this city. Information of the BSs' coordinates, heights, azimuths, and transmit power is introduced in the simulation software. Antenneregister also has details of antennas for Television and radio broadcasting, point to point links and radio amateur antennas, which are not contemplated in this replication.

The simulation environment also has clutter zones for the city of Enschede [32] accounting for the different penetration losses and propagation characteristics due to the materials involved. A DEM (Digital Elevation Map) is used and was leveraged from [33] in the past, but which cannot be obtained anymore through those means as its access has been restricted to require NASA credentials. This map provides a good representation of the propagation environment, considering the different building heights and vegetation profiling within the area under consideration.

3.2 mmWave Cell-free Massive MIMO Topology

There are two variants of the topology for the mmWave BSs deployment:

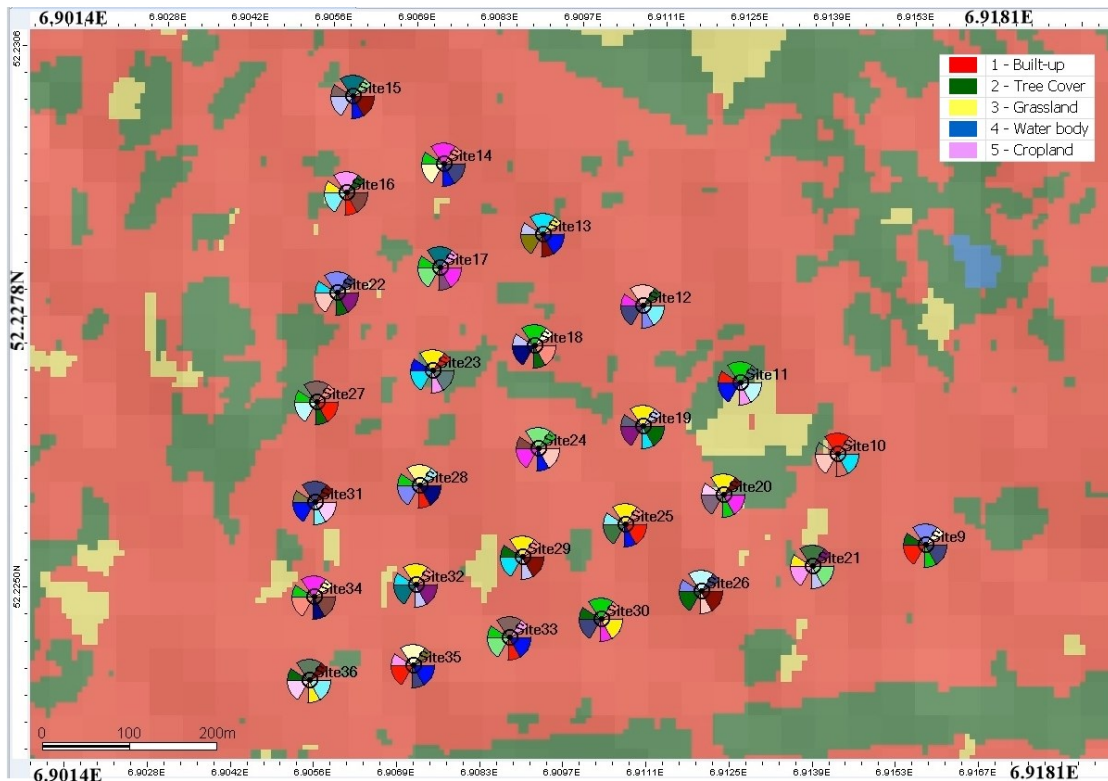


Figure 7. Topology 1 mmWave deployment with 28 BSs.

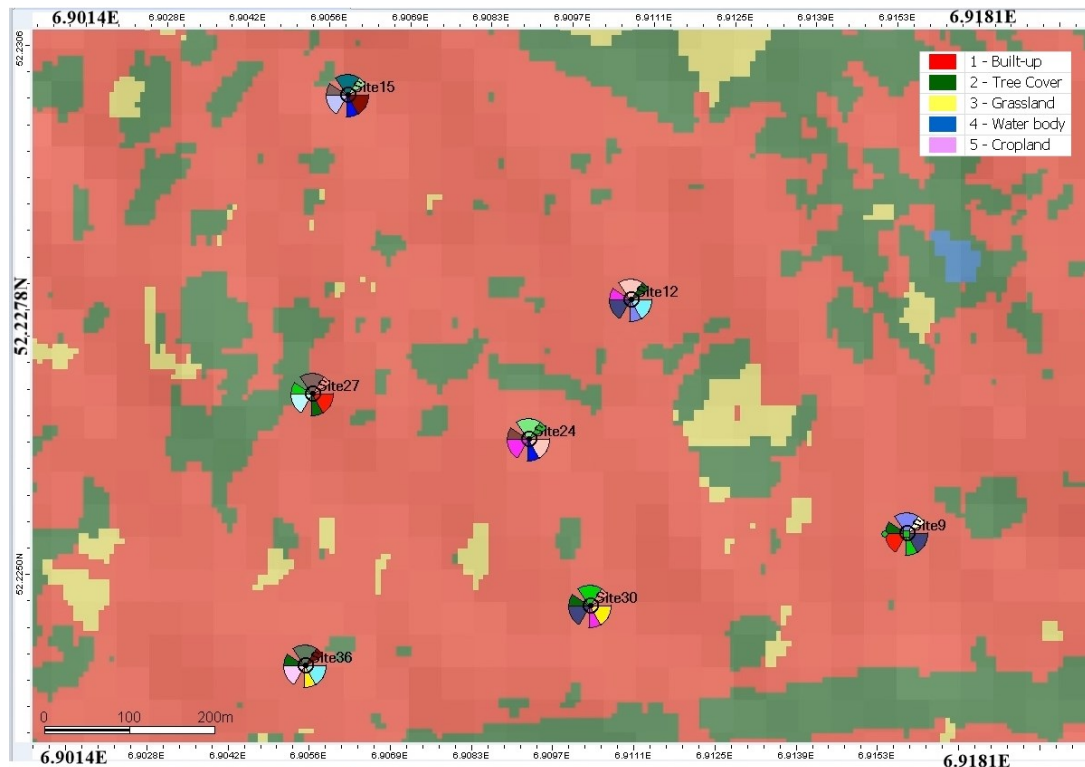


Figure 8. Topology 2 mmWave deployment with 7 BSs.

Fig. 7 shows Topology 1 with an increased amount for a total of 28 mmWave BSs, where distances range between 130 and 150 meters defined by the theoretical link budget in section 2.2.2. BSs could be approximately 296 meters apart from each other to still be aligned with the link budget. Both Topology 1 and Topology 2 are equipped with 6 Transmitters able to have 128x128 antennas each. A transmitter configuration along with the antenna used can be found in Annex O, and the beam patterns can be found in Annex B. Topology 2 is shown in Fig. 8 with a reduced number of 7 BSs. The separation distances between them is mostly between 200 and 300 meters, which is still aligned with the link budget.

Note that the placement of this hypothetical mmWave deployment are not necessarily feasible placements in Enschede, as the actual coordinate locations may not be all suited or available for the placement of antennas. However as some BSs deployments are starting to require less hardware and more software defined, the future of BSs deployments could facilitate such deployment. Furthermore the distances between these BSs are not uncommon when comparing them to other mmWave deployments such as the case of Japan [23].

3.3 Computational Zones

The simulation setup has two different computational zones, where one is used for the mmWave deployment, and the second one for the rest of the network’s area of interest. Note that zones shown in Fig. 9 and Fig. 10 do not necessarily represent the area of coverage, but are created in order to focus and simplify the computational processing.

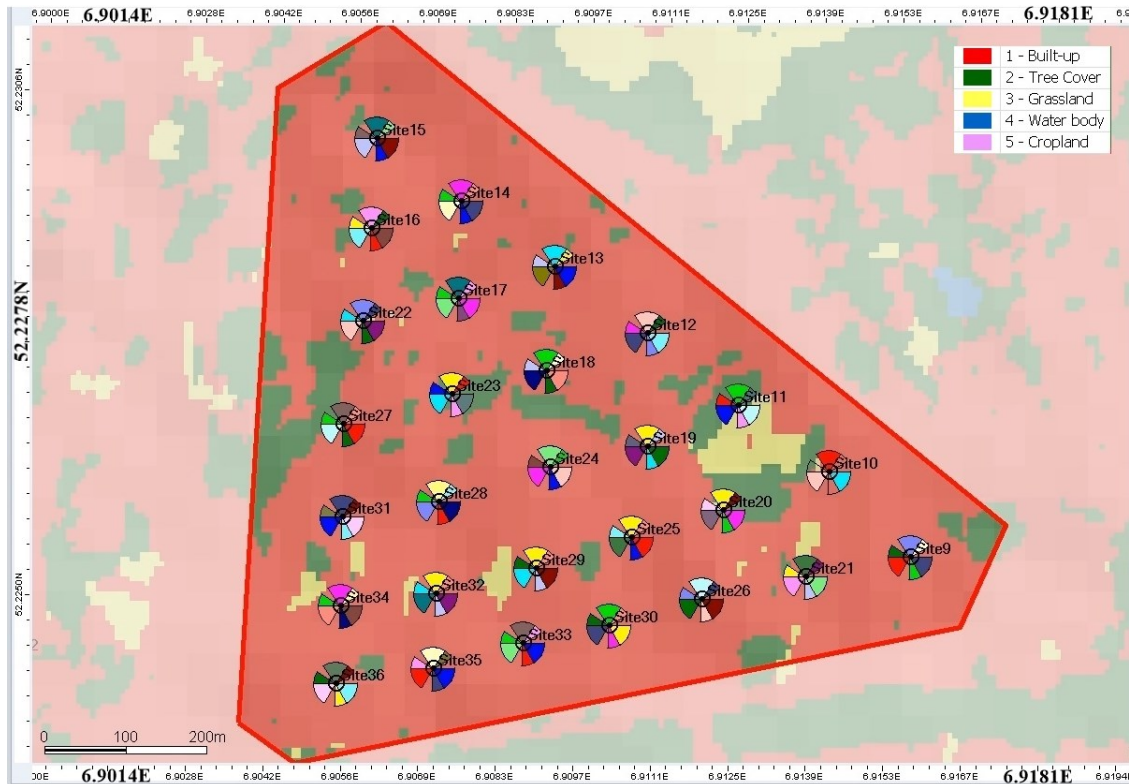


Figure 9. Computational Zone 1.

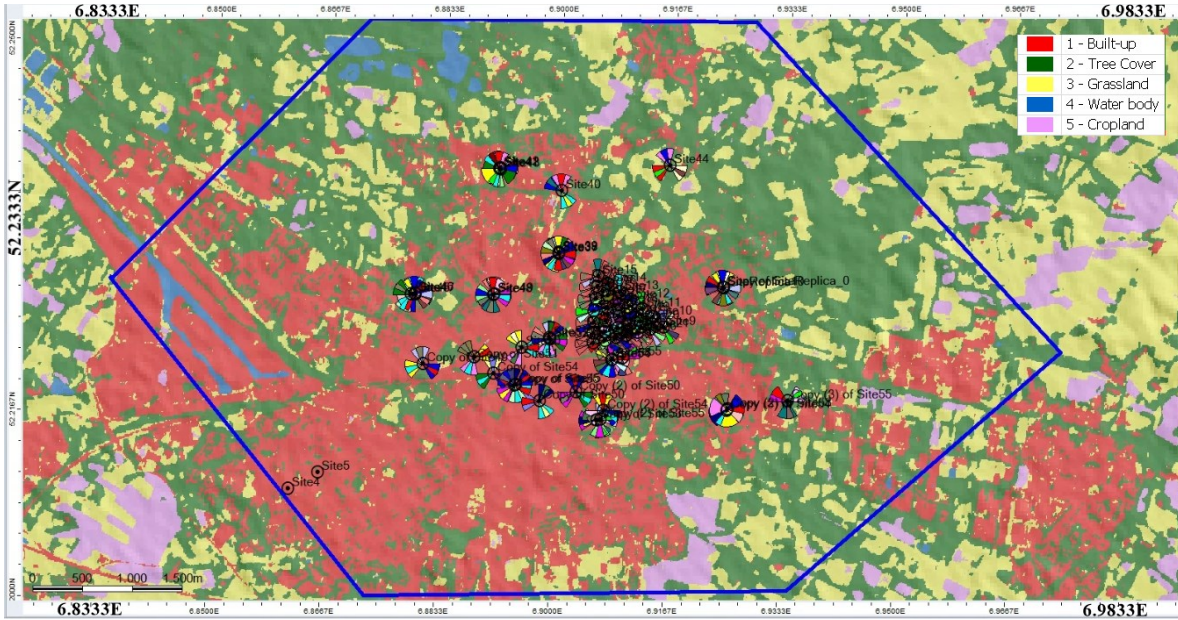


Figure 10. Computational Zone 2.

3.4 Simulation Parameters

The parameters for the already existing network in Enschede were leveraged from Antenneregister. The basis for the choice of parameters in the mmWave Cell-free Massive MIMO scenario is defined through different premises.

3.4.1 Transmit Power

The transmit power of 40 dBm was chosen because it is in between what is commonly found commercially, such as the case of [19] using an antenna power of 36.5 dBm and what is the maximum transmit power defined by regulatory agencies such as the FCC with their limit set on 43 dBm [35]. The transmit power of 60 dBm was chosen to push the boundaries of mmWave Tx. Powers that would not be commonly found. This is to assess if even under those conditions E. field levels would result in a violation of reference levels from the ICNIRP guidelines.

3.4.2 BS Antenna Configuration

The choice of 4x4 antenna elements was to evaluate the effect of having a configuration with less capabilities for beamforming and that is at the same time a non-Massive MIMO configuration. The 128x128 configuration is Massive MIMO and more capable of beamforming.

3.4.3 mmWave Frequency

The choice of the mmWave frequency band of n257 is related to be close to what was commonly found in the literature [17], [18], [19]. Moreover, it is the frequency range that the Netherlands may be interested in for commissioning mmWave, judging from the advice from the health council of The Netherlands [11].

3.4.4 User Density

The Urban scenario is based on a calculation shown in Annex J. This considers a percentage of the total area of Enschede related to the same percentage of its total population and assuming a 10% market penetration in terms of subscribers. This to take into account that only a fraction of the population would be using the network in each simulation. The Dense Urban scenario assumes a 30% market penetration instead, to account for more exceptional scenarios and to push the boundaries of the assessments.

3.4.5 Number of Base Stations

As Tokyo - Japan is one of the cities with a significant number of mmWave BSs deployments [34], it is used as a reference for determining the mmWave hypothetical deployment in Enschede. The amount of BSs in the topologies is determined by two estimations found in Annex K relating the total population of Enschede and making a comparison ratio wise to the population of Tokyo Japan. There are around 1100 mmWave antennas deployed in Tokyo alone, and an estimated 21000 in all Japan [34].

3.4.6 Sub-Carrier Spacing and Bandwidth

The choice of the Bandwidth and Sub-Carrier Spacing is related to what is technically possible for the n257 band, where the only channel bandwidths range from 50 to 400 MHz, for which possible SCSs are 120 kHz and 240 kHz. For instance, the n257 band could not possibly sustain a channel bandwidth of 20 MHz, since it already supports 120 kHz, and the minimum bandwidth due to the 240 Sub-Carriers found in the Synchronization Signal Block (SSB) is 120×240 or 28.8 MHz [36]. So these are strictly technical constraints due to the choice in frequency.

3.5 Simulation's Propagation Models

This section describes the small scale fading and large scale fading considerations in the simulation setup.

3.5.1 Small scale Fading Propagation modeling

The simulation software Atoll provides various features and functionalities to address small-scale fading phenomena in network design. Small-scale fading refers to the rapid fluctuation of signal strength caused by multipath propagation, which occurs due to reflections, diffraction, and scattering of the radio signal in the environment. The environment refers to the geographical characteristics or obstacles, which are defined with the help of a DEM and a clutter zone map, and user presence in a simulation.

Atoll addresses small-scale fading phenomena in network design through the following methods:

- Propagation Models: Atoll incorporates advanced propagation models, such as Ray Tracing and Ray Launching, which accurately predict the signal behavior in complex

urban environments, indoor scenarios, and microcellular environments. These models take into account the impact of small-scale fading caused by multipath propagation.

- Path Loss and Shadowing: The software considers path loss and shadowing effects, which are essential factors contributing to small-scale fading. It accounts for the signal attenuation due to distance and obstacles, and also models the spatial variation of signal strength caused by shadowing effects.
- Monte Carlo simulations: The Generator initialization of these simulations accounts for shadowing effects by the default, the user and shadowing error distribution will be random.

3.5.2 GSM and UMTS Propagation Model - Okumura-Hata

The Okumura-Hata model is applicable up to 1500 MHz, while the Okumura model can handle frequencies up to 1920 MHz. The Okumura-Hata model is suitable for both point-to-point and broadcast communications and considers various parameters such as mobile station antenna heights ranging from 1 to 10 meters, BS antenna heights ranging from 30 to 200 meters, and link distances spanning from 1 to 10 kilometers.

The fundamental formulation of the Okumura-Hata model for urban environments is derived from Okumura's measurements conducted in densely populated areas of Tokyo. The Hata model [37] is formulated as follows:

$$L_U = 69,55 + 26,16 \log_{10} f - 13,82 \log_{10} h_B - C_H + [44,9 - 6,55 \log_{10} h_B] \log_{10} d \quad (19)$$

Where

L_U = Path loss in urban areas in [dB]

h_B = Height of the BS [m]

h_M = Height of mobile station antenna [m]

f = Frequency of transmission [MHz]

C_H = Antenna height correction factor

d = Distance between the base and mobile stations [km]

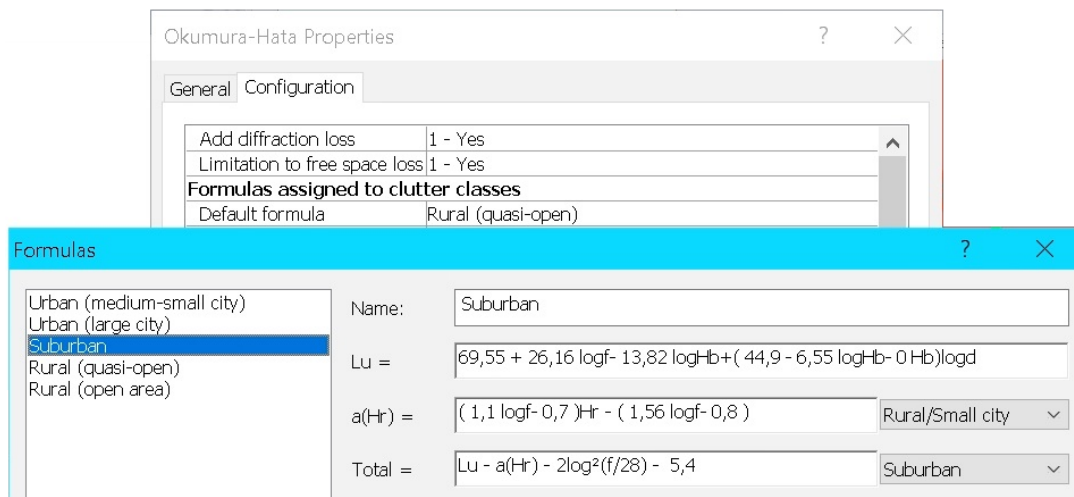


Figure 11. Okumura Hata configuration in the simulation software Atoll.

Fig. 11 shows some of the details considered by the simulation software Atoll in regard to the Okumura-Hata propagation model. The formulas shown in Fig. 11 are specific to a Suburban scenario where L_U is the Pathloss, $a(Hr)$ is the same as C_H in Eq. (19), the Antenna Height correction factor. The Total shown in Fig. 11 accounts for the Pathloss L_U , the correction factor $a(Hr)$ and values specific to the different environments. Based on the simulation environment, the simulation software can automatically choose the appropriate formulas.

3.5.3 LTE Propagation Model - COST 231 Hata

With the first GSM generation, which operated in the 900 [MHz] band, the Hata model could be used, which is valid for frequencies between 100 and 1500 [MHz]. With the increase in users and the evolution of the services offered, other bands such as 1800 and 1900 [MHz] began to be used. Due to the above, the European COST 231 group proposed a new model that complements the Hata model and is valid for frequencies between 1500 and 2000 [MHz]. The COST 231 Hata model [38] provides the following Equation for propagation losses.

$$L = 46.3 + 33.9\log_{10}f - 13.82\log_{10}h_b - a(h_m) + (44.9 - 6.55\log_{10}h_b)\log_{10}R + C_m \quad (20)$$

Equation (10) represents the losses due to propagation given by the COST 231 Hata model. where h_m is the height of the mobile antenna and C_m is a correction factor to take into account the propagation environment.

Environment	Value [dB]
For dense urban cities (tall buildings, more than 7 floors)	3
For less dense urban cities (Smaller streets and buildings)	0
For urban cities with wide streets	-5
For sub-urban with small buildings	-12
For mixed scenarios, Town and rural	-20
For rural scenarios with few trees and almost without hills	-26

Table 12. COST 231 values for different environments.

$$a = 3.2\log_{10}^2(11.75h_m) - 4.97 \quad (21)$$

Equation (11) accounts for the variations in propagation losses when the mobile moves vertically.

Parameters	Validity Range
Frequency in [MHz]	1500 to 2000
Effective height from the BS [m]	30 to 200
UE height	1 to 10
Distance [km]	1 to 20

Table 13. COST 231 Parameters Validity Ranges.

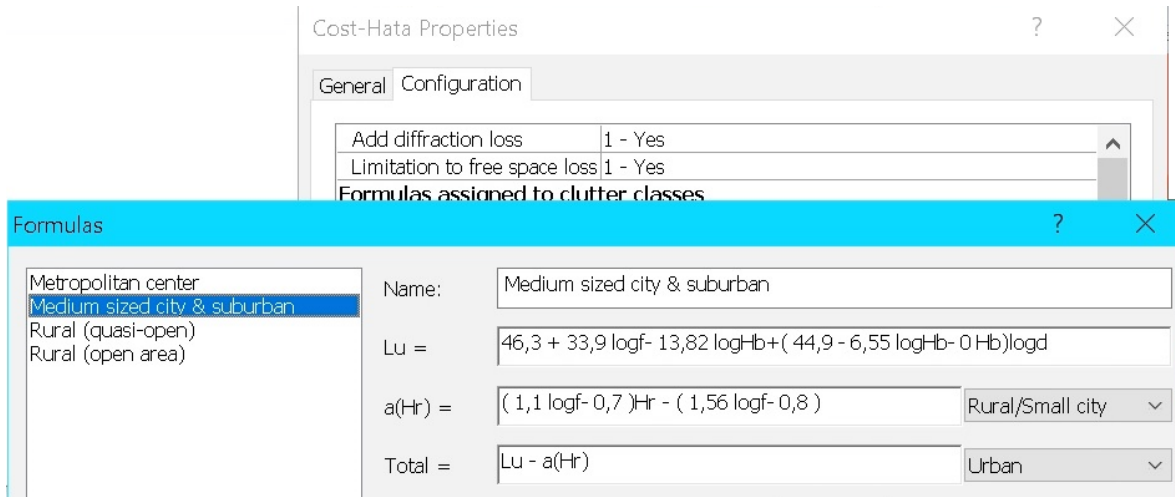


Figure 12. Cost-231 Hata configuration in the simulation software Atoll.

For the case of Cost-231 Hata, the simulation software Atoll also auto calibrates according to the geographic available details, and assigns $a(Hr)$ depending on the specific scenarios.

Figure 12 illustrates the key parameters considered by the simulation software Atoll concerning the Cost-231 Hata propagation model. The displayed formulas are used in a medium-sized city scenario, where L_U represents the Pathloss, and $a(Hr)$ is equivalent to C_m in Equation (20), which is the correction factor based on the propagation environment. The "Total" value in Figure 12 encompasses the Pathloss L_U , the correction factor $a(Hr)$, and environment-specific values. The simulation software can also automatically select the adequate formulas based on the simulation environment.

3.5.4 5G NR Propagation Model - 3GPP 38.901

The 3GPP 38.901 standard [22] includes a propagation model specifically designed for mmWave frequencies, such as the frequency band n257. This model takes into account the unique characteristics of mmWave propagation, which differ significantly from lower frequency bands. At mmWave frequencies, several propagation phenomena come into play, including high path loss, significant atmospheric absorption, and sensitivity to blockages. The 3GPP 38.901 propagation model addresses these factors to provide accurate predictions of signal coverage and quality in mmWave environments.

The model considers parameters such as building density, street layout, antenna heights, and environmental conditions to estimate path loss, shadow fading, and other effects. It also incorporates advanced techniques like beamforming and beam tracking to enhance signal strength and reliability in mmWave communications. The UMi (Urban Microcell) framework is used for the mmWave hypothetical deployment in Enschede. The UMi framework is a radio propagation model used to characterize the signal propagation in urban microcell environments, which include smaller areas with more obstacles and significant small-scale fading effects. Because of this, it is better suited to characterize the propagation environment in mmWave cell-free networks operating in urban settings, where multiple scatterers and reflections play a significant role in signal propagation. Table 14 describes the LoS and NLoS equations for the 3GPP 38.901 propagation model for the UMi settings.

UMi - Street Canyon	LOS	$PL_{UMi-LOS} = \begin{cases} PL_1 & 10m \leq d_{2D} \leq d'_{BP} \\ PL_2 & d'_{BP} \leq d_{2D} \leq 5km \end{cases}$ $PL_1 = 32.4 + 21\log_{10}(d_{3D}) + 20\log_{10}(f_c) \quad (22)$ $PL_2 = 32.4 + 40\log_{10}(d_{3D}) + 20\log_{10}(f_c) - 9.5\log_{10}((d'_{BP})^2 + (h_{BS} - h_{UT})^2) \quad (23)$	$\sigma_{SF} = 4$	$1.5m \leq h_{UT} \leq 22.5m$ $h_{BS} = 10m$
	NLOS	$PL_{UMi-NLOS} = \max(PL_{UMi-LOS}, PL'_{UMi-NLOS}) \quad (24)$ <p style="text-align: center;">for $10m \leq d_{2D} \leq 5km$</p> $PL'_{UMi-NLOS} = 35.3\log_{10}(d_{3D}) + 22.4 + 21.3\log_{10}(f_c) - 0.3(h_{UT} - 1.5) \quad (25)$	$\sigma_{SF} = 7.82$	$1.5m \leq h_{UT} \leq 22.5m$ $h_{BS} = 10m$

Table 14. 3GPP 38.901 UMi for NLOS and LOS Pathloss equations [22].

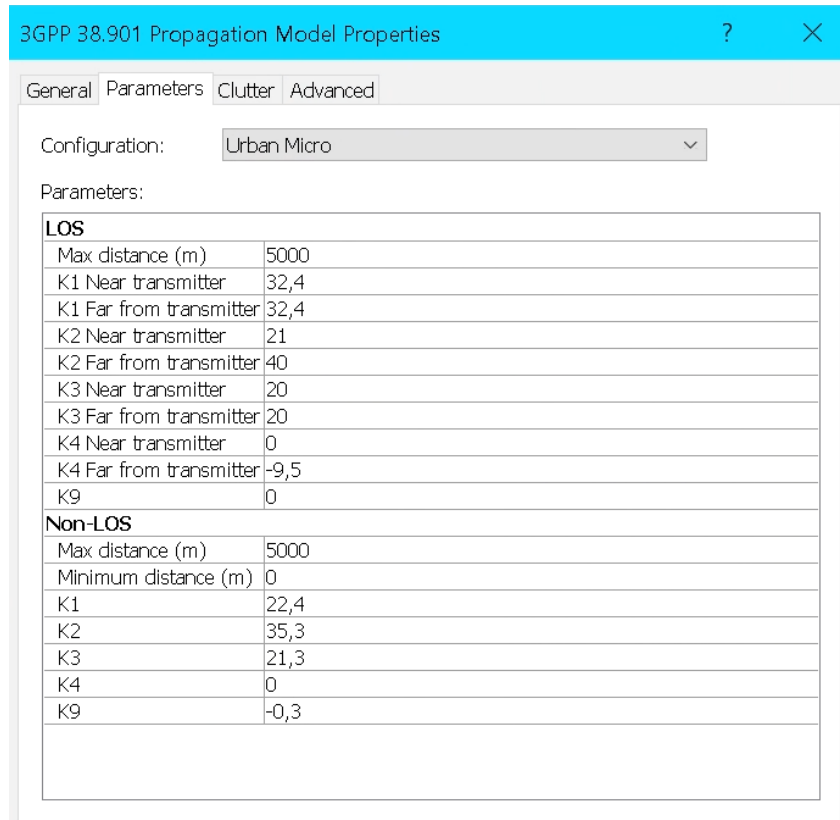


Figure 13. 3GPP 38.901 Propagation Model properties in Atoll.

The simulation software Atoll can automatically determine whether to utilize the UMa (Urban Macro) or UMi (Urban Micro) conditions based on the specific scenario. This calibration process takes into account the K factor parameters shown in Fig. 13, which align with the configurations specified in the 3GPP 38.901 specifications [22] shown in Table 14.

For the LOS (Line of Sight) scenario, Figure 13 shows the different K parameters applied in the UMi expressions with a validity distance of 5000 meters. Different K factors in the LOS scenario can be used depending on the considered position of the UE in relation

to the BS. If the UE is close to the BS as shown in Fig. 13, a certain K1 to K4 factor is accounted. “Near transmitter” values correspond to equation (22) in Table 14 and “Far from transmitter” correspond to equation (23) in the LOS scenario. This differentiation takes into account a breakpoint distance cited in the equation distance validity ranges in Table 14 to either use PL_1 or PL_2 from equations (22) and (23). On the other hand, the NLOS K factors are fixed and also correspond with the terms found in equation (24) for PL' in Table 14.

Through the inclusion of the K factors corresponding to the different configurations, Atoll accurately models and analyzes wireless communication systems in the considered environments. This ensures that the simulations align with industry standards, facilitating meaningful comparisons. The software’s capability to automatically select the appropriate UMa or UMi conditions, coupled with its adherence to the 3GPP specifications, guarantees a reliable simulation framework.

4 Results and Analysis

This chapter presents the simulation environment calibration, simulation results on different scenarios and discussion of the mmWave Cell-free Massive MIMO network overlapped with the legacy technologies considered and present in the city of Enschede.

4.1 EMF validation simulation

To calibrate the simulation environment to output results that would approximate real life measurements, a portion of Enschede's network is replicated in the simulation software, and the built-in EMF exposure report feature is used to determine levels at specific measurement points available through Antenneregister [21].

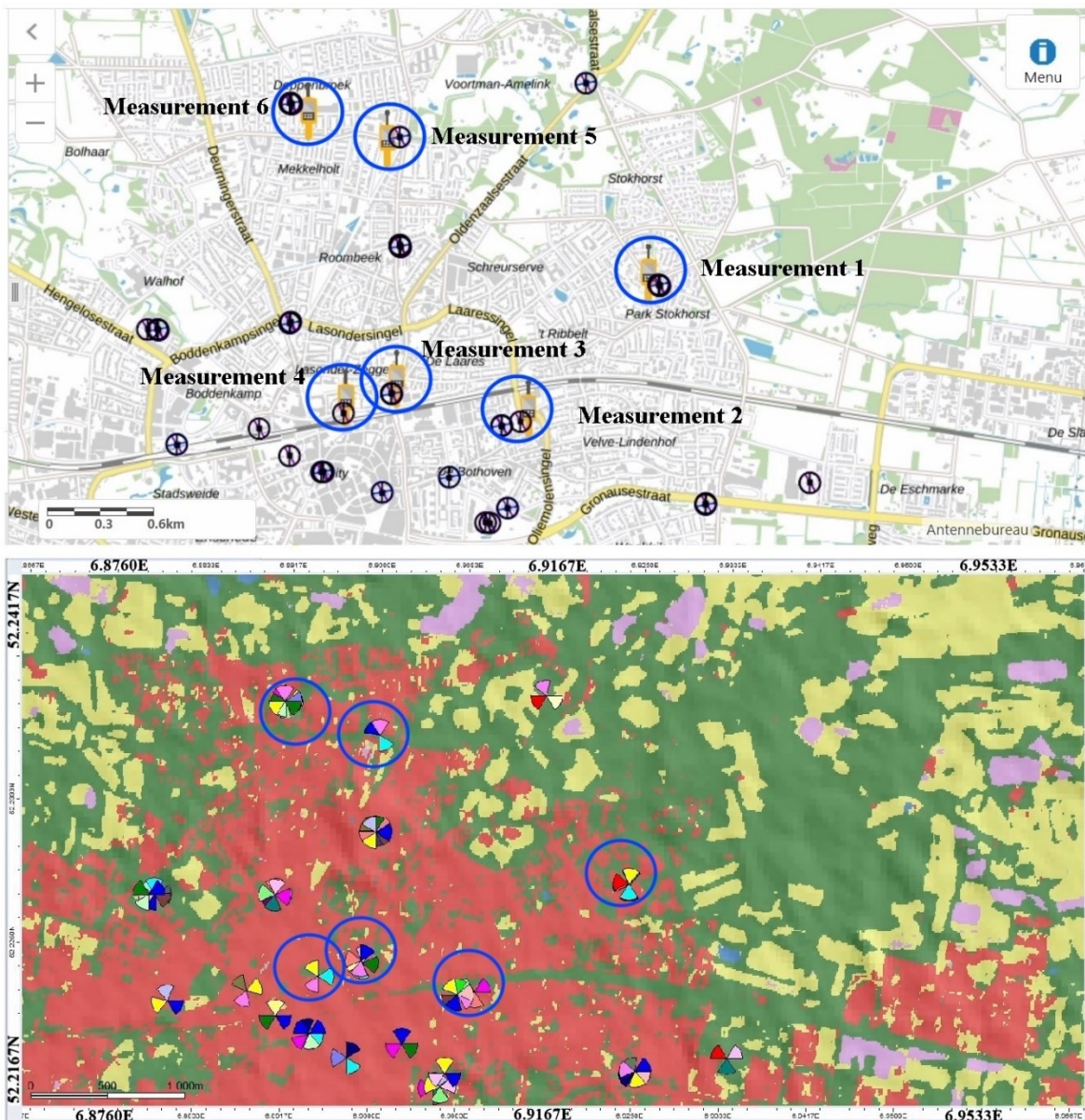


Figure 14. Top: Antenneregister Map with the considered BSs and measurements in Enschede.
Bottom: Replication of Enschede's network on the simulation software Atoll.

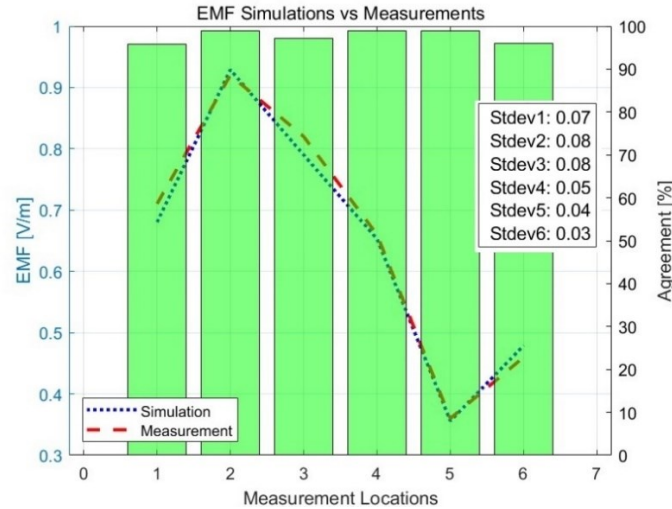


Figure 15. EMF verification of the replicated network vs Agentschap Telecom measurements.

The blue circles in Fig. 14 show the 6 measurement locations available in Antenneregister [21] relevant to the replicated portion of the network. Fig. 14 also shows the replicated network where EMF level simulation samples are taken.

The EMF report given by the simulation software Atoll does not include a list of EMF levels related to specific coordinates, hence a comparison with measurement locations from Antenneregister is not directly possible. However the EMF simulation includes the radiation representation in the displayed map within the simulation software as shown in Fig. 16. By hovering the cursor over different coordinates in this map, the corresponding EMF levels are illustrated, as it is the case in Fig. 16 for coordinates 6,898186894E 52,224244261N displaying 1.09 V/m. In this way ten samples per measurement location are taken as shown in Annex M, surrounding the coordinates of the measurements available in Antenneregister. The standard deviations of the samples taken for each measurement location are shown in the top right of Fig. 15. Figures presented in Annex P show examples of the samples taken. The samples' averages are then compared with the available measurements for the considered region, and presented in Fig. 15, where the green bars represent the percentage agreement between them, measured on the right vertical axis and with values above 95%.

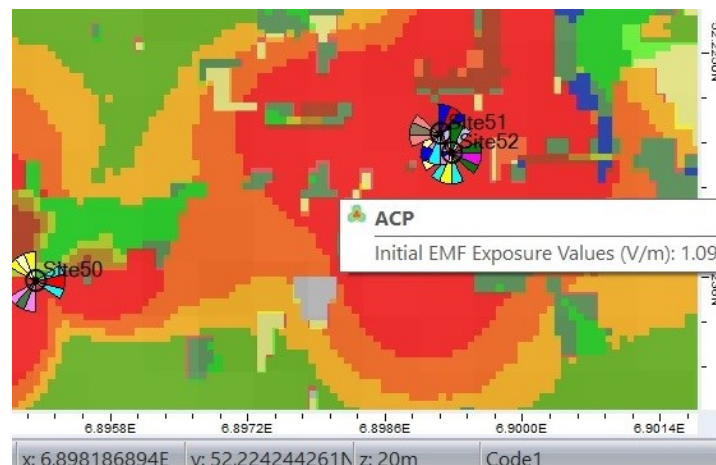


Figure 16. EMF value example in the simulation software Atoll.

4.2 EMF exposure assessment of Legacy Cellular Technologies and Cell-free Massive MIMO

Using Atoll's feature for EMF exposure, reports are created overlapping the EMF levels for the access technologies from GSM, UMTS, LTE, 5G NR, including the added mmWave BSs for the Cell-free Massive MIMO network. The parameters for Enschede's former network are maintained, while changes are made for the introduced mmWave BSs.

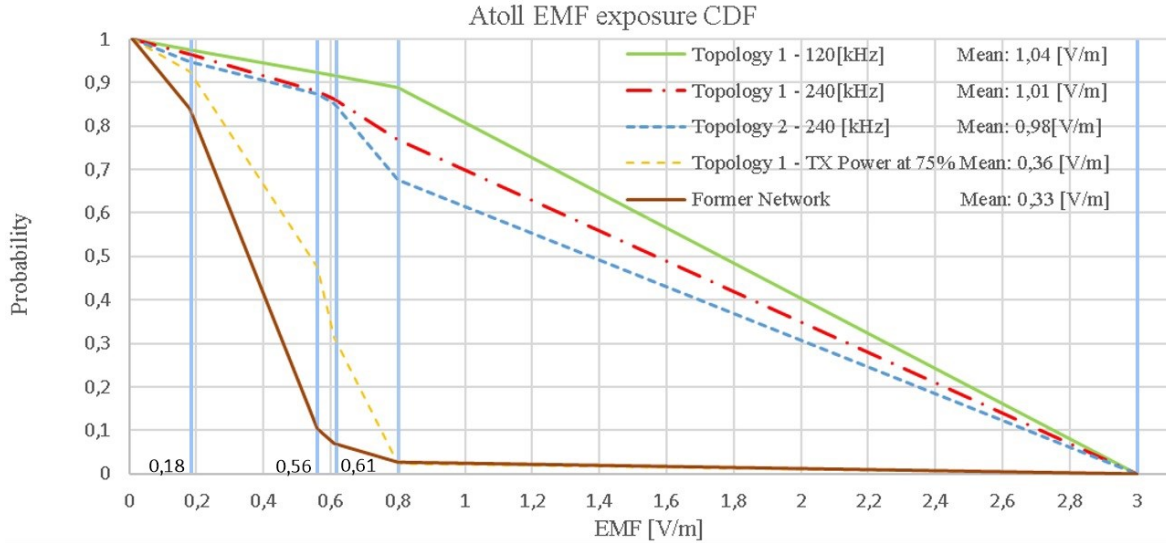


Figure 17. Atoll EMF reports CDF.

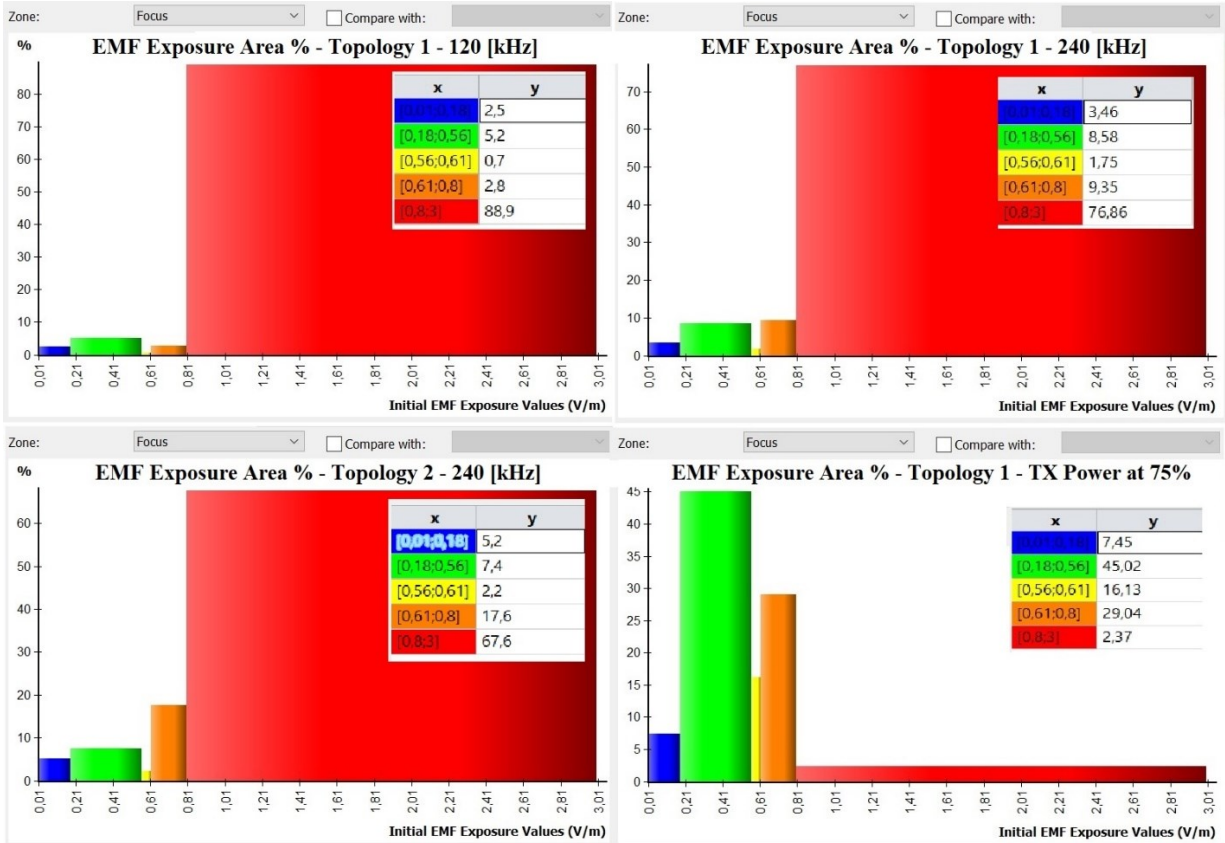


Figure 18. Atoll EMF reports area percentage histogram.

Running the simulation using the computational zone shown on Figure 10, limits the ability to effectively observe variations resulting from different configurations. For this reason the smaller computational zone shown on Figure 9 is used. Figures 17 and 18 are applying this computational zone as the total considered area. Figure 18 presents the areas' percentages covered by different EMF levels, with ranges defined in colored bars. Specific Electric field ranges, found in Annex I, were defined for these EMF simulations to reduce processing times. Note that ranges in Annex I are only applicable on section 4.2, since EMF reports in this section are generated directly by the simulation software.

Fig. 17 shows the CDF provided by the simulation software while using different conditions for the mmWave part of the network. The light blue gridlines correspond to specific EMF ranges defined for the simulation in this section, also available in Annex I. Figures 17 and 18 are related and present the following:

- The first simulation for the 120 kHz SCS, represented as the solid green line in Fig. 17, has a mean E. field value higher than the 240 kHz SCS configuration represented by the red dash-dotted line. The top two plots in Fig. 18 show a similar insight with the area percentage representation. This shows 89% for the 120 kHz SCS and 77% for the 240 kHz SCS when considering the red bar range.
- Figure 18 also shows that with the reduced amount of BSs, Topology 2 has an E. field level of 68% in the red bar range.
- In Fig. 18 reducing the maximum Transmit power to 75% produces a drastic E. field reduction in the red bar range down to 2,37% when considered the red bar, and most of the E. fields registered are in the green bar range.
- The upgraded network can represent as much as 215% Increase, or 9 dB, in relation to the former network, when comparing it to a Topology 1 – 120 SCS kHz configuration from Fig. 17.

It is worth emphasizing that the simulation environment was calibrated by using Agentschap Telecom measurements available in [21], so that simulation results would represent levels close to what would be measured in the real world. Without performing a calibration, Atoll EMF reports can output levels close to the high E. fields found in case study 4 in Table 6 from [20], as can be shown in Annex R. The works in [20] do not make mention of a calibration attempt on the simulation environment, hence it is possible that the higher levels found in that case could have been related to an uncalibrated simulation environment.

Measurements by Agentschap are often realized in the Far field and not very close to the BSs. This means that fields evaluated closer to BSs could reach higher levels than most of the available measurements. All of the measurement locations used from Antenneregister are made in between 50 and 200 meters away from the closest BSs. Since the simulation takes into account every pixel including those close to the BSs, some of the levels are higher than the measurements, although these represent the minority. The EMF exposure from reports shown in Fig. 17 are all below the reference levels from ICNIRP, but mostly above the BioInitiative assessment, which is one of the most strict limits someone could find in regard to EMF exposure. However, if compared to limits from more EMF exposure conservative countries from Table 1, such as Italy, Turkey and Bulgaria, these levels would still be considered below the limits.

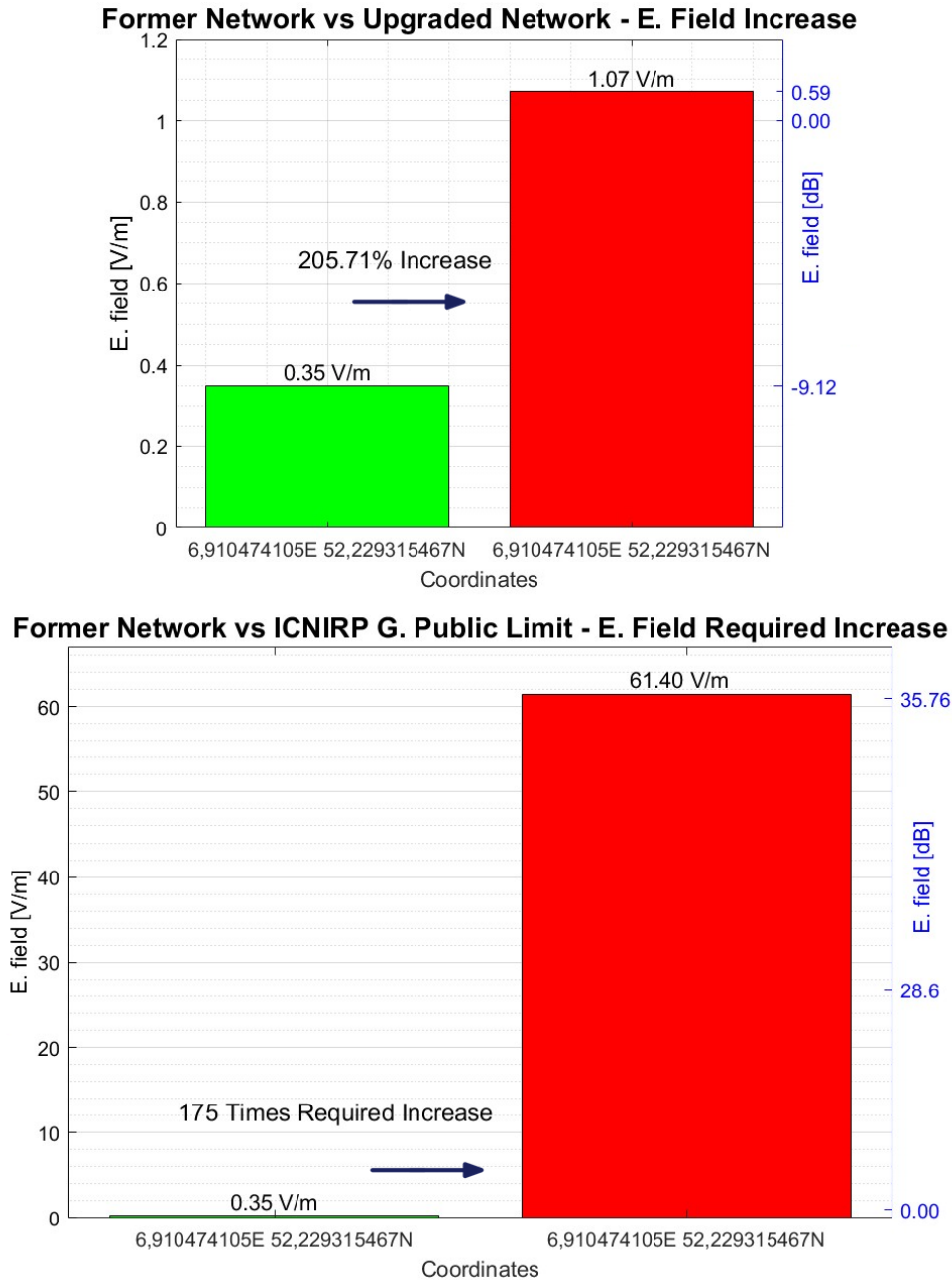


Figure 19. Former vs Upgraded Network E. Field Increase & Required E. field Increase to reach ICNIRP limits.

The example comparison shown in Fig. 19 shows the E. field level increase at one specific set of coordinates, namely 6,910474105E 52,229315467N. The green bar representing the former network, and the red bar representing the same network plus the additional mmWave BSs introduced, referred as the Upgraded network. As the purpose is to illustrate an example, this set of coordinates was simply chosen as it is nearby a location from a different type of study discussed in section 4.3.1, however there is no intent in making a direct relationship between the studies through this choice of coordinates.

The green bar in the left side of Fig. 19, exhibit an E. field level of 0,35 V/m, while the upgraded network shows 1,07 V/m, which would represent an approximate 206% increase on the E. field registered on those specific coordinates. In terms of the difference between former versus upgraded network, it is a significant increase in the E. field level. However on the right side of Fig. 19, an additional perspective is provided which shows that the E. field increase would require to be around 175 times larger to reach a reading that would equal ICNIRP reference limits for the general public.

Most of the measurements in Enschede available in [21] do not divert far from each other, and some measurements remain close to the one shown on the example in the left part of Fig 19.

It is worth to note that, although rare, higher measurement readings are possible in other cities such as Amsterdam, where a measurement of 19,63 V/m can be found. This would represent 55 times increase if compared with the example on the left of Fig. 19.

It should be emphasized that the hypothetical mmWave Cell-free Massive MIMO upgrade resulting in a 206% increase as shown in the left graph of Fig. 19, would only apply near to the coordinates shown in this Figure. This is because the influence area and coverage from the introduced BSs decay more rapidly as they operate on the mmWave frequencies.

4.3 Cell-free Massive MIMO analysis

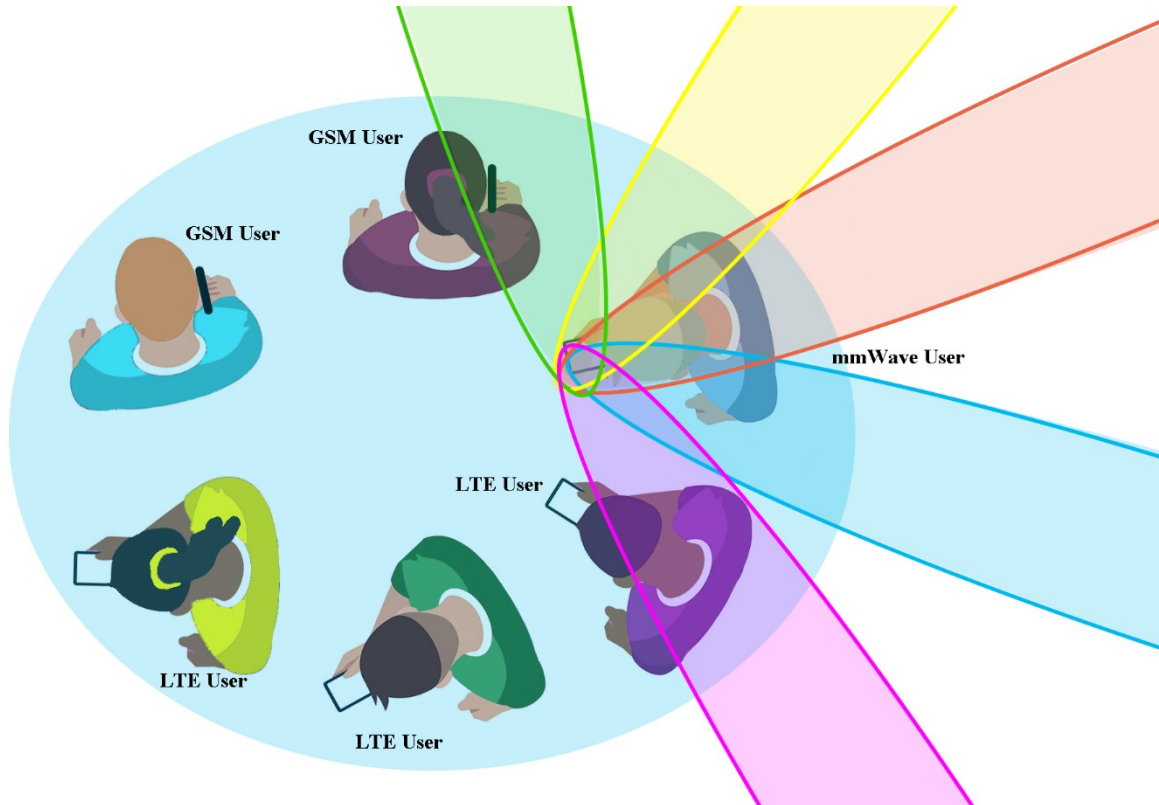


Figure 20. Simulation scenario layout applicable to section 4.3.

Within section 4.3, various evaluations are realized using the same User layout as shown in Fig. 20. This figure shows a single mmWave user in a fixed position being served by 5 beams denoted by different colors beams from 5 different BSs in a Cell-free Massive MIMO scheme. There are other five users nearby the mmWave user (approximately 1 [m] away),

also in a fixed position using the GSM and LTE access technologies as shown in Fig. 20. The light blue circle in Fig. 20 surrounding the users is merely a simplified representation of the overlapped EMF from the GSM and LTE BSs. The beamwidths in Fig. 20 are also meant as an illustrative representation of the beams from the Cell-free Massive MIMO mmWave BSs. Note that these studies do not account for the EMF fields emitted by the UEs, but only by the potentially present EMF field from the BSs for the given specific scenario.

All the available input data from Antenneregister [21] such as maximum Transmit powers are accounted in this study, with the assumption that 70% of the maximum power and technology duty cycle are used for LTE and mmWave. For GSM 80% of the maximum power is used, and it is assumed that the recorded field happens on the assigned timeslot for the GSM transmission. The duty cycle for GSM is already accounted in the simulation software for averaging the EMF reports, but in this specific scenario the GSM network is on an active call transmitting under general TDMA conditions with assigned timeslots with transmission bursts in the order of ~ 0.6 milliseconds.

In addition to the fixed parameters belonging to LTE and GSM on Enschede's former network, configuration variations shown in Table 15, are applied to the mmWave BSs in each scenario within section 4.3, in terms of SCS, BS Antenna Configuration and maximum Transmit Power.

The Cell-free user association is fixed to always use 5 beams at the same time per user. Each single beam comes from a single transmitter, capable of having different receiving and transmitting antennas' configurations, as shown in Table 15 in the BS Antenna Configuration column. Precoding techniques such as distributed LP-MMSE are bypassed and not in effect, however BSs are chosen in terms of a best server protocol, which usually selects BSs that are close to the user.

Figures in this section include scatter plots and percentage representations of the sum levels for all of the considered access technologies. While they are not in comparable conditions in terms of number of users from each technology, it does provide an additional perspective under this specific scenario. There are in total 5 studies followed by a grouped analysis of the Cell-free mmWave BSs of all the considered studies in this section. The considered parameters are shown in Table 15.

Location	mmWave User Coordinates	SCS [kHz]	BS Antenna Configuration	TX Power [dBm]
1	6.910578096E 52.22939321N	120	4x4	40
2	6.91616565E 52.227287341N	240	128x128	40
3	6.908992749E 52.225072443N	240	128x128	60
4	6.904865057E 52.226198992N	120	128x128	60
5	6.9056398E 52.223594875N	120	4x4	60

Table 15. Details for the 5 Cell-free Massive MIMO specific scenario studies.

Since the E. fields for each access technology are sourced from different BSs, and because these are not studies about the interactions between the E. fields from each technology but rather the sum of the E. fields, studies in this section are realized in parts.

Simulations in this section are realized in 3 parts, each corresponding to a different access technology, namely GSM, LTE, and mmWave 5G NR. Simulations are carried in relation to the coordinates set in Table 15 for the mmWave User for each location, in a way that they correspond to the layout setup shown in Figure 20. Results are then put together to realize the analysis.

4.3.1 Cell-free study location 1

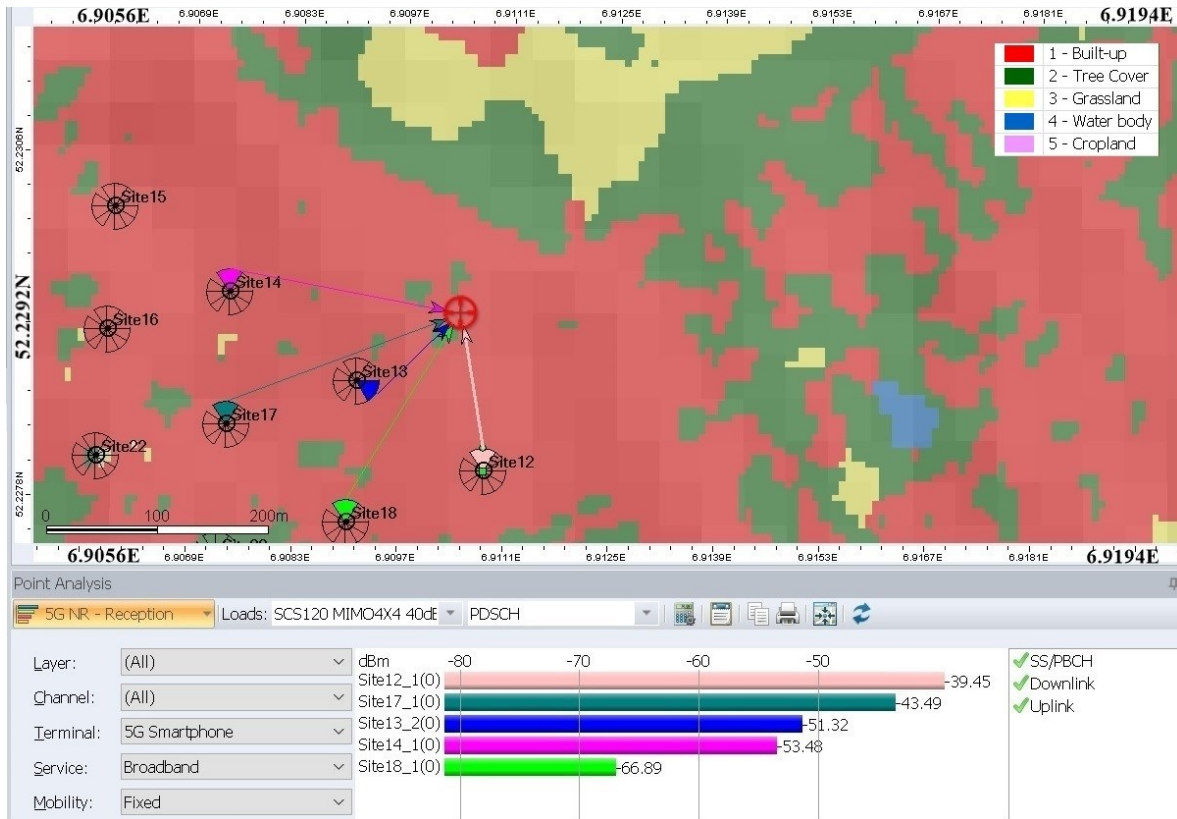


Figure 21. Cell-free MIMO study Location 1.

Location	mmWave User Coordinates	SCS [kHz]	BS Antenna Configuration	TX Power [dBm]
1	6.910578096E 52.22939321N	120	4x4	40

Table 16. Location 1 mmWave Cell-free MIMO configuration.

Figure 21 shows the simulation for the mmWave User alone represented by the red cross, where all the beams from different BSs point and meet in the direction of this user. The red cross also represents the location where the PDSCH signal is measured by the simulator. Table 16 shows the configurations and details relevant to this sub-section.

The simulations for the GSM and LTE users for this location can be found in Fig. 61 and Fig. 62 in Annex Q. Data related to simulations in the location considered by this sub-section are shown in Table 22 in Annex G.

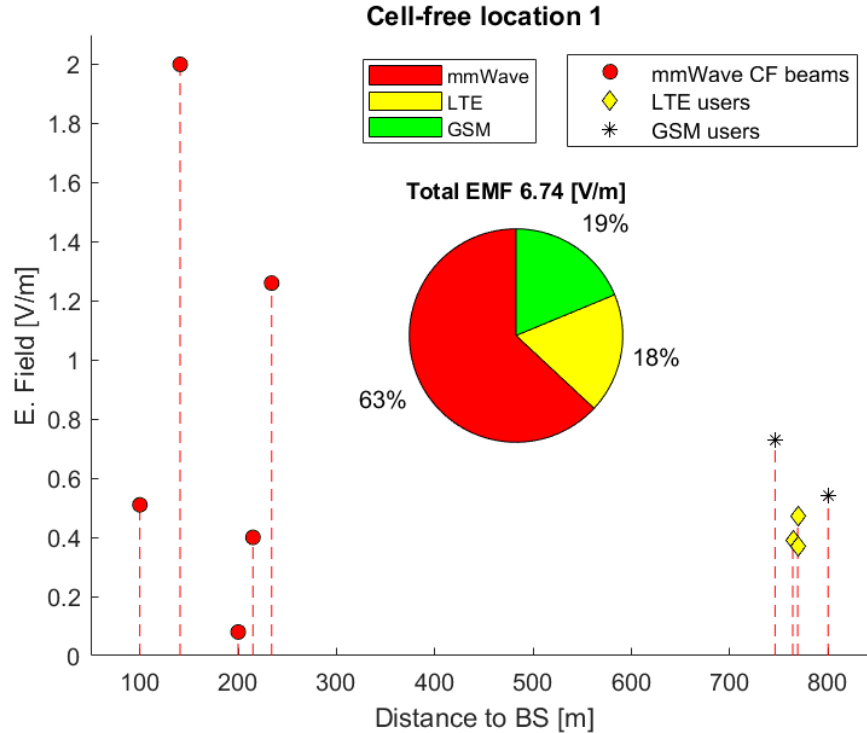


Figure 22. Cell-free MIMO study Location 1 E. field vs Distance.

As shown in Fig. 22 Beams coming from mmWave BSs are approximately 3.5 times closer to the user in comparison to users with other technologies from the network, with distances ranging between 100 - 234 meters for mmWave, and 746 – 800 meters for LTE and GSM.

When considering distance however, a higher frequency such as the one used in the mmWave configuration, is presented with a more challenging propagation environment than with lower frequency technologies such as GSM and LTE.

Some of the beam's E. field intensity can vary substantially even when having comparable distances such as the case for the beams between 200 and 234 meters shown in Fig. 22. This can be attributed to the difference in the specific propagation environments. On the other hand, EMF levels for LTE and GSM on this location are found to be relatively close to each other when compared to users with the same technology.

In this first scenario, most of the EMF exposure contribution belongs to mmWave with 63% of the total EMF as shown in Fig. 22, while the EMF level attribution for LTE and GSM are 18% and 19% respectively. The sum of the E. fields of all beams and access technologies have a total of 6,74 V/m, which is still lower than ICNIRP's reference levels for the general public [6].

4.3.2 Cell-free study location 2

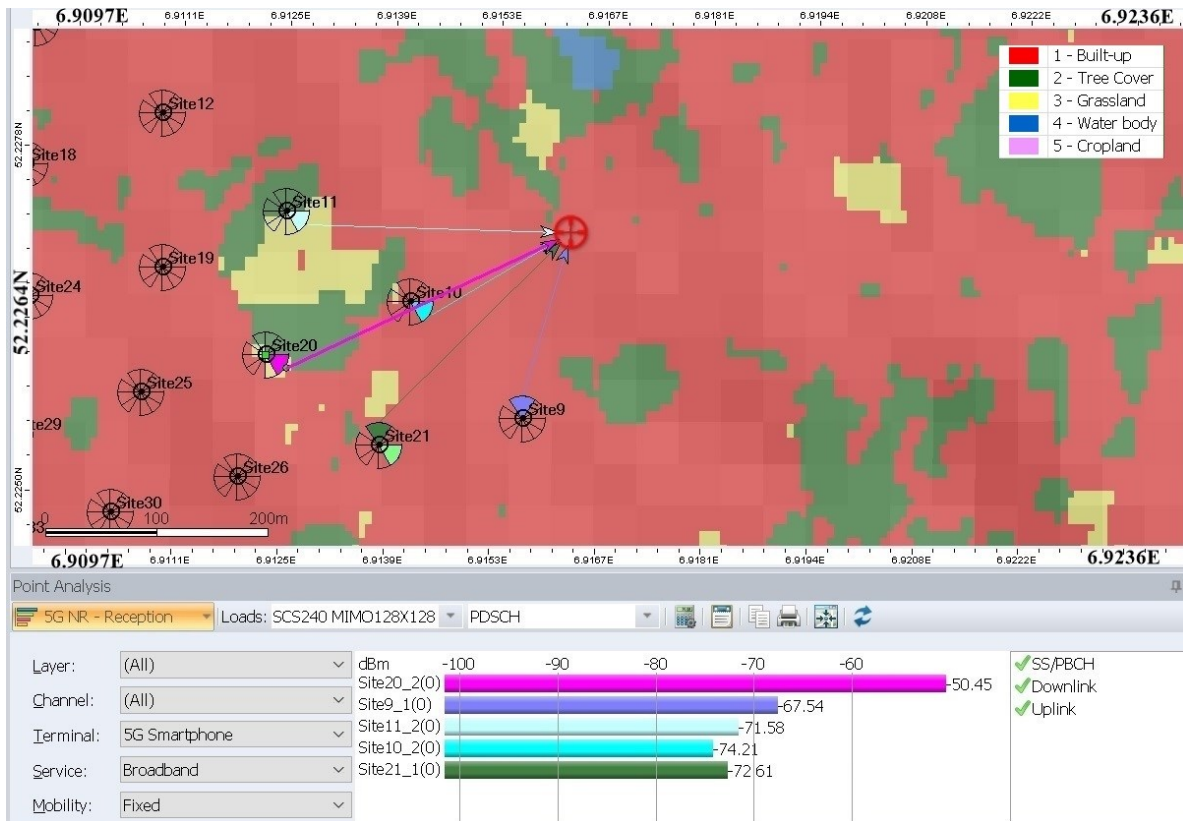


Figure 23. Cell-free Massive MIMO study Location 2.

Location	mmWave User Coordinates	SCS [kHz]	BS Antenna Configuration	TX Power [dBm]
2	6.91616565E 52.227287341N	240	128x128	40

Table 17. Location 2 mmWave Cell-free Massive MIMO configuration.

For location 2, Fig.23 shows the simulation for the mmWave User, represented by the red cross, where beams from different BSs meet in the location of this user. Table 17 shows the configurations and details relevant to this sub-section.

The simulations for the GSM and LTE users for this location can be found in Fig. 63 and Fig. 64 in Annex Q. Data related to simulations in the location considered by this sub-section are shown in Table 23 in Annex G.

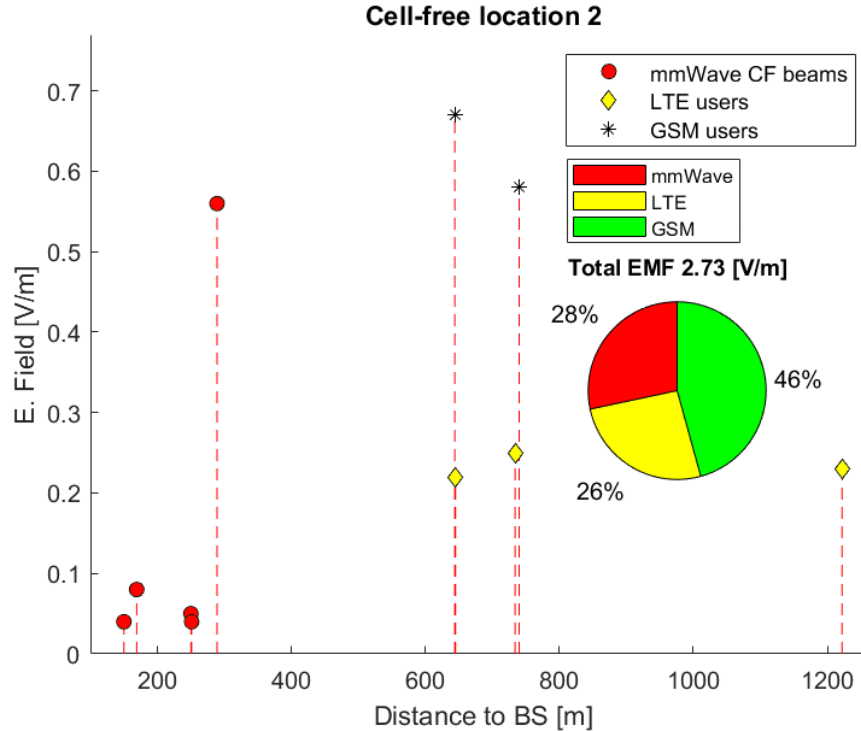


Figure 24. Cell-free Massive MIMO study Location 2 E. field vs Distance.

In location 2, E. fields registered by the mmWave user shown in Fig. 24 are in general lower when compared to levels registered in location 1 shown in Figure 22. This could be attributed to the variation in subcarrier spacing, higher beamforming capability from the increased number of antennas resulting in a lower assigned power to the mmWave user, or the specific propagation environment.

Unlike the first location, GSM users have the most contribution in this location with 46% of the total EMF, while the mmWave BSs from the Cell-free Massive MIMO and LTE represent 28% and 26% of the total EMF respectively.

In this location it can be appreciated that LTE users despite having very different separation distances from their serving BSs, such as 645 and 1222 meters, can present very similar E. field individual levels of 0,22 and 0,23 V/m.

Although the coordinate locations between location 1 in Figure 22 and location 2 in Figure 24 are not far different, LTE EMF levels display a noticeable difference in levels with 42% decrease in EMF level for the second location, while GSM EMF levels are maintained nearly the same.

The second location simulations for the Cell-free Massive MIMO network present a lower EMF exposure than the previous one, with a total EMF of 2,73 V/m, and it is still lower than ICNIRP limitations [6].

4.3.3 Cell-free study location 3

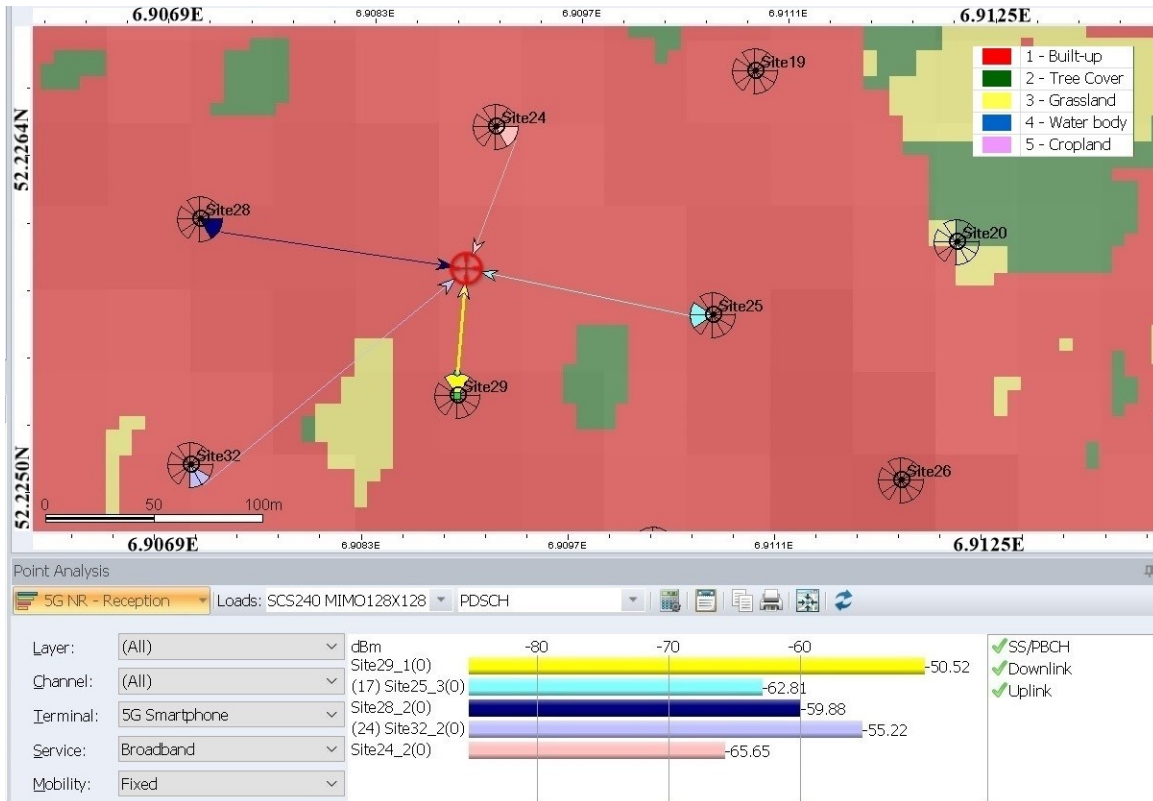


Figure 25. Cell-free study Location 3.

Location	mmWave User Coordinates	SCS [kHz]	BS Antenna Configuration	TX Power [dBm]
3	6.908992749E 52.225072443N	240	128x128	60

Table 18. Location 3 mmWave Cell-free Massive MIMO configuration.

In Figure 25, the simulation depicts the mmWave User's position, represented by the red cross. At this location, beams from various BSs converge towards the user. Table 18 shows the configurations applicable to this sub-section.

The simulations for GSM and LTE users in this specific location can be found in Fig. 65 and Fig. 66 in Annex Q. Furthermore, the detailed data corresponding to the simulations in this location is presented in Table 24 within Annex G.

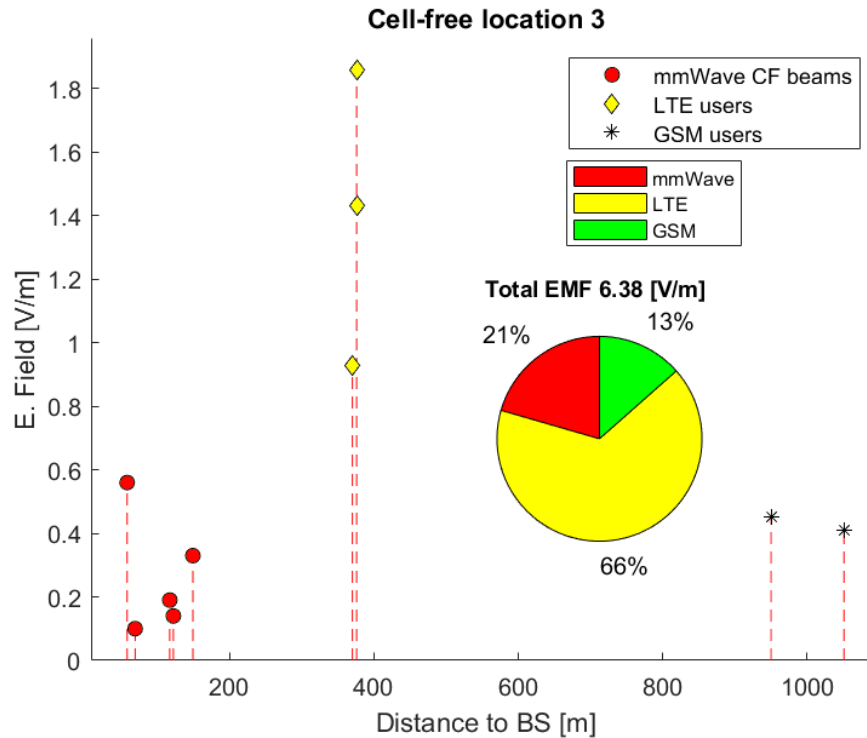


Figure 26. Cell-free Massive MIMO study Location 3 E. field vs Distance.

The beams shown in Figure 26 present similar E. field levels between 0,1 and 0,56 V/m, as well as comparable separation distances from the BSs of 58 - 149 meters. Two of the LTE users are being served by the same BS in this case, and one that is very close to it, which is shown by the aligned distances of 376 meters.

Unlike location 1 and location 2, the LTE users are closer to their serving BS in location 3, and are representing the higher EMF contribution to this study with 66%, while mmWave and GSM represent 21% and 13% respectively.

The total EMF is comparable to location 1, with 6,38 V/m, but there is no close relationship between them in terms of specific configurations for the mmWave Cell-free Massive MIMO BSs, location or separation distances to serving BSs.

The registered individual and total E. field levels for location 3 are also still below the ICNIRP limitations [6].

4.3.4 Cell-free study location 4

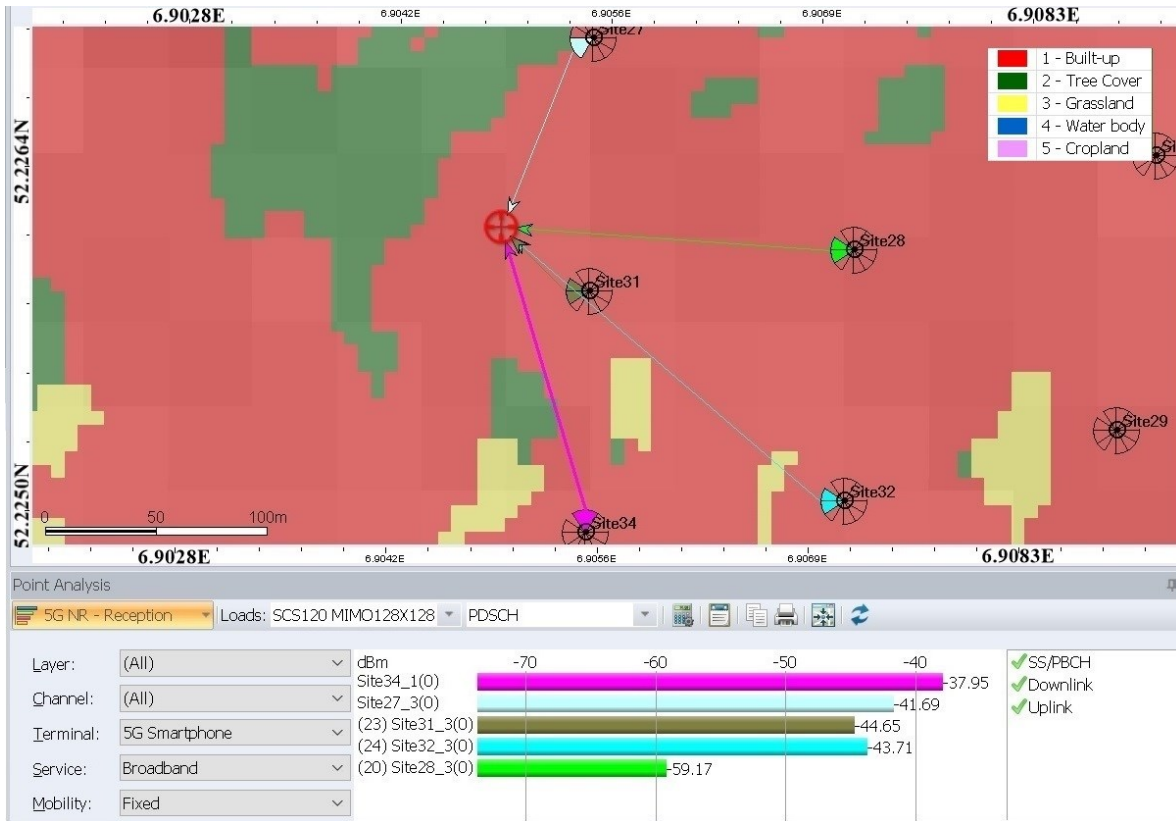


Figure 27. Cell-free study Location 4.

Location	mmWave User Coordinates	SCS [kHz]	BS Antenna Configuration	TX Power [dBm]
4	6.904865057E 52.226198992N	120	128x128	60

Table 19. Location 4 mmWave Cell-free Massive MIMO configuration.

Figure 27 illustrates the simulation of the mmWave User's position, depicted by the red cross. The relevant configurations for this sub-section are outlined in Table 19.

For GSM and LTE users in this specific location, their respective simulations can be found in Fig. 67 and Fig. 68 in the Annex Q. Additionally, detailed data related to the simulations in this location can be found in Table 25 within the Annex G.

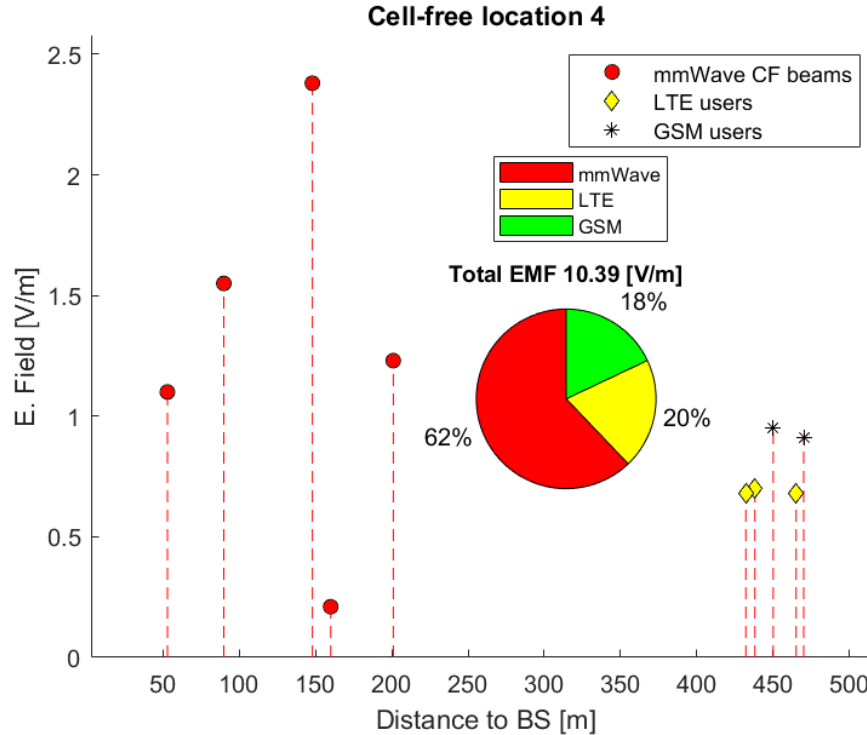


Figure 28. Cell-free Massive MIMO study Location 4 E. field vs Distance.

In Location 4 the mmWave beams shown in Fig. 28 from the Cell-free Massive MIMO BSs have E. field levels that are less equalized despite having comparable separation distances, but this is likely a result from specific propagations in the mmWave frequency band. On the other hand, E. field levels for LTE and GSM are again more equalized in terms of their levels despite having different serving BSs.

In this location it is the beams for the mmWave Cell-free Massive MIMO user which have the higher EMF contribution, with 62% while LTE and GSM add the 20% and 18% respectively. The higher EMF contribution for the mmWave user could be attributed to the parameter configuration of 120 kHz subcarrier spacing, the higher TX Power for this study or the specific propagation environment.

It can also be appreciated that even if one of the beams comes from a BS that is very close to the user, it still does not necessarily output the highest E. field contribution to the specific scenario.

The individual fields for each beam from the mmWave Cell-free Massive MIMO BSs range between 0,21 and 2,38 V/m while LTE and GSM levels range between 0,68 and 0,91 V/m, having an overall total of 10,39 V/m for this location. The individual and total EMF levels are also lower than the general public reference levels from ICNIRP [6] for location 4.

4.3.5 Cell-free study location 5

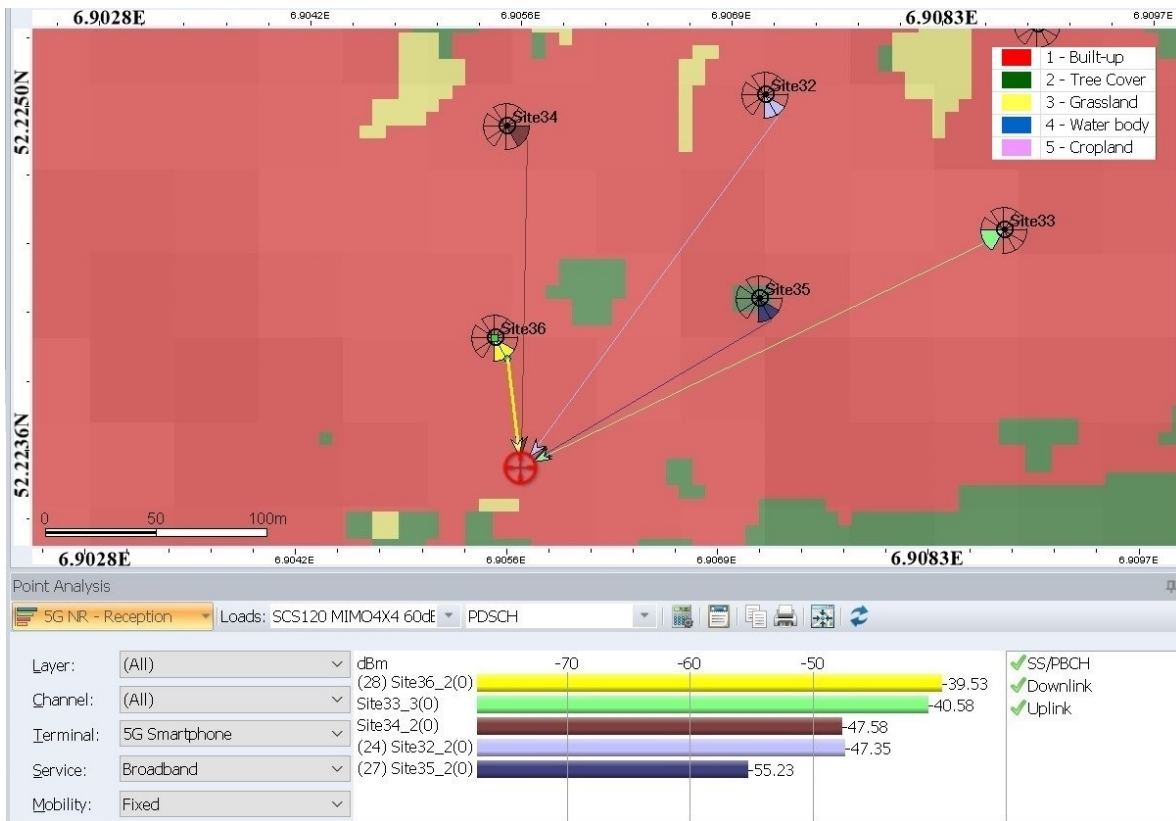


Figure 29. Cell-free MIMO study Location 5.

Location	mmWave User Coordinates	SCS [kHz]	BS Antenna Configuration	TX Power [dBm]
5	6.9056398E 52.223594875N	120	4x4	60

Table 20. Location 5 mmWave Cell-free MIMO configuration.

In Figure 29, the simulation depicts a red cross which is the position of the mmWave User. Configurations for this sub-section are provided in Table 20.

The simulations for GSM and LTE users in this specific location can be found in Fig. 69 and Fig. 70 in the Annex Q. Furthermore, detailed data related to the simulations in this location is presented in Table 26 within the Annex G.

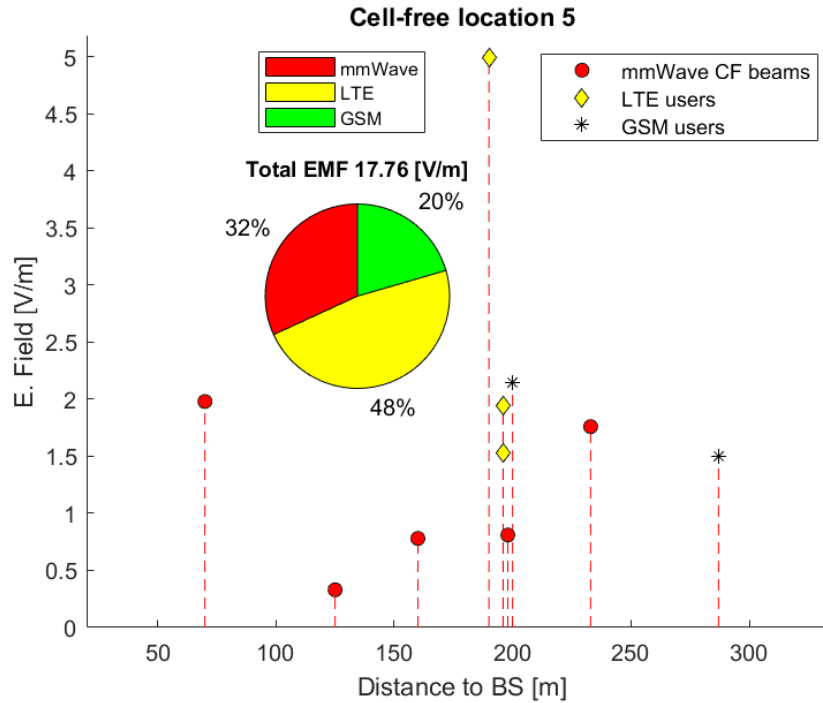


Figure 30. Cell-free MIMO study Location 5 E. field vs Distance.

In the results of location 5, shown in Figure 30, average distances to all the BSs for each technology are in general closer than in previous studies. Beams from the Cell-free MIMO BSs in location 5 present slightly more equalized E. field levels from each other, and are in general lower than the study in location 4. Unlike location 4, location 5 has a non-Massive MIMO BS Antenna configuration with 4x4 antennas. Location 5 also has a different Subcarrier spacing, which along the BS Antenna Configuration, could be influential factors on the lower E. field levels aside from the specific propagation conditions of location 5.

The most significant contribution in this study is from LTE with 48%, while mmWave and GSM add 32% and 20% respectively. In this case LTE receives a significant individual contribution from one of the signals that is significantly larger, possibly due to the fact that the separation distance is much smaller in comparison to any of the other LTE users in the previous studies. Individual and total EMF levels for this study are below the reference levels from ICNIRP [6].

It is worth noting that one of the main purposes of this section was to make a hypothetical scenario where many users are close to each other using different technologies to assess if the total E. field levels were still below regulation levels, and it is shown this is true for all the tested locations. On the other hand, levels within four of five cases would trigger the rule of thumb protocol by Agentschap Telecom. The so called rule of thumb simply involves conducting measurements only for 5 minutes, as long as the E. field level registered is below 5% of the relevant limitations given by ICNIRP guidelines. If an E. field level surpasses this threshold, the rule of thumb is to conduct measurements of 30 minutes. Agentschap Telecom reasoning behind this rule is to be capable of covering more measurement locations thanks to the spared time. However, measurements realized by Agentschap Telecom do not consider specific scenarios such as the ones shown in section 4.3, but as technologies evolve, new ways of assessments would be beneficial for the general public.

4.3.6 Overall Cell-free Massive MIMO assessment - Location 1 to 5

Next the mmWave beams are separated and compared in a grouped plot according to variations in the configurations from their BSs.

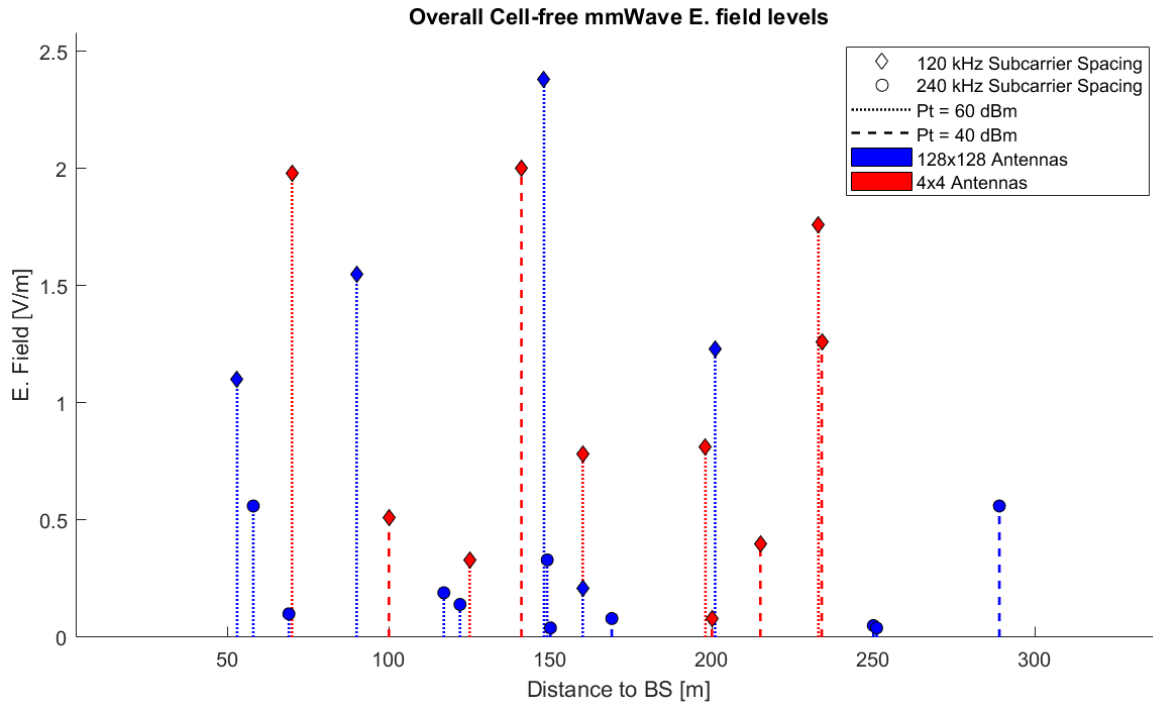


Figure 31. Overall Cell-free mmWave E. field levels.

The main purpose of section 4.3 was to evaluate the possible total EMF exposure values for a layout as the one in Figure 20. A direct comparison of the E. field levels in sub-section 4.3.6, due to configuration changes, for the mmWave user on all locations is not the most fair as the propagation environments are changing. However, some insights can be identified.

Figure 31 shows all the beams from all locations with all the various configurations represented on the plot. When comparing the mmWave beam E. field levels, it can be seen that most of the higher levels belong to configurations using 60 dBm as the TX power, and a subcarrier spacing 120 kHz subcarrier spacing. On average, all the beams from BSs using 240 kHz Subcarrier spacing in Fig. 31, represents 20% in EMF levels in relation to 120 kHz. Data used for these calculations can be found in Annex G.

Note that some of the E. fields corresponding to the 120 kHz subcarrier spacing configuration also exhibited low E. field levels. This is also the case for 60 dBm TX power configurations which is counter intuitive. However, as mentioned before, the locations related to beams shown in Fig. 31 are changing, and it can happen that a higher TX (Transmit) power configuration has less performance due to less favorable propagation conditions, leading to a lower E. field. This is particularly the case when operating in the mmWave frequencies, and subtle environment changes can lead to significant propagation conditions. A possible example of this phenomena could be seen in Fig. 32 from [39]. The red circle “A” has better propagation environment conditions when compared to the blue circle “D” which exhibits a higher BLER of 75%, hinting a lower E. field, despite being in close proximity to the BS, represented by the yellow star shape.

4.4.1 Dense Urban vs Urban CDF

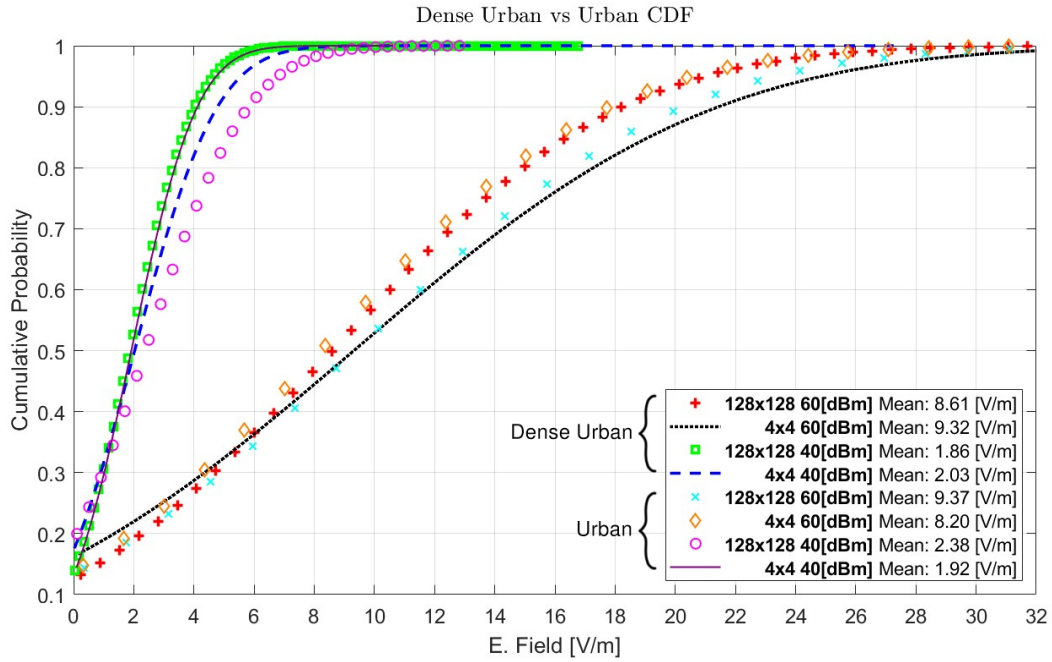


Figure 33. Dense Urban vs Urban Monte Carlo simulations' CDF.

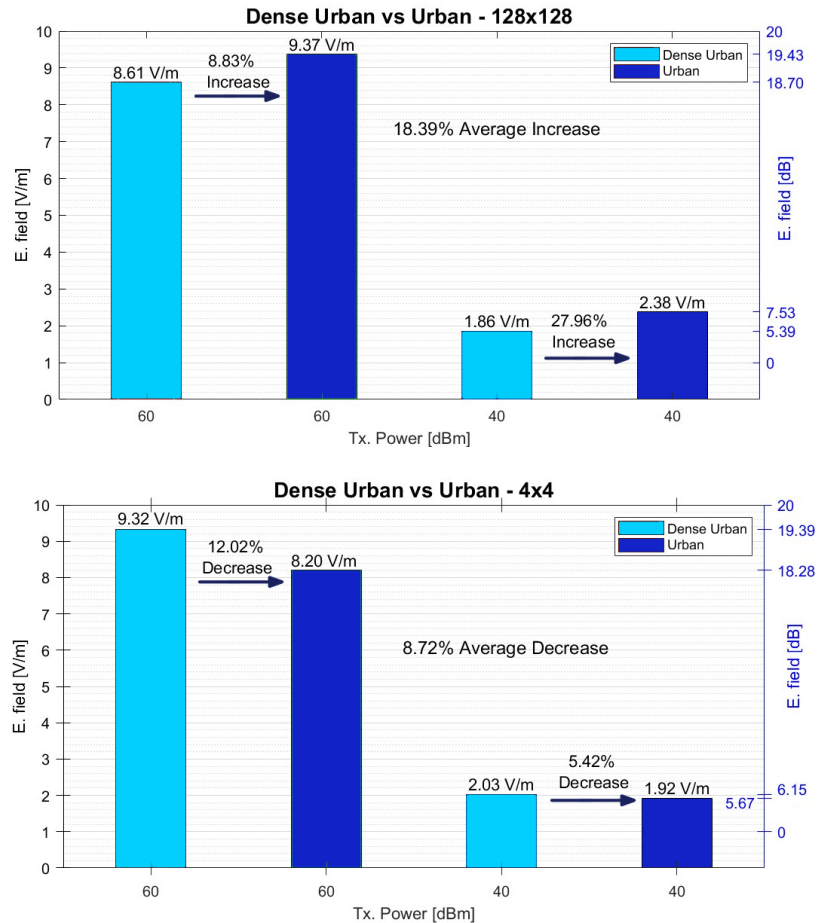


Figure 34. Dense Urban vs Urban Average Increased and decreased E. field levels.

Monte Carlo simulations were performed in this sub-section aimed to compare the Dense Urban and Urban conditions according to the simulation settings defined in Table 10. For all simulations shown in Fig. 33, the following configurations are used: 240 [kHz] SCS, 400 [MHz] Channel BW, and Topology 2.

In this combined study of E. fields shown in Figure 33 there is a clear distinction between the configuration using a maximum Transmit Power of 60 dBm in comparison to 40 dBm. From these simulations on average the difference in E. field level between the different TX Powers is approximately 7 V/m or an increase of 333% (12 dB) from using 40 to 60 dBm transmitters on the BSs.

The simulations depicted in Fig. 33 exhibit a mixed trend when comparing Dense Urban to Urban in relation to their BS Antenna Configuration. While using a 128x128 configuration there is an average increase in the E. fields of 18% (1.4 dB) from Dense Urban to Urban shown in Fig. 34. This could be related to the more efficient power allocation in the Dense Urban scenario due to the increased beamforming ability of a 128x128 configuration, or due to the fact that the network has to spread its power among more users on the Cell-free Massive MIMO network. It could also be related to the propagation scenario losing some diversity gain from the missing pathways of a broader beam that a lower antenna element configuration would give.

On the other hand, while using a 4x4 configuration there is a decrease in the E. field shown in Fig. 34 of 8,7% (-0,8 dB) on average from Dense Urban to Urban. This could be related to the decreased beamforming ability and having more power allocated on the Dense Urban scenario, or due to the less amount of users in the Urban scenario.

4.4.2 Topology 2 vs Topology 1 Simulations

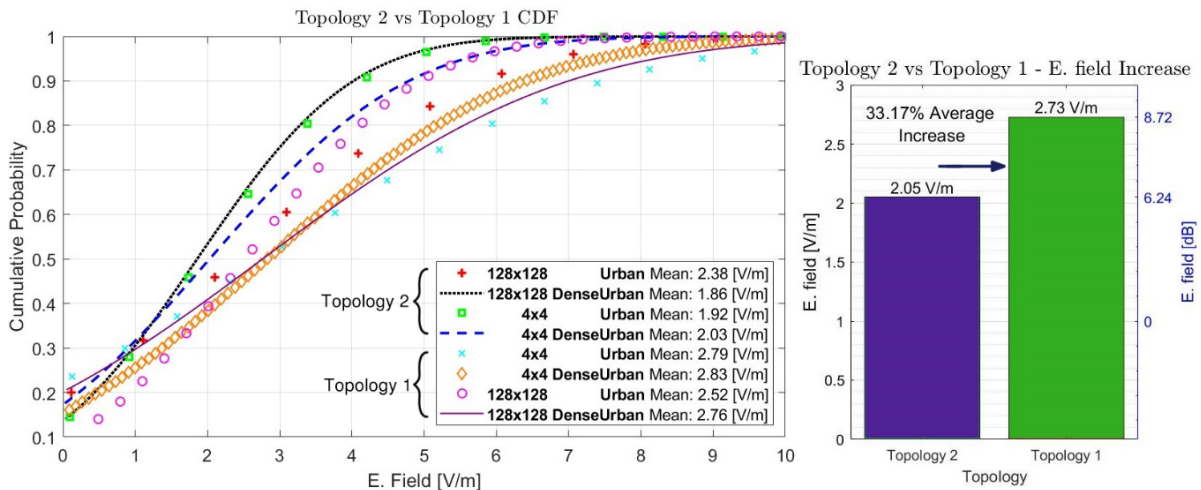


Figure 35. Topology 2 vs Topology 1 Monte Carlo simulations' CDF and E. field Increase.

Simulations were performed in this sub-section, which aim to compare “Topology 2” and “Topology 1”, corresponding to BSs’ layouts shown in Figure 8 and Figure 7. For all simulations shown in Fig. 35, the following configurations are used: 240 [kHz] Subcarrier spacing, 400 [MHz] Channel BW, and 40 [dBm] Tx Power.

This combined study shown in Fig. 35, the second subset of markers tend to have a higher E. field level due to the increased amount of BSs in Topology 1. This difference is noticeable but it is not as substantial as the difference observed due to the different transmit powers in the previous study shown in Figure 33. On average, the difference between

Topology 2 and Topology 1 is 0,68 V/m or an increase of 33% (2,5 dB) on Topology 1 which has more BSs.

Markers belonging to Topology 2 are mostly confined to each other, with the exception of the plus marker in Fig. 35. The mean value of the plus marker deviates the most from the overall Mean values present in the Topology 2 group in Fig. 35. Similarly, the circle marker presents the same behavior within its Topology 1 group. Aside from these exceptions, Mean values still align with the previously identified trend of increased E. field levels on Topology 1.

The trend identified in section 4.4.1 is repeated under Topology 2 when considering the BS Antenna Configuration and User Density. Using a 128x128 configuration results in an increased E. field from Dense Urban to the Urban scenario of 28% under Topology 2. Under Topology 1 there is a decrease of 9% from Dense Urban to Urban when using the 128x128 configuration which points to the increased number of BSs being a dominating factor in the higher E. field with a Dense Urban user distribution.

In this case using a 4x4 configuration results in a decreased E. field of 3,4% on average from Dense Urban to Urban on both Topologies. The analysis provided in 4.4.1 applies to this part of the study.

4.4.3 240 kHz vs 120 kHz Subcarrier spacing simulations - 40 dBm

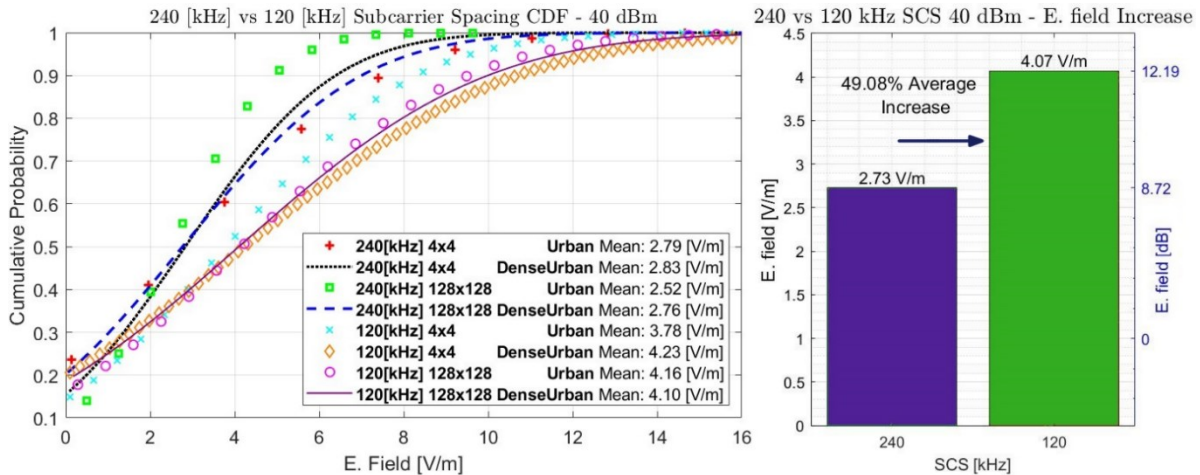


Figure 36. 240 kHz vs 120 kHz SCS - 40 dBm Monte Carlo simulations' CDF and E. field Increase.

In this sub-section, the Cell-free Massive MIMO network utilizes two distinct Sub-Carrier Spacing (SCS) configurations for each transmitter. These configurations include 240 kHz and 120 kHz SCS. For all simulations shown in Fig. 36, the following configurations are used: Topology 1, 400 [MHz] Channel BW, and 40 [dBm] Tx Power.

The difference between using a 240 and 120 kHz SCS configuration shown in Fig. 36 results in an increased E. field of 1,34 V/m or 49% (3 dB) by using 120 kHz and having a Tx Power of 40 dBm.

The trend identified in section 4.4.2 is repeated for this study when considering BS Antenna Configurations, user density and Topology. Using a 128x128 BS Antenna Configuration, results in a negligible E. field increase from Dense Urban to the Urban scenario when comparing the circled and solid lines in Fig. 36. A decrease of 8,7% in the E. field is present when comparing the squared and dashed line in Fig. 36. This repeats the trend found in section 4.4.2, where the increased amount of BSs from Topology 1 has a dominating factor in the increased E. field levels exhibited.

In this set of simulations using a 4x4 BS Antenna Configuration still results in a decreased E. field of 6,03% on average from Dense Urban to Urban. Aside from the increased amount of BSs exhibiting a dominating behavior, the analysis provided in 4.4.1 for the reasoning behind these observations also applies to this part of the study.

4.4.4 240 kHz vs 120 kHz Subcarrier spacing simulations – 60 dBm

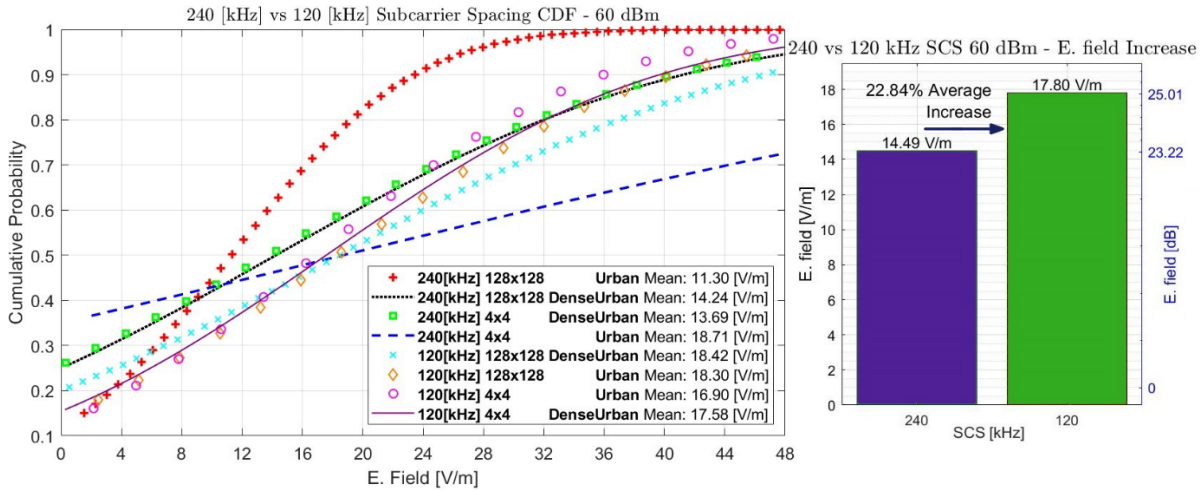


Figure 37. 240 kHz vs 120 kHz SCS - 60 dBm Monte Carlo simulations' CDF and E. field Increase.

This sub-section presents a second group of simulation configurations, incorporating a Tx Power of 60 dBm configuration with the 240 kHz and 120 kHz SCS settings. For all simulations shown in Fig. 37, the following configurations are used: Topology 1, 400 [MHz] Channel BW, and 60 [dBm] Tx Power.

In the simulations shown in Fig. 37, the same trend found in section 4.4.3 is repeated. Switching between the 240 and 120 kHz SCS configuration results in an increased E. field of 3,32 V/m or 23% (2 dB) by using 120 kHz and using a Tx Power of 60 dBm.

In the Monte Carlo simulation represented by the dashed blue line in Fig. 37, there is one outlier reading of 392 V/m that significantly affects the plot and Mean value. The E. field value corresponding to this exceptional reading is approximately 30 times larger than the Mean value of that simulation, which would be 12.88 V/m if the outlier were not present. However, the current display in Fig. 37 shows a Mean value of 18.71 V/m due to the presence of the exceptional reading. Due to the time-consuming nature of setting up specific configurations in the simulations, no re-runs were conducted once the data was plotted. The presence of an exceptionally high E. field value in comparison to the rest of the data from the same simulation suggests the possibility of a glitch. Additionally, the Mean value of the simulation represented by the dashed line in Fig. 37, without the exceptional reading, closely aligns with the other Mean values from the first group of four markers, which correspond to the 240 kHz SCS configuration.

The trend identified in section 4.4.2 is present for this study as well when considering the BS Antenna Configuration, User Density and Topology. Using a 128x128 BS Antenna Configuration results in a decrease of 10,82 % on average going from Dense Urban to Urban. This aligns with the trend in section 4.4.2 where the increased amount of BSs from Topology 1 has a dominating behavior in the increased E. field levels exhibited.

The utilization of a 4x4 BS Antenna Configuration on the BS maintains the same behavior as previous studies. This leads to an average decrease in the E. field of 15,35% from Dense Urban to Urban environments. The analysis discussion in 4.4.1 is relevant to this part of the study as well.

It is feasible for a smaller Subcarrier spacing to have a higher received power and hence a higher E. field. This is due to the higher spectral efficiency when packing subcarriers in a given channel bandwidth. Therefore, it is worth exploring the impact of the wider channel bandwidth from the previous studies of 400 MHz.

In some scenarios, a wider bandwidth can provide more frequency diversity and potentially improve frequency selectivity, aiding in mitigating the effects of frequency-selective fading caused by multipath propagation. This could explain the observed higher received power for the lower Subcarrier spacing, as the wider bandwidth enables better utilization of available frequency components or subcarriers. To further investigate this, a comparison study between different Channel bandwidths that are compatible with the frequency band n257 is carried out next.

4.4.5 400 MHz vs 100 MHz Channel Bandwidth simulation

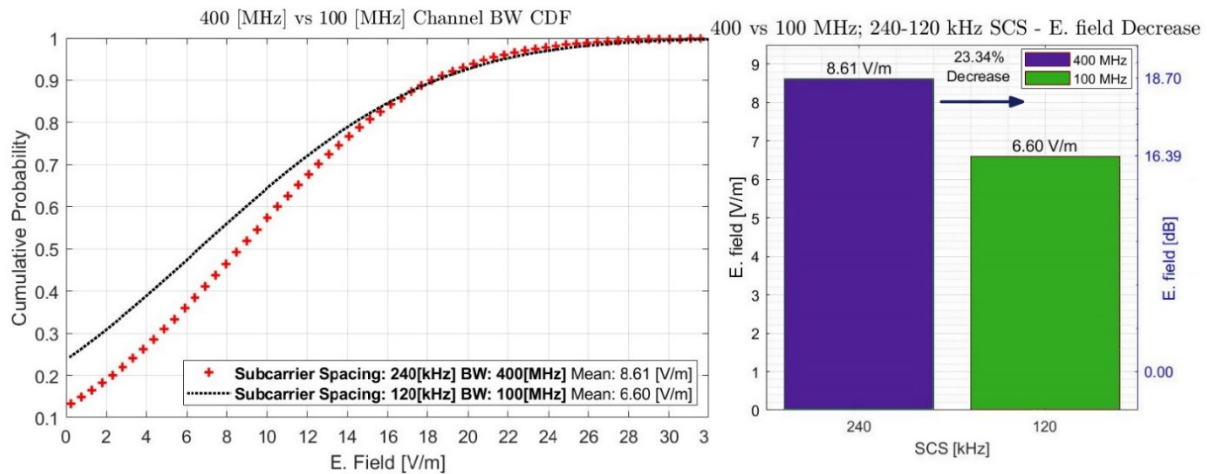


Figure 38. 400 vs 100 MHz Channel BW Monte Carlo simulations' CDF and E. field Decrease.

The purpose of this sub-section is to compare simulations involving different Channel Bandwidths, specifically 400 MHz and 100 MHz. For all simulations shown in Fig. 38, the following configurations are used: Topology 2, 128x128 BS Antenna Configuration, Dense Urban and 60 [dBm] Tx Power.

The results shown in Fig. 38 for this specific case, the utilization of a lower channel bandwidth has the effect of reducing the disparity between electric fields compared to previous studies that examined different subcarrier spacings. When employing a 240 kHz subcarrier spacing, it is observed that the E. field level increases by 2 V/m, representing a growth of 23% (2,3 dB). This suggests that a wider channel bandwidth could have potentially played a role in facilitating greater frequency diversity and improving the frequency selectivity of the system.

The observed higher E. field level with the 240 kHz subcarrier spacing signifies the potential benefits of employing a wider channel bandwidth, as it could provide additional frequency diversity and potentially enhance the frequency selectivity of the system.

This finding is significant, indicating that a 240 kHz Subcarrier spacing resulting in lower electric field readings has the requirement of having a sufficiently large channel bandwidth. The compatible channel bandwidth for the band n257 of 28 GHz that would achieve this is 400 MHz.

4.5 BLER and RSRQ Results

In order to ensure the quality of connection regardless of switching between the different configurations, BLER (Block Error Rate) reports are acknowledged throughout the simulations performed in previous studies.

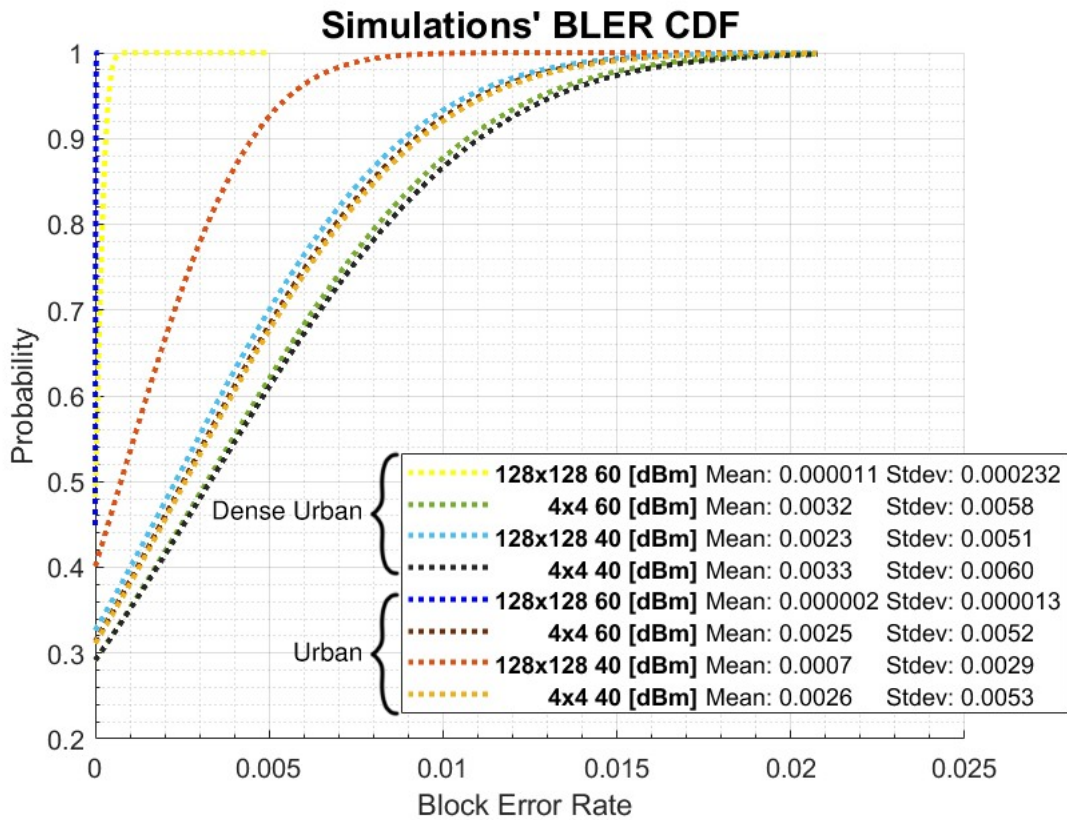


Figure 39. BLER CDF plots for 4.4.1.

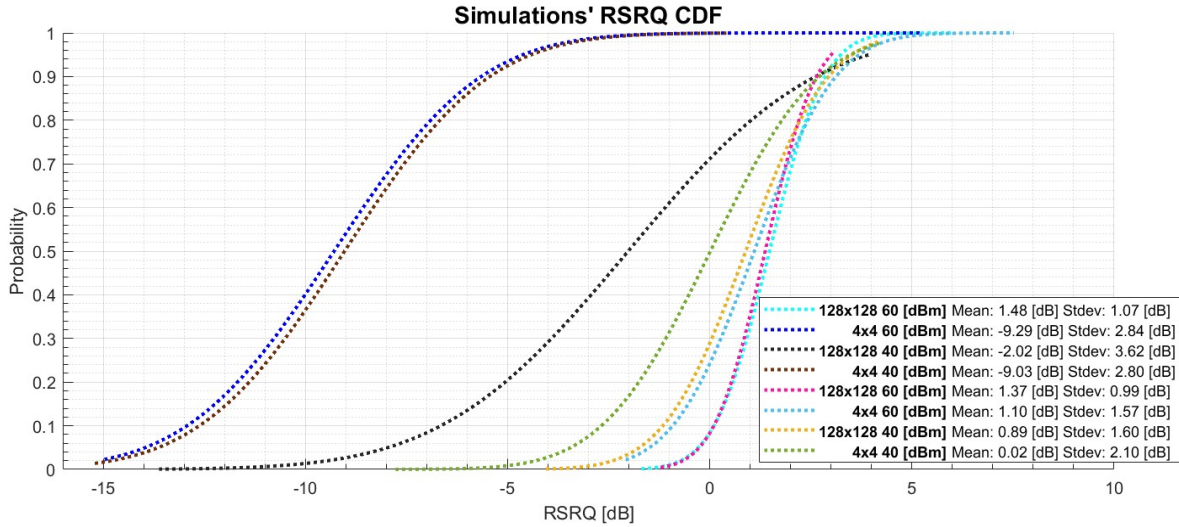


Figure 40. RSRQ CDF plots for 4.4.1.

All of the simulation results consistently exhibit a similar trend as the ones shown in Fig. 39 and Fig. 39, which represents the Cumulative Distribution Function for BLER. The CDF depicted in the figure corresponds specifically to configurations found in 4.4.1 and 4 simulations from 4.4.2.

In Fig. 39, the lowest BLER belongs to configurations with 60 dBm Tx Power and BS Antenna Configuration of 128x128. These individual plots can be found in Annex S. The CDF shown in Fig. 39 demonstrates that the higher probabilities primarily cluster below a BLER value of 0.01. This indicates that only 1% of the users may experience errors, which aligns with the desired optimal error rate for 5G transmissions. Furthermore, the RSRQ levels experienced by users sit in fair Mean levels of -9.29 dB on the least performing simulations in Fig. 40, belonging to 4x4 BS Antenna Configurations in Dense Urban scenarios as evidenced in Annex S. Most of the RSRQ levels in Fig. 40 show optimal Mean values around 1 dB. Moreover, the low standard deviation values suggest that the RSRQ levels are clustered closely together around the mean, indicating relatively uniform signal quality across the considered area. Monte Carlo simulations also provide statistical summaries, such as the one in Figure 80. This suggests other configurations applied to this network design will deliver optimal performance, successfully meeting the objective of maintaining good network conditions.

4.6 Throughput simulation results

Downlink prediction simulations were realized to get an overall perspective of the data rates that can be expected in the considered computational area. The configuration used in Fig. 41 is 120 kHz SCS, 40 dBm Tx Power, 400 MHz Channel BW under Topology 1. Note that user density is not considered by the simulator in this type of prediction, but Monte Carlo simulations have Throughput data reflecting the same prediction consistently.



Figure 41. User Throughput prediction in the mmWave portion of the network.

Most areas on Fig. 41 exhibit high data rate predictions, as indicated by the red and orange regions representing data rates above 800 Mbps. These levels are anticipated due to the presence of mmWave BSs in this specific network segment, which represents a hypothetical upgrade. It is important to note that the BS numbers might seem somewhat unrealistic for a city like Enschede, but which are more common in densely populated metropolitan cities.

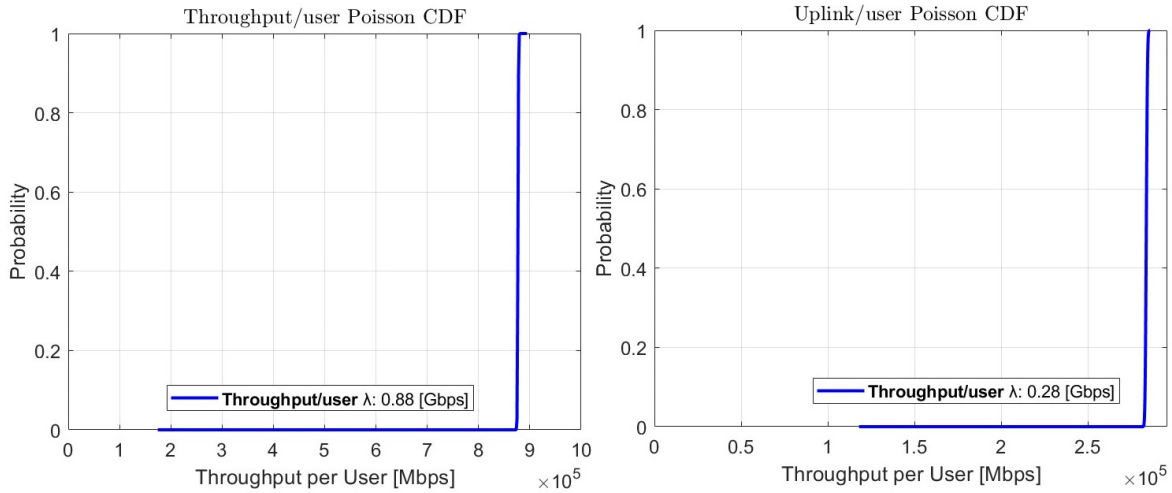


Figure 42. Downlink and Uplink Throughputs per User CDF.

In terms of the application throughput per user, the data rates shown in Fig. 42 consistently hover around the range of 0,8 to 0,9 Gbps in Downlink and above 0,28 Gbps in Uplink. This reflects the successful transmissions and high QoS (Quality of Service) achieved through the well-designed network configuration, as evidenced by the previous Block Error Rate study and the throughput simulations.

It is important to mention that the throughput prediction is based on the broadband service defined within the simulation software, with some of its settings outlined in Annex L. Additionally, a snapshot of user throughputs obtained from the simulation is provided in Annex H.

This particular service has high data rate demands, which explains why the majority of users exhibit elevated data rates, compared to the nominal values shown in Annex L, in both the Downlink and Uplink directions. As the maximum Uplink throughput for this service is defined with 300 Mbps, the Uplink simulation experiences relatively fewer variations as it represents a smaller portion of the demand within this network's design. This means that the network has less trouble allocating resources to satisfy a smaller UL demand of ~300 Mbps, as opposed as the DL demand of 950 Mbps, both defined in Annex L.

5 Conclusion Recommendations and Future Work

5.1 Conclusion

This thesis aimed to analyze the impact of various parameters on EMF exposure in a Cell-free Massive MIMO deployment in Enschede, considering existing GSM, 3G, 4G, and 5G technologies. The study assessed the influence of User Density, Base Station Quantity, BS Antenna Configuration, Channel Bandwidth, Subcarrier Spacing, and Transmit Power, while taking into account BLER and Throughput performance and ensuring compliance with EMF general public reference limits.

The results from section 4.2 indicate a prediction of a 215% (9 dB) increase in the E. field level for the area covered by the hypothetical mmWave Cell-free Massive MIMO added BSs. However, it is important to note that this increase remains well below the ICNIRP reference limitations for the general public. In a specific scenario involving a single user from the mmWave Cell-free Massive MIMO network surrounded by three LTE users and two GSM users, the EMF levels showed an increase but still stayed below the referential limits set by ICNIRP.

The studies also revealed higher E. field levels for a subcarrier spacing of 120 kHz, which is further simulated in section 4.4. Comparing the Tx powers from 40 to 60 dBm resulted in a 333% increase in the E. field. Additionally, comparing a co-located 4x4 MIMO configuration with a 128x128 Massive MIMO configuration showed differences depending on user density and the considered topology.

In the 128x128 configuration, there was an increase ranging between 18% and 28% from Dense Urban to Urban user density environments, considering the reduced number of BSs in Topology 2. However, the same 128x128 configuration showed a decrease in the E. field level ranging between 9% and 11% from Dense Urban to Urban environments, but this time under the Topology 1 conditions with more BSs.

The first effect, equivalent to a lower E. field level in a Dense Urban scenario compared to an Urban one under the reduced number of BSs in Topology 2, can be attributed to the increased beamforming ability of the 128x128 configuration in a Dense Urban environment or the need to distribute available power among more users. It could also be related to the loss of diversity gain in the propagation scenario due to the absence of broader beams that a lower antenna element configuration would provide.

The second effect, equivalent to a higher E. field level in the Dense Urban environment compared to the Urban one under Topology 1 conditions with more BSs, can be attributed to the dominating factor of the increased number of BSs, particularly evident in the Dense Urban conditions.

On the other hand, the 4x4 configuration consistently showed a decrease in the E. field level from Dense Urban to Urban ranging between 3% and 15%. This effect indicates a higher E. field level in the Dense Urban environment and a lower level in the Urban one. This behavior can be attributed to the reduced beamforming ability and less efficient power allocation in the Dense Urban environment, along with a smaller number of users in the Urban environment.

Comparing Topology 2 with fewer BSs to Topology 1, an average increase of 33% in the E. field level was observed. The results also revealed an increase ranging between 23% and 49% in the E. field level for subcarrier spacings from 240 kHz to 120 kHz. It is worth noting that this trend requires a sufficiently large channel bandwidth, such as 400 MHz, which is compatible with the considered n257 frequency band of 28 GHz.

The BLER values obtained from all simulations were below 0.01, indicating that only 1% of the users could experience errors. Additionally, the RSRQ levels exhibit Mean values close to 1 dB for most configurations, demonstrating the optimal performance of the network. The application throughput per user shows data rates mainly between 0,8 and 0,9 Gbps in Downlink and 0,28 Gbps in Uplink for the most demanding service simulated. These results suggest that the network achieves optimal quality of service based on the BLER, RSRQ, and throughput outcomes. The results of the conducted studies also complied with the reference E. field levels set by ICNIRP for the general public [6]. Results are summarized in Table 21.

Section	Considered change or parameters	Additional context	EMF Impact
4.2	Introduction of a significant amount of mmWave Cell-free Massive MIMO BSs in Enschede	Legacy Technologies vs mmWave Cell-free Massive MIMO 5G NR	215% (9 dB) increase
4.2, 4.3	Sub-Carrier Spacing	240 kHz vs 120 kHz	Preliminary identification of EMF increase for the 120 kHz SCS
4.4.3		240 kHz vs 120 kHz	49% (3 dB) EMF Increase for 240 kHz SCS – 40 dBm TX Power
4.4.4		240 kHz vs 120 kHz	23% (2 dB) EMF Increase for 240 kHz SCS – 60 dBm TX Power
4.2,4.3	Transmit Power	40 dBm vs 60 dBm	Observable EMF increase for 60 dBm, but not applicable on every instance.
			333% (12 dB) EMF Increase from 40 to 60 dBm
4.4.1	User Density	Dense Urban vs Urban	In general, more EMF on Dense Urban, but conditional in relation to BS Antenna Configuration
	BS Antenna Configuration	128x128	EMF Increase of 18% (1,4 dB) in the Dense Urban scenario.
		4x4	EMF Decrease of 9% (-0,8 dB) in the Urban scenario.
4.4.2	BS Quantity	Topology 2 vs Topology 1	EMF Increase of 33% (2,5 dB)
4.4.5	Channel BW	400 [MHz] vs 100 [MHz]	23% (2,3 dB) EMF Decrease while switching between 120 kHz and 240 kHz SCS

Table 21. Summary of the EMF findings in relation to the considered parameters.

5.2 Recommendations

Considering the normalized EMF exposure reports in section 4.2, this thesis indicates that measurements following Agentschap protocols would generally stay below ICNIRP reference levels. Even with the addition of numerous mmWave antennas, EMF levels are expected to remain below the general public reference limits. There is a substantial difference between ICNIRP's reference limit of 61,4 V/m to overall measurements that range from 0,3 to 1,48 V/m belonging to the former mobile network in Enschede. With a substantial amount of additional mmWave antennas introduced, measurements are projected to still be much lower than ICNIRP's reference limits, shown in sections 4.2, 4.3 and 4.4. This prediction would mean that Agentschap would likely continue using its resources to measure low levels in the regular cases for years to come.

Electric fields from section 4.3 showed higher levels than the ones shown in 4.2, which are still below ICNIRP's reference levels. Section 4.2 presents results derived from the simulation software's EMF exposure tool in the context of both the former network and the upgraded network, encompassing various configurations such as BS Quantity (Topologies 1 and 2), 120 - 240 kHz SCS, and Transmit Power. In contrast, Section 4.3 uses the same parameters, including the additional consideration of BS Antenna Configuration, focusing on a specific assumed scenario that primarily contributes to the EMF disparities between Sections 4.2 and 4.3. Nonetheless, there is the possibility of even more specific scenarios that might lead to higher exposure levels beyond those presented in this thesis.

In countries like Italy, places such as parks and sport fields where children are usually present, adhere to more strict EMF limits. Considering the implementation of similar precautionary measures in The Netherlands may be beneficial as well. The Health Council from The Netherlands advised to conduct further research before commissioning mmWaves [11]. For this reason, local entities such as Agentschap Telecom could contemplate introducing additional measuring protocols that take into account more considerations.

5.3 Future work

The use of mmWave technology alone does not necessarily result in an exponential increase in the Electric field. However, under certain scenarios within a Cell-free Massive MIMO scheme, there can be instances where E. field levels are heightened.

In addition, if we were to address the concerns raised by the BioInitiative group, the intensity of the E. field and thermal effects would not be the sole determining factors for safety. Factors such as modulation and long-term exposures would also need to be taken into consideration.

Optimizing system parameters to minimize exposure and maximize throughput for the cellular networks remains a path to explore.

This research focuses on the received E. fields from BSs, but it does not account for the fields emitted by the User Equipment itself. With the increase of data usage in next generation of communication, the UL exposure is also an important factor, due to the extreme short distance between human and devices. This aspect could be explored in future work. If the ICNIRP guidelines continue to dominate and remain unchanged, it is essential to consider the combined effect of exposure resulting from both the UE and BS. This is particularly crucial if the levels indicated in section 1.2.2 are in proximity to the actual EMF exposure levels originating from mmWave UE devices, as these devices are intended for use in close proximity to the user.

References

[1] “Exposure limits for radio-frequency fields (public) Data by country,” 2017. Available: <https://apps.who.int/gho/data/view.main.EMFLIMITSPUBCRADIOFREQUENCYv>

[2] Ts. Shalamanova et al., “Results of Measurements of Electromagnetic Fields around Base Stations for Mobile Communication in Bulgaria,” in Proc. 9th Nat. Conf. Biomedical Physics and Engineering, Bulgaria, 2004, pp. 129 – 134.

[3] M. Ivanova, Ts. Shalamanova, “Measurements of RF radiation around base stations for mobile communication in Bulgaria,” J. Environ. Prot. Ecol., vol. 6, no. 2, pp. 328 – 336, Jan. 2005.

[4] “Ordinance No. 9 from 14.03.1991 on the limit values of electromagnetic fields in populated areas and the determination of hygienic-protective zones around radiating objects.,” 1991. Available:

<https://econ.bg/Нормативни-актове/Наредба-9-от-14-03-1991-г-за-предельно-допустими-нивана-електромагнитни-полета-в-населени- 1.1 i.128561 at.5.html>

[5] “ICNIRP GUIDELINES FOR LIMITING EXPOSURE TO TIME-VARYING ELECTRIC, MAGNETIC AND ELECTROMAGNETIC FIELDS (UP TO 300 GHZ),” 1998. Available:

<https://www.icnirp.org/cms/upload/publications/ICNIRPemfgdl.pdf>

[6] “ICNIRP GUIDELINES FOR LIMITING EXPOSURE TO ELECTROMAGNETIC FIELDS (100 KHZ TO 300 GHZ),” 2020. Available:

<https://www.icnirp.org/cms/upload/publications/ICNIRPrfgdl2020.pdf>

[7] “BioInitiative: A Rationale for Biologically-based Exposure Standards for Low-Intensity Electromagnetic Radiation,” 2023. Available:

<https://bioinitiative.org/table-of-contents/>

[8] “Literature on Neurological Effects of Radiofrequency Radiation (2007-2022),” 2022. Available:

<https://bioinitiative.org/wp-content/uploads/2022/06/RFR-Neurological-Effects-Abstracts-2022.pdf>

[9] “BioInitiative reports conclusions: Defining a new ‘Effect Level’ for RFR,” 2023. Available:

<https://bioinitiative.org/conclusions/>

[10] “Achtergronddocument advies 5G en gezondheid,” 2020. Available:

<https://www.gezondheidsraad.nl/binaries/gezondheidsraad/documenten/adviezen/2020/09/02/5g-en-gezondheid/Achtergronddocument-advies-5G-en-gezondheid.pdf>

[11] “Kernadvies 5G en gezondheid,” 2020. Available:

<https://www.gezondheidsraad.nl/binaries/gezondheidsraad/documenten/adviezen/2020/09/02/5g-en-gezondheid/Advies-5G-en-gezondheid.pdf>

- [12] "Meetprotocol EMV," 2021. Available: <https://www.rdi.nl/binaries/agentschap-telecom/documenten/publicaties/2020/11/meerjarenplan-emv-en-meetprotocol/meerjarenplan-emv-en-meetprotocol/Meetprotocol+EMV.pdf>
- [13] "Ray-Tracing Simulation & Propagation Methods," 2023. Available: <https://www.remcom.com/electromagnetic-simulation-numerical-methods/ray-tracing-simulation-methods>
- [14] "Ray Tracing for Wireless Communications," 2023. Available: <https://www.mathworks.com/help/comm/ug/ray-tracing-for-wireless-communications.html>
- [15] S. Dhalbisoi, A. Rout, R. K. Sahoo and S. Sethi, "A Comparative Analysis On 5G Cell Free Massive Mimo In Next Generation Networking Environment," 2022 International Conference on Intelligent Controller and Computing for Smart Power (ICICCSP), Hyderabad, India, 2022, pp. 1-5, doi: 10.1109/ICICCSP53532.2022.9862350.
- [16] K. Zhao, Z. Ying and S. He, "EMF Exposure Study Concerning mmWave Phased Array in Mobile Devices for 5G Communication," in IEEE Antennas and Wireless Propagation Letters, vol. 15, pp. 1132-1135, 2016, doi: 10.1109/LAWP.2015.2496229.
- [17] S. Q. Wali, A. Sali, J. K. Allami and A. F. Osman, "RF-EMF Exposure Measurement for 5G Over Mm-Wave Base Station With MIMO Antenna," in IEEE Access, vol. 10, pp. 9048-9058, 2022, doi: 10.1109/ACCESS.2022.3143805.
- [18] S. Liu et al., "E-Field Strength Measurements of a 5G Base Station in 28 GHz Band for EMF Exposure Assessment," 2021 IEEE USNC-URSI Radio Science Meeting (Joint with AP-S Symposium), Singapore, Singapore, 2021, pp. 49-50, doi: 10.23919/USNC-URSI51813.2021.9703567.
- [19] L. Chiaraviglio et al., "EMF Exposure in 5G Standalone mm-Wave Deployments: What Is the Impact of Downlink Traffic?," in IEEE Open Journal of the Communications Society, vol. 3, pp. 1445-1465, 2022, doi: 10.1109/OJCOMS.2022.3200423.
- [20] L. Chiaraviglio et al., "Planning 5G Networks Under EMF Constraints: State of the Art and Vision," in IEEE Access, vol. 6, pp. 51021-51037, 2018, doi: 10.1109/ACCESS.2018.2868347.
- [21] "Antenneregister," 2023. Available: https://www.Antenneregister.nl/Html5Viewer/Index.html?viewer=Antenneregister_extern
- [22] "Study on channel model for frequencies from 0.5 to 100 GHz," 2017. Available: <https://portal.3gpp.org/desktopmodules/Specifications/SpecificationDetails.aspx?specificationId=3173>
- [23] "5G Link Budget," 2021. Available: <https://www.telecomhall.net/t/5g-link-budget/12264>
- [24] S. Kusmariyanto, D. Fadilla, F. H. Partiansyah, G. Asmungi and W. A. Priyono, "5G NR Network Planning in Malang City East Java Using Atoll Software," 2022 11th Electrical Power, Electronics, Communications, Controls and Informatics Seminar (EECCIS), Malang, Indonesia, 2022, pp. 191-196, doi: 10.1109/EECCIS54468.2022.9902947.

- [25] S. Rahmatia, A. A. Azzahra, M. Ismail, O. N. Samijayani and D. Astharini, "Long Term Evolution (LTE) Network Design Frequency Division Duplex (FDD) of 1800 MHz Based on Subscriber Growth Forecasting in 2025 at Denpasar, Indonesia," 2018 IEEE 5th International Conference on Engineering Technologies and Applied Sciences (ICETAS), Bangkok, Thailand, 2018, pp. 1-6, doi: 10.1109/ICETAS.2018.8629164.
- [26] J. Zhang, L. Xu, R. Zhang, W. He and Y. Wang, "Atoll-based Propagation Model Correction and Actual Measurement," 2019 IEEE 4th Advanced Information Technology, Electronic and Automation Control Conference (IAEAC), Chengdu, China, 2019, pp. 662-666, doi: 10.1109/IAEAC47372.2019.8997802.
- [27] "3GPP TSG RAN WG1 #101," 2023. Available: https://www.3gpp.org/ftp/tsg_ran/WG1_RL1/TSGR1_101-e/Inbox/drafts/8.4.1%20Baseline%20coverage%20performance/R1-20xxxxx%20-%20%5B101-e-NR-Cov-Enh%5D-updated%20-%20v024_SONY_VZ.docx
- [28] Forsk, "EMF Exposure," Atoll Documentation, Version 3.4.0, Blagnac, France, 2020.
- [29] "Distance on a sphere: The Haversine Formula," 2022. Available: [https://community.esri.com/t5/coordinate-reference-systems-blog/distance-on-a-sphere-the-haversine-formula/ba-p/902128#:~:text=For%20example%2C%20haversine\(%CE%B8\),longitude%20of%20the%20two%20points.](https://community.esri.com/t5/coordinate-reference-systems-blog/distance-on-a-sphere-the-haversine-formula/ba-p/902128#:~:text=For%20example%2C%20haversine(%CE%B8),longitude%20of%20the%20two%20points.)
- [30] He, Qing & Yang, Wan & Hu, Yan. (2014). Accurate method to estimate EM radiation from a GSM base station. Progress In Electromagnetics Research M. 34. 19-27. 10.2528/PIERM13091301.
- [31] "Received Field Intensity and Power Density Calculation," 2023. Available: <https://www.ahsystems.com/EMC-formulas-equations/power-density.php>
- [32] "Clutter Zones: World Cover V2," 2021. Available: https://viewer.esa-worldcover.org/worldcover/?language=en&bbox=139.67920809523235,35.65265658283407,139.792680525461,35.69651336074148&overlay=false&bgLayer=OSM&date=2023-06-29&layer=WORLDCOVER_2021_MAP
- [33] "USGS Earth Explorer," 2023. Available: <http://earthexplorer.usgs.gov/>
- [34] "5G mmWave is alive and well in Tokyo Japan ," 2023. Available: <https://assets.qualcomm.com/SRG-5G-mmWave-Performance-JP.html>
- [35] "FCC 16-89," 2016. Available: <https://docs.fcc.gov/public/attachments/FCC-16-89A1.pdf>
- [36] "5G NR: Synchronization Signal/PBCH block (SSB)," 2022. Available: <https://howltestuffworks.blogspot.com/2019/10/5g-nr-synchronization-signalpbch-block.html>
- [37] Hata, M., "Empirical Formula for Propagation Loss in Land Mobile Radio Service" IEEE Trans. on Vehicular Technology, vol. VT-29, no. 3, August 1980, pp. 317-325.

[38] COST 231 TD(90) 73, "Digital mobile radio towards future generation systems: Final Report," European Commission, Directorate-General for the Information Society and Media, 1991.

[39] W. Roh et al., "Millimeter-wave beamforming as an enabling technology for 5G cellular communications: theoretical feasibility and prototype results," in *IEEE Communications Magazine*, vol. 52, no. 2, pp. 106-113, February 2014, doi: 10.1109/MCOM.2014.6736750.

Annexes

Annex A: Agentschap Telecom sample measurement

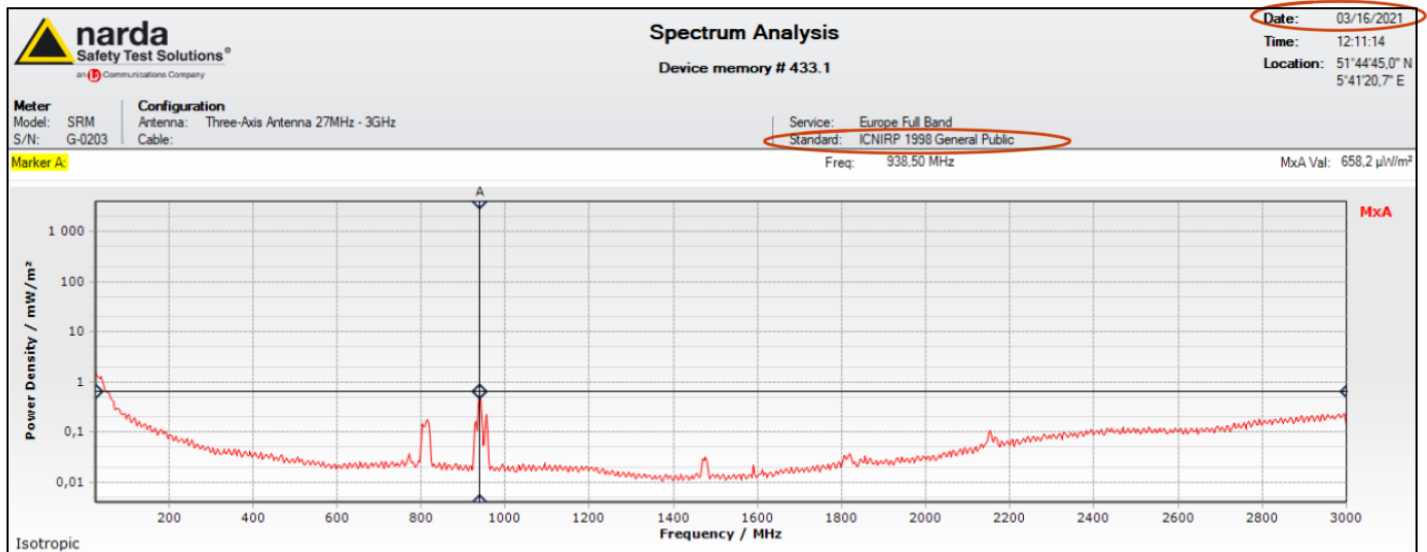


Figure 43. E. field measurement from the latest released measurement reports using the older guidelines.

Annex B: mmWave Antenna Pattern and beamforming pattern

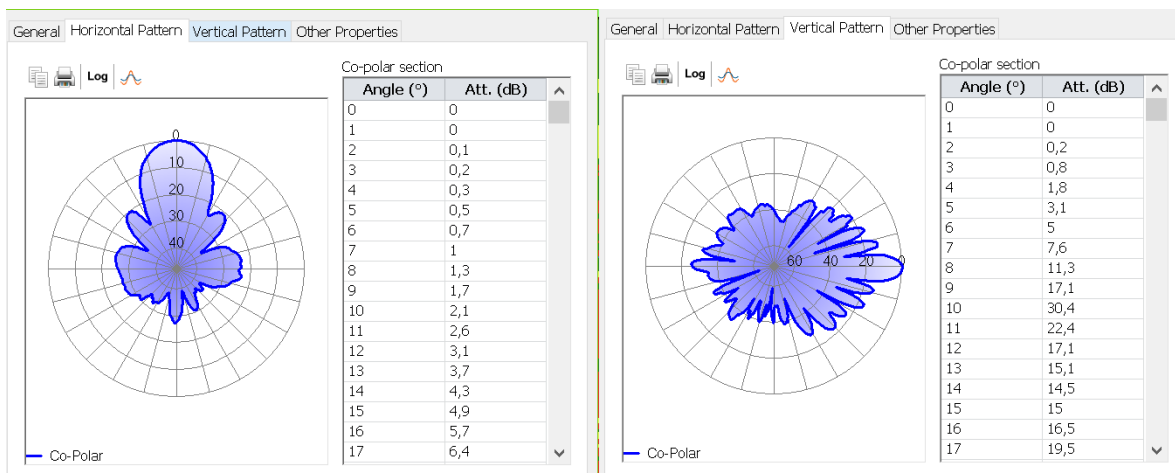
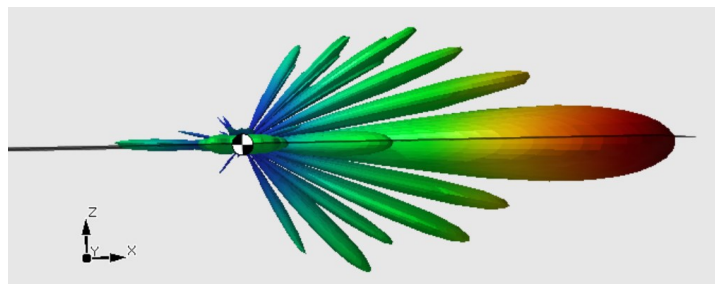


Figure 44. mmWave Antenna beam pattern.

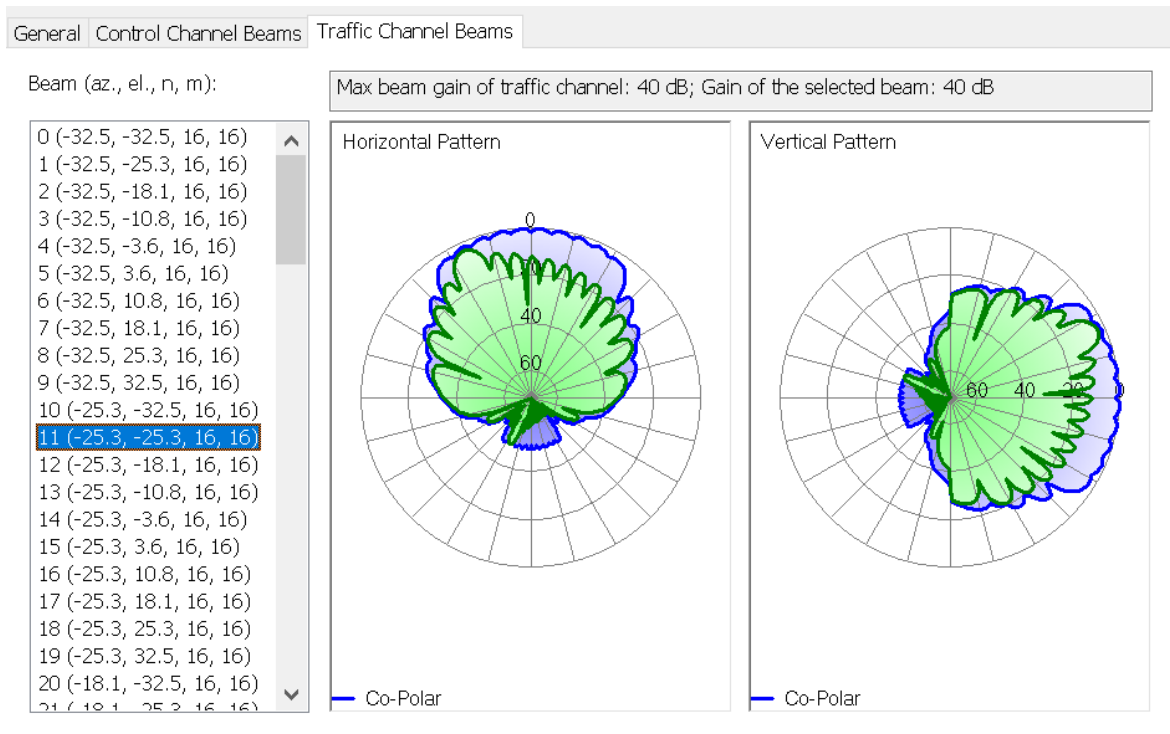


Figure 45. Beamforming patterns.

Annex C: Electric field equation 1 derivation

$$E \left[\frac{dB\mu V}{m} \right] = V[dB\mu V] + AF \left[\frac{dB}{m} \right]$$

$$20 \log \left(E \left[\frac{\mu V}{m} \right] \right) = P_r[dBm] + 107 + AF \left[\frac{dB}{m} \right]$$

$$20 \log(E) = P_r + 20 \log \left(\frac{1}{\sqrt{20}} \right) + AF$$

$$20 \log \left(\frac{E}{\frac{1}{\sqrt{20}}} \right) = P_r + AF$$

$$E = \frac{1}{\sqrt{20}} * 10^{\frac{P_r + AF}{20}}$$

Annex D: Electric field equation 2 derivation

From the Friis Transmission formula:

$$P_r = P_t * G_t * G_r * \left(\frac{\lambda}{4 * \pi * d} \right)^2$$

$$P_r = P_t * G_t * G_r * \left(\frac{c/f}{4 * \pi * d} \right)^2$$

$$Pr = Pt * Gt * Gr * \left(\frac{c}{16 * \pi^2 * d^2 * f^2} \right)^2$$

Expressing (Pr) in terms of the electric field strength (E) using the equation $Pr = (E_{field}^2 * Z_0) / 2$, where Z_0 is the characteristic impedance:

$$(E_{field}^2 * Z_0) / 2 = Pt * Gt * Gr * (c^2 / (16 * \pi^2 * d^2 * f^2))$$

Solving for E:

$$E_{field}^2 = (2 * Pt * Gt * Gr * (c^2 / (16 * \pi^2 * d^2 * f^2))) / Z_0$$

$$E_{field}^2 = (Pt * Gt * Gr * c^2) / (16 * \pi^2 * d^2 * f^2 * Z_0)$$

$$E_{field} = \sqrt{\frac{(Pt * Gt * Gr * c^2)}{16 * \pi^2 * d^2 * f^2 * Z_0}}$$

substituting $c = 3 * 10^8$ m/s and $Z_0 = 377$ ohms:

$$E_{field} = \sqrt{\frac{(30 * 10^{-3} * Pt * Gt * Gr)}{4 * \pi^2 * d^2 * f^2}}$$

From Friis transmission formula solving for Gr:

$$G_r = d^2 \left(\frac{3 * 10^8}{f} \right)^2 \left(\frac{P_r}{P_t * G_t} \right)$$

$$E_{field} = \sqrt{\frac{\left(30 * 10^{-3} * Pt * Gt * \left(d^2 \left(\frac{3 * 10^8}{f} \right)^2 \left(\frac{P_r}{P_t * G_t} \right) \right) \right)}{4 * \pi^2 * R^2 * f^2}}$$

$$E_{field} = \sqrt{\left(\left(30 * 10^{-3} * 10^{\frac{P_r}{10}} \right) * \left(\frac{3 * 10^8}{(4 * \pi * d * f)} \right) * (4 * \pi * d)^2 / G_t \right)}$$

Annex E: MatLab scripts calculating Electric fields

1. pdsch_array1=table2array(PDSCH1);
2. pdsch_array2=table2array(PDSCH2);
3. pdsch_array3=table2array(PDSCH3);
4. pdsch_array4=table2array(PDSCH4);
- 5.
6. figure
7. legend_strings = {};
- 8.
9. myArray_1 = pdsch_array1;
10. meanVal1 = mean(myArray_1);
11. stdVal1 = std(myArray_1);

```
12. myArray_2 = pdsch_array2;
13. meanVal2 = round(mean(myArray_2),2);
14. stdVal2 = std(myArray_2);
15. myArray_3 = pdsch_array3;
16. meanVal3 = mean(myArray_3);
17. stdVal3 = std(myArray_3);
18. myArray_4 = pdsch_array4;
19. meanVal4 = mean(myArray_4);
20. stdVal4 = std(myArray_4);
21.
22. legend_strings = {sprintf('\bfSubcarrier Spacing: 240[kHz] BW: 400[MHz]
    \rmMean: %.2f [V/m]', meanVal1), ...
23.     sprintf('\bfSubcarrier Spacing: 120[kHz] BW: 100[MHz] \rmMean:
    %.2f [V/m]', meanVal2)};
24.
25. x = linspace(min(myArray_1), max(myArray_1), length(myArray_1));
26. y = cdf('Normal', x, mean(myArray_1), std(myArray_1));
27. h(1) = plot(x, y, '+r', 'LineWidth', 1.8, 'MarkerIndices',1:4:length(x));
28. hold on;
29. x = linspace(min(myArray_2), max(myArray_2), length(myArray_2));
30. y = cdf('Normal', x, mean(myArray_2), std(myArray_2));
31. h(2)= plot(x, y, 'k', 'LineWidth', 1.8, 'MarkerIndices',1:4:length(x));
32. x = linspace(min(myArray_3), max(myArray_3), length(myArray_3));
33. y = cdf('Normal', x, mean(myArray_3), std(myArray_3));
34. h(3)= plot(x, y, 'sg', 'LineWidth', 1.8, 'MarkerIndices',1:3:length(x));
35. x = linspace(min(myArray_4), max(myArray_4), length(myArray_4));
36. y = cdf('Normal', x, mean(myArray_4), std(myArray_4));
37. h(4)= plot(x, y, '--b', 'LineWidth', 1.8, 'MarkerIndices',1:3:length(x));
38.
39. xlim([0 3.1]);
40. xticks(0:0.01:3.1);
41. title(['CDF']);
42. xlabel('E. Field [V/m]');
43. ylabel('Cumulative Probability');
44. % legend(h, legend_strings,'Location', 'southeast');
45. set(gca,'FontSize',12)
46. grid
```

Annex F: Haversine implementation to calculate exact distances from users to the serving antennas in the software Atoll on Java

```
1. const fs = require('fs');
2. const XLSX = require('xlsx');
3. const workbook = XLSX.readFile('table1.xlsx');
4. const sheet = workbook.Sheets[workbook.SheetNames[0]];
5. const table = XLSX.utils.sheet_to_json(sheet, { header: 1 });
```

```

6. let distances = [];
7. const R = 6371; // Earth's radius in km
8. for (let i = 0; i < table.length; i++) {

9.   if (table[i][2] === table[i][3]) {
10.    for (let j = 0; j < table.length; j++) {
11.     if (table[i][2] === table[j][3]) {
12.      let x1 = parseFloat(table[i][0].toString().replace(',', '.'));
13.      let y1 = parseFloat(table[i][1].toString().replace(',', '.'));
14.      let x2 = parseFloat(table[j][4].toString().replace(',', '.'));
15.      let y2 = parseFloat(table[j][5].toString().replace(',', '.'));

16.      const dLat = (x1 - x2) * Math.PI / 180;
17.      const dLon = (y1 - y2) * Math.PI / 180;
18.      const a = Math.sin(dLat / 2) * Math.sin(dLat / 2) +
          a. Math.cos(x2 * Math.PI / 180) * Math.cos(x1 * Math.PI / 180) *
          b. Math.sin(dLon / 2) * Math.sin(dLon / 2);
19.      const c = 2 * Math.atan2(Math.sqrt(a), Math.sqrt(1 - a));
20.      let factor1=0.62608
21.      const distance = R * c*1000*factor1;
22.      distances.push(distance);
23.      //console.log(`Distance between ${table[i][2]} and ${table[j][3]} is ${distance}
          meters`);
24.    }
25.  }
26. }
27. if (table[i][2] !== table[i][3]) {
28.   for (let j = 0; j < table.length; j++) {
29.     if (table[i][2] === table[j][3]) {
30.      let x1 = parseFloat(table[i][0].toString().replace(',', '.'));
31.      let y1 = parseFloat(table[i][1].toString().replace(',', '.'));
32.      let x2 = parseFloat(table[j][4].toString().replace(',', '.'));
33.      let y2 = parseFloat(table[j][5].toString().replace(',', '.'));

34.      const dLat = (x1 - x2) * Math.PI / 180;
35.      const dLon = (y1 - y2) * Math.PI / 180;
36.      const a = Math.sin(dLat / 2) * Math.sin(dLat / 2) +
          a. Math.cos(x2 * Math.PI / 180) * Math.cos(x1 * Math.PI / 180) *
          b. Math.sin(dLon / 2) * Math.sin(dLon / 2);
37.      const c = 2 * Math.atan2(Math.sqrt(a), Math.sqrt(1 - a));
38.      let factor1=0.62608
39.      const distance = R * c*1000*factor1;
40.      distances.push(distance);
41.      //console.log(`Distance between ${table[i][2]} and ${table[j][3]} is ${distance}
          meters`);
42.    }
43.  }

```

```

44. }
45. //j=0;
46. // if(i===table.length){break;}
47. }
48. const distancesSheet = XLSX.utils.aoa_to_sheet(distances.map(distance =>
    [distance]));
49. const distancesWorkbook = XLSX.utils.book_new();
50. XLSX.utils.book_append_sheet(distancesWorkbook, distancesSheet, 'Distances');
51. try {
52. XLSX.writeFile(distancesWorkbook, 'distances.xlsx');
53. console.log('Distances file saved successfully');
54. } catch (error) {
55. console.log(`Error saving distances file: ${error}`);
56. }

```

Annex G: Cell-free studies data tables

The following Tables contain data used in Figures from section 4.3 and Annex Q. Tables show data for E. fields, distance from user to serving BS, E. field corresponding percentage, Access technology to the Network and PDSCH levels from 5G NR & LTE users and BCCH (Broadcast Control Channel) for GSM.

	E. field [V/m]	Distance [m]	E. field Percentage [%]	Network Access	PDSCH - BCCH [dBm]
User 1 (beam 1)	2,00	141	29,68	5G mmWave	-39,45
User 1 (beam 2)	1,26	234	18,64	5G mmWave	-43,49
User 1 (beam 3)	0,51	100	7,57	5G mmWave	-51,32
User 1 (beam 4)	0,40	215	5,90	5G mmWave	-53,48
User 1 (beam 5)	0,08	200	1,26	5G mmWave	-66,89
User 2	0,47	769	6,94	4G LTE	-53,48
User 3	0,39	764	5,75	4G LTE	-55,11
User 4	0,37	769	5,51	4G LTE	-55,48
User 5	0,54	800	7,96	GSM	-51,25
User 6	0,73	746	10,79	GSM	-56,5
Total EMF [V/m]	6,741968418				

Table 22. Cell-free study location 1 data.

	E. field [V/m]	Distance [m]	E. field Percentage [%]	Network Access	PDSCH - BCCH [dBm]
User 1 (beam 1)	0,56	289	20,69	5G mmWave	-50,45
User 1 (beam 2)	0,08	169	2,89	5G mmWave	-67,54
User 1 (beam 3)	0,05	250	1,82	5G mmWave	-71,58
User 1 (beam 4)	0,04	150	1,34	5G mmWave	-74,21
User 1 (beam 5)	0,04	251	1,61	5G mmWave	-72,61
User 2	0,25	734	9,10	4G LTE	-58,98
User 3	0,23	1222	8,60	4G LTE	-59,48
User 4	0,22	645	8,23	4G LTE	-59,86
User 5	0,67	644	24,45	GSM	-48,13
User 6	0,58	740	21,27	GSM	-53,63
Total EMF [V/m]	2,72622676				

Table 23. Cell-free study location 2 data.

	E. field [V/m]	Distance [m]	E. field Percentage [%]	Network Access	PDSCH - BCCH [dBm]
User 1 (beam 1)	0,56	58	8,77	5G mmWave	-50,52
User 1 (beam 2)	0,14	122	2,13	5G mmWave	-62,81
User 1 (beam 3)	0,19	117	2,98	5G mmWave	-59,88
User 1 (beam 4)	0,33	149	5,10	5G mmWave	-55,22
User 1 (beam 5)	0,10	69	1,54	5G mmWave	-65,65
User 2	1,86	376	29,17	4G LTE	-41,48
User 3	1,43	376	22,33	4G LTE	-43,8
User 4	0,93	370	14,50	4G LTE	-47,55
User 5	0,45	950	7,08	GSM	-40,13
User 6	0,41	1051	6,40	GSM	-45,88
Total EMF [V/m]	6,381599842				

Table 24. Cell-free study location 3 data.

	E. field [V/m]	Distance [m]	E. field Percentage [%]	Network Access	PDSCH - BCCH [dBm]
User 1 (beam 1)	2,38	148	22,89	5G mmWave	-37,95
User 1 (beam 2)	1,55	90	14,88	5G mmWave	-41,69
User 1 (beam 3)	1,10	53	10,58	5G mmWave	-44,65
User 1 (beam 4)	1,23	201	11,79	5G mmWave	-43,71
User 1 (beam 5)	0,21	160	1,99	5G mmWave	-59,17
User 2	0,70	438	6,78	4G LTE	-49,92
User 3	0,68	432	6,59	4G LTE	-50,17
User 4	0,68	465	6,54	4G LTE	-50,23
User 5	0,95	450	9,18	GSM	-44,5
User 6	0,91	470	8,79	GSM	-44,88
Total EMF [V/m]	10,39212853				

Table 25. Cell-free study location 4 data.

	E. field [V/m]	Distance [m]	E. field Percentage [%]	Network Access	PDSCH - BCCH [dBm]
User 1 (beam 1)	1,98	70	11,17	5G mmWave	-39,53
User 1 (beam 2)	1,76	233	9,89	5G mmWave	-40,58
User 1 (beam 3)	0,78	160	4,42	5G mmWave	-47,58
User 1 (beam 4)	0,81	198	4,54	5G mmWave	-47,35
User 1 (beam 5)	0,33	125	1,83	5G mmWave	-55,23
User 2	4,99	190	28,08	4G LTE	-32,92
User 3	1,94	196	10,94	4G LTE	-41,11
User 4	1,53	196	8,63	4G LTE	-43,17
User 5	2,15	200	12,08	GSM	-29,69
User 6	1,50	287	8,42	GSM	-36,44
Total EMF [V/m]	17,75906491				

Table 26. Cell-free study location 5 data.

Annex H: Throughput simulation data

Total: 515

Effective RLC Aggregate Channel Throughput (UL) (kbps)	Application Aggregate Channel Throughput (UL) (kbps)	Peak RLC Aggregated User Throughput (DL) (kbps)	Effective RLC Aggregated User Throughput (DL) (kbps)	Application Aggregated User Throughput (DL) (kbps)	Peak RLC Aggregated User Throughput (UL) (kbps)	Effective RLC Aggregated User Throughput (UL) (kbps)	Application Aggregated User Throughput (UL) (kbps)	Connection Status
0	0	940.878,25	921.986,06	875.886,75	0	0	0	Connected DL
0	0	940.550,63	940.550,63	893.523,13	0	0	0	Connected DL
0	0	480.999,31	480.999,31	456.949,34	0	0	0	Connected DL
0	0	940.319,5	940.319,5	893.303,5	0	0	0	Connected DL
0	0	940.184,94	924.091,19	877.886,63	0	0	0	Connected DL
0	0	940.550,63	935.117,56	888.361,69	0	0	0	Connected DL
0	0	594.881,19	582.758,81	553.620,88	0	0	0	Connected DL
0	0	941.202,06	941.202,06	894.141,94	0	0	0	Connected DL
87.348.412,4	82.980.995,0	0	0	0	50.318,9	50.318,9	47.802,95	Connected UL
0	0	940.009,19	940.009,19	893.008,75	0	0	0	Connected DL
87.348.412,4	82.980.995,0	0	0	0	50.318,9	50.318,9	47.802,95	Connected UL
0	0	940.550,63	940.550,63	893.523,13	0	0	0	Connected DL
0	0	941.202,06	923.429,88	877.258,38	0	0	0	Connected DL

Figure 46. Snapshot of the simulation data showing some of the user throughputs.

Annex I: Atoll EMF simulation generated report ranges applicable on section 4.2

Display type: Value intervals Field: EMF Exposure

		Min	Max	Legend
1		0,8000	3	EMF Exposure: 0.8 V/m < x < 3 V/m
2		0,6100	0,8000	EMF Exposure: 0.61 V/m < x < 0.8 V/m
3		0,5600	0,6100	EMF Exposure: 0.56 V/m < x < 0.61 V/m
4		0,1800	0,5600	EMF Exposure: 0.18 V/m < x < 0.56 V/m
5		0,0100	0,1800	EMF Exposure: 0.01 V/m < x < 0.18 V/m

Figure 47. EMF Atoll simulation generated report display range applicable on section 4.2.

Annex J: User densities estimation

Total area surface of Enschede: 142.7 km²Total area surface of the city of Enschede estimated through the simulation software: 42.8 km²

Total population of Enschede: 158553

Urban:

Assumed subscriber penetration: 10%

$$Ratio_1 = \frac{142.7}{42.8} = 3.33$$

$$\frac{158553}{47613} = 47613$$

$$47613 * 0,1 = 4761$$

$$\frac{4761}{42.8} = 111 \text{ Active_users/km}^2$$

Dense Urban:

Assumed subscriber penetration: 45%

$$\begin{aligned} 47613 * 0,3 &= 14283 \\ \frac{21425}{42.8} &= 500 \text{ Active_users/km}^2 \end{aligned}$$

Annex K: Base Station quantity estimations

Estimation of the number of mmWave BSs for the simulation scenario based on already deployed networks:

Estimation 1:

Measuring the area of the most heavily populated area of the city of Enschede, and determining the number of BSs based on the area and number of BSs of an already deployed network, in this case Tokyo:

$$6700 \text{ m} \times 6400 \text{ m} = 42,88 \text{ km}^2$$

$$\text{Ratio} = 2194\text{km}^2/1100 \text{ BSs} = 1,99$$

$$42,88/\text{Ratio} = 22 \text{ BSs}$$

Estimation 2:

Ratio of Japan's population to deployed mmWave BSs:

$$\text{Ratio} = 125.7 \text{ million people} / 21000 \text{ BSs} = 5985$$

$$158553 \text{ people}/\text{Ratio} = 27 \text{ BSs}$$

Annex L: Broadband service properties in Atoll



Broadband Properties ? X

General | 5G NR | LTE | NB-IoT | UMTS | GSM

QoS class identifier (QCI): QCI priority:

Priority:

	Uplink	Downlink
Highest modulation:	<input type="text" value="16QAM"/>	<input type="text" value="64QAM"/>
Lowest modulation:	<input type="text" value="BPSK"/>	<input type="text" value="BPSK"/>
Highest coding rate:	<input type="text" value="0,95"/>	<input type="text" value="0,95"/>
Lowest coding rate:	<input type="text" value="0,3"/>	<input type="text" value="0,3"/>
Max throughput demand:	<input type="text" value="310.000 kbps"/>	<input type="text" value="950.000 kbps"/>
Min throughput demand:	<input type="text" value="500 kbps"/>	<input type="text" value="1.000 kbps"/>
Min PRBs:	<input type="text" value="1"/>	

Application throughput

Scaling factor: Offset:

Body loss:

Figure 48. Broadband service properties.

Annex M: Electric field level calibration with Agentschap Measurements.

	Coordinates	Measurement Location 1 (6,92363736E 52,229663145 N)	Measurement Location 2 (6,910870215 E 52,223141334 N)	Measurement Location 3 (6,899848772 E 52,225328789 N)	Measurement Location 4 (6,895028731 E 52,224303122 N)	Measurement Location 5 (6,899744167 E 52,237434087 N)	Measurement Location 6 (6,899744167 E 52,237434087 N)
Electric field level [V/m]	EMF Simulator Samples	0,69	0,98	0,89	0,71	0,36	0,46
		0,64	0,8	0,78	0,65	0,37	0,48
		0,52	0,97	0,8	0,69	0,4	0,48
		0,71	0,92	0,74	0,64	0,32	0,49
		0,75	0,89	0,96	0,56	0,33	0,49
		0,68	0,88	0,75	0,59	0,35	0,5
		0,77	0,85	0,68	0,66	0,44	0,51
		0,69	1,05	0,73	0,72	0,34	0,52
		0,7	0,95	0,75	0,63	0,37	0,44
		0,65	1	0,82	0,68	0,28	0,42
	Samples Average	0,68	0,929	0,79	0,653	0,356	0,479
	Measurement	0,71	0,92	0,82	0,66	0,36	0,46
	Comparison (%)	95,77	98,92	97,21	98,94	98,89	96,03

Table 27. Electric field level calibration with Agentschap Measurements.

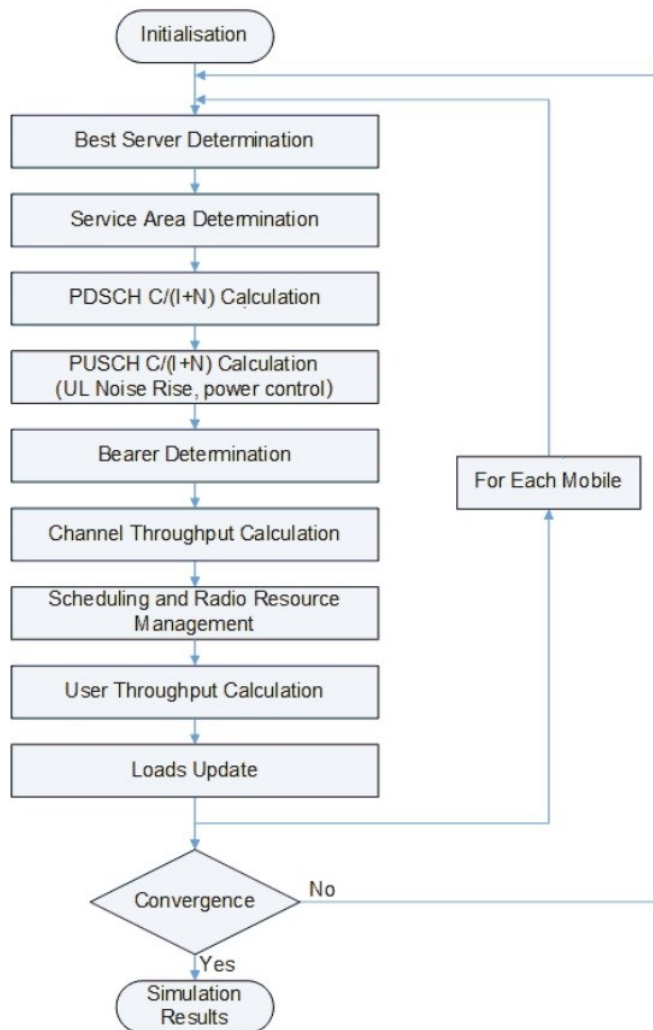
Annex N: Atoll simulation algorithm

Figure 49. Atoll Simulation algorithm.

Annex O: mmWave transmitter configuration

General Transmitter 5G NR Cells LTE Cells NB-IoT Cells Propagation Display

Active Transmitter type: Intra-network (Server and Interferer) ▾

Transmission/Reception

	Transmission		Reception		Equipment...
	Real	Computed	Real	Computed	
Total losses:	6,06 dB	6,06 dB	-0,16 dB	-0,16 dB	Detail
Noise figure:			4 dB	4 dB	

Antennas

Height/ground: 26 m ▾

Antenna model and parameters

Broadcast: Antel RWA-80020/20 ▾ ... Select...

Beamforming: Default Beamformer ▾ ...

Mechanical azimuth: 240 ° ▾ Mechanical downtilt: 0 ° ▾

Electrical azimuth: ° Electrical downtilt: 0,5 ° ▾

Additional electrical downtilt: 0 ° ▾

Number of antennas

Transmission: 128 ▾ Reception: 128 ▾

Number of PAs: 1 ▾

Figure 50. mmWave Transmitter configuration example.

Annex P: Figures for the taken samples for Measurement location 1

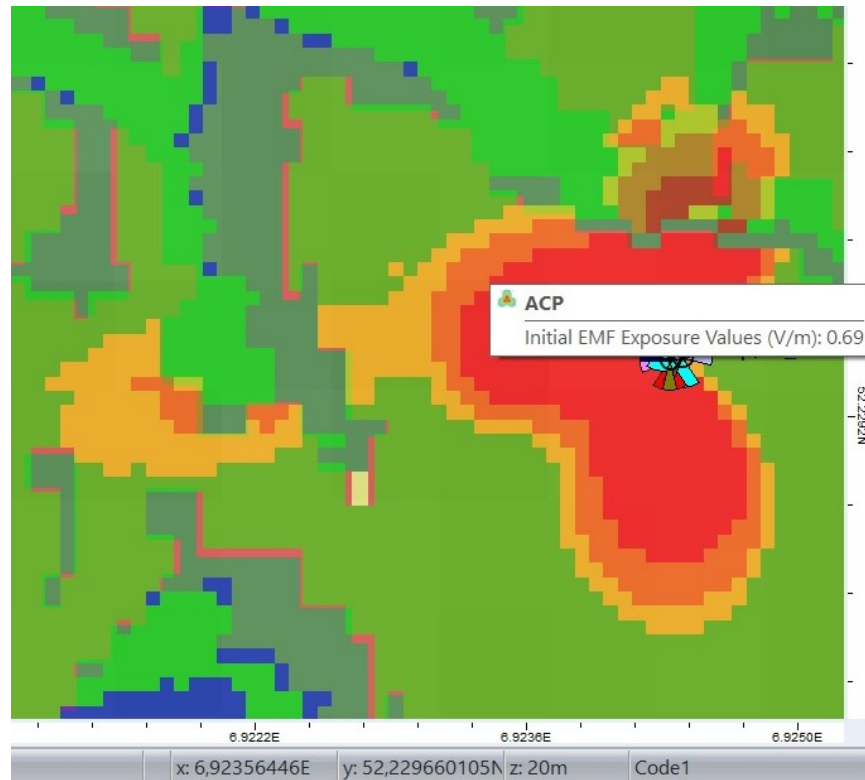


Figure 51. Sample 1 for measurement location 1.

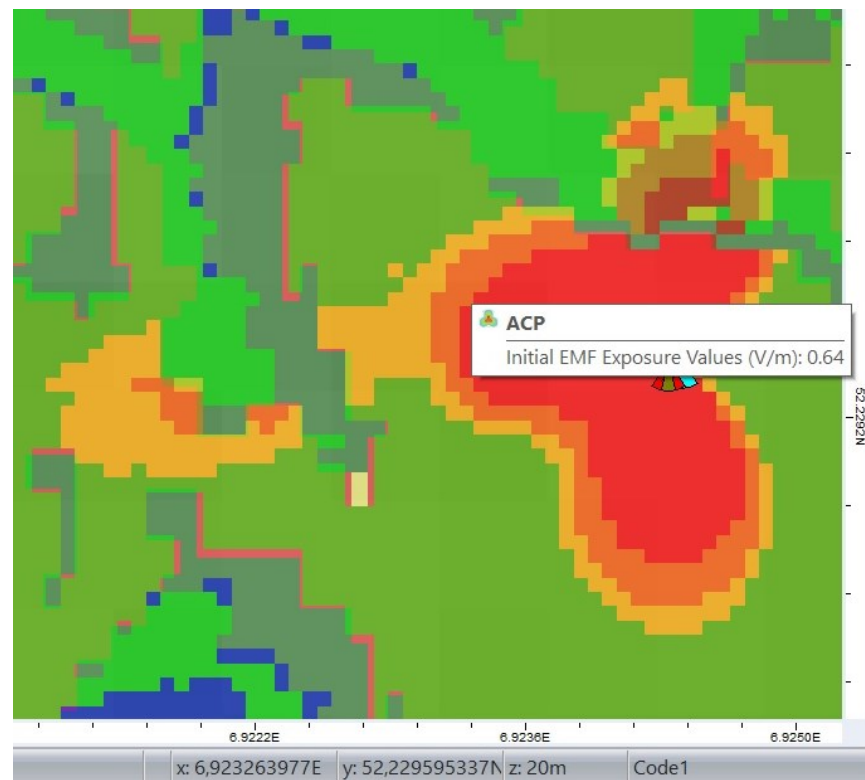


Figure 52. Sample 2 for measurement location 1.

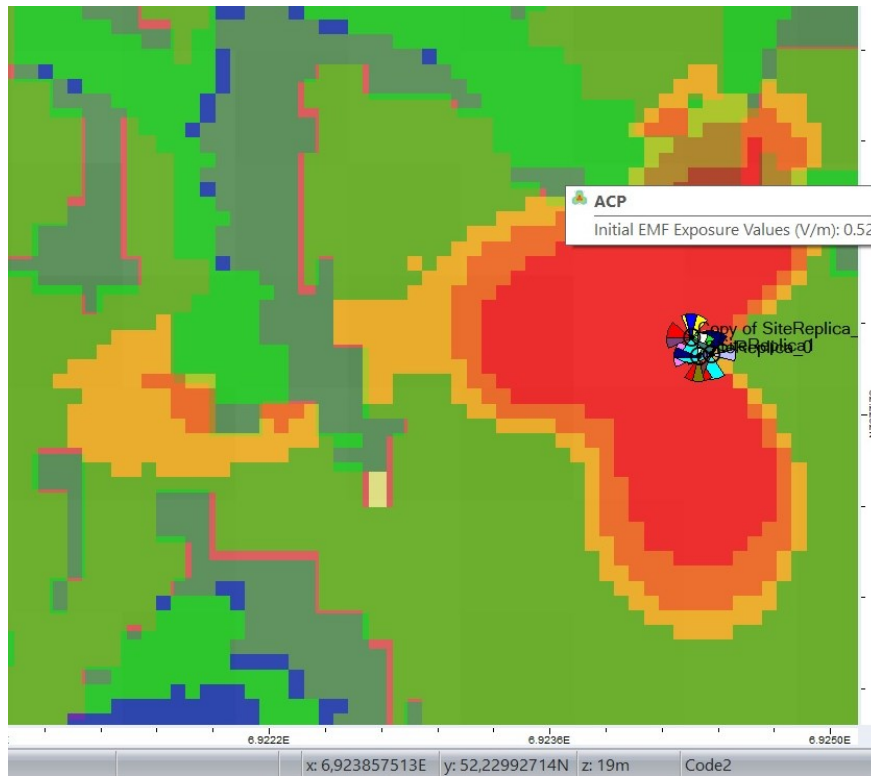


Figure 53. Sample 3 for measurement location 1.

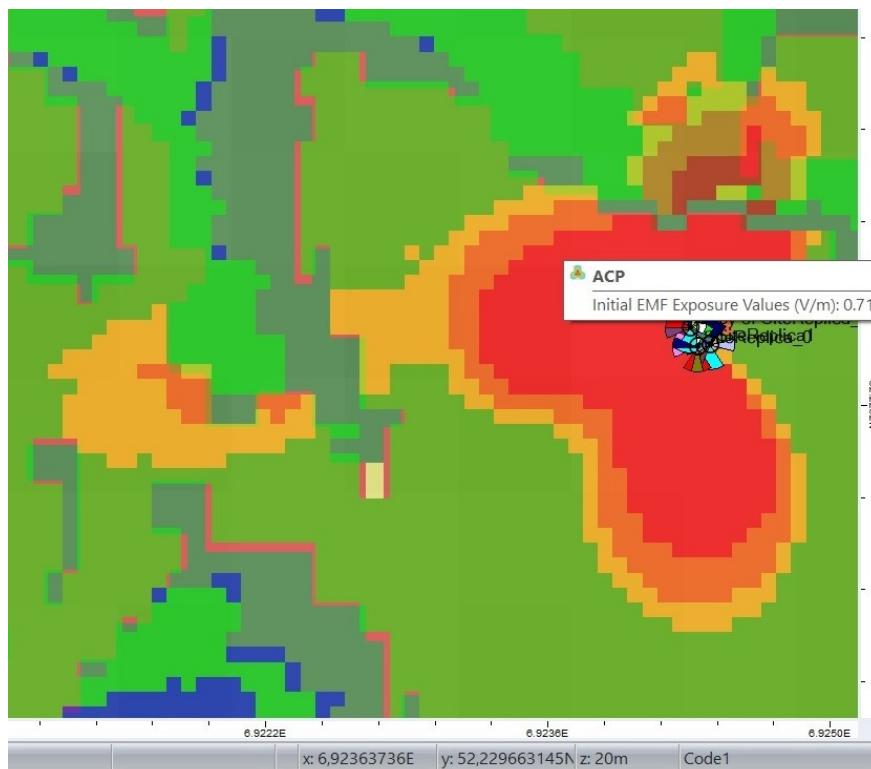


Figure 54. Sample 4 for measurement location 1.

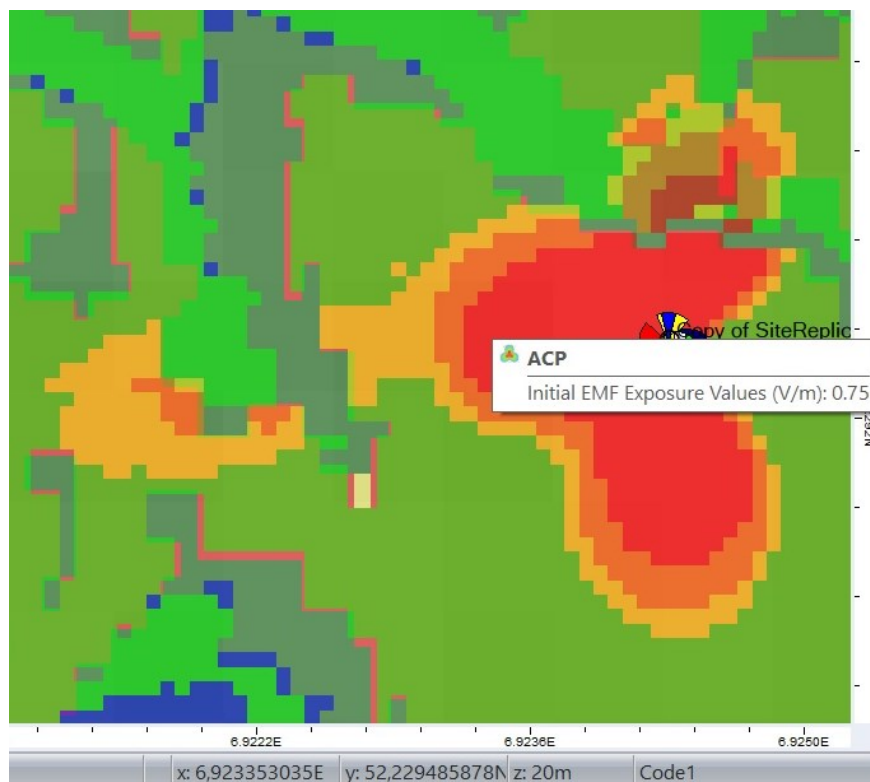


Figure 55. Sample 5 for measurement location 1.

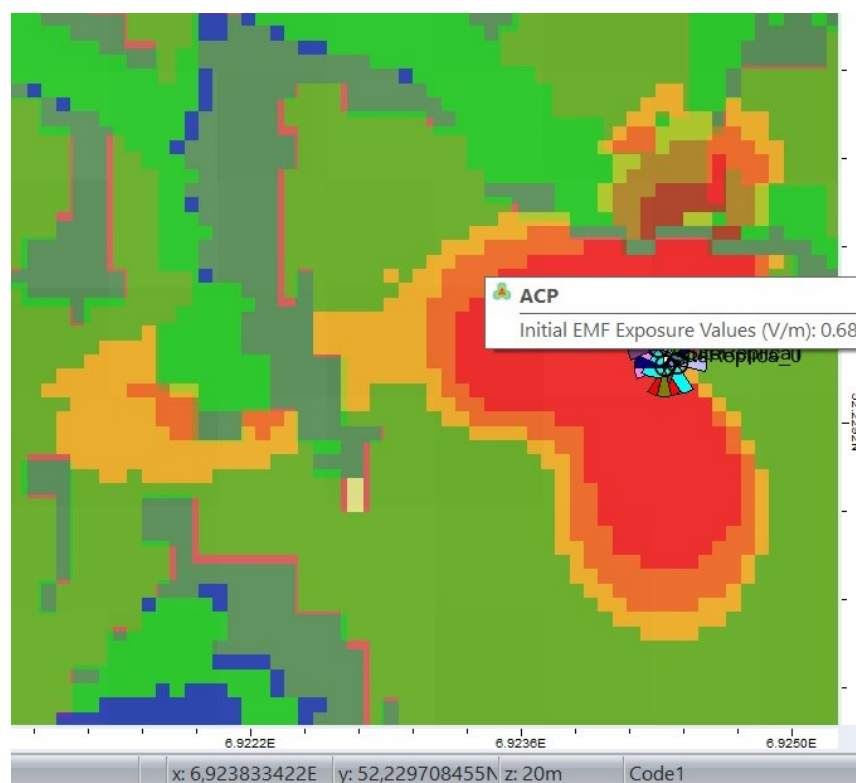


Figure 56. Sample 6 for measurement location 1.

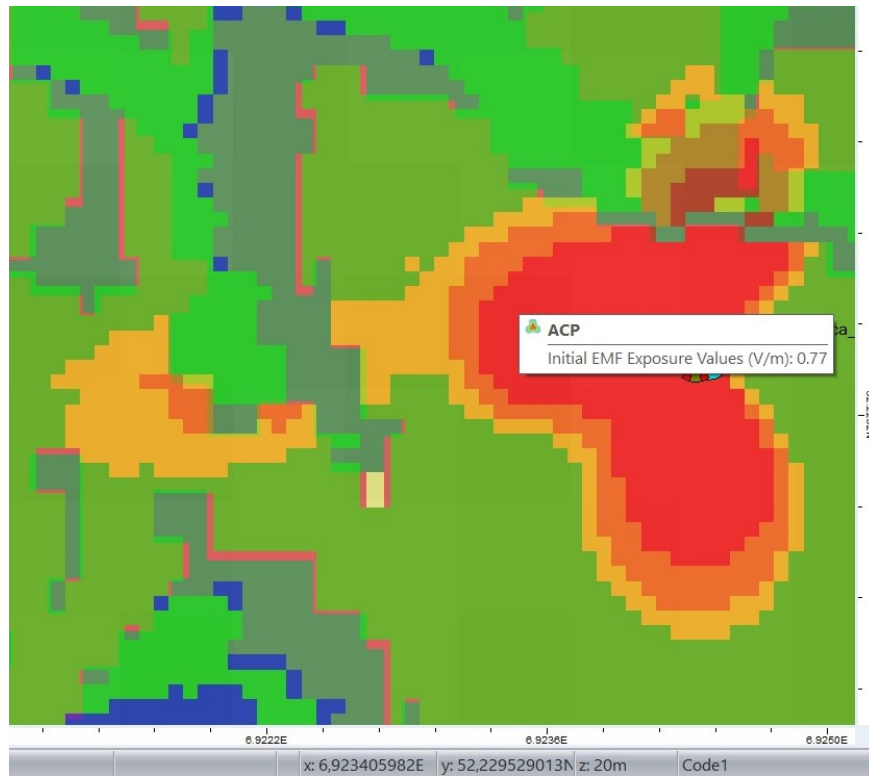


Figure 57. Sample 7 for measurement location 1.

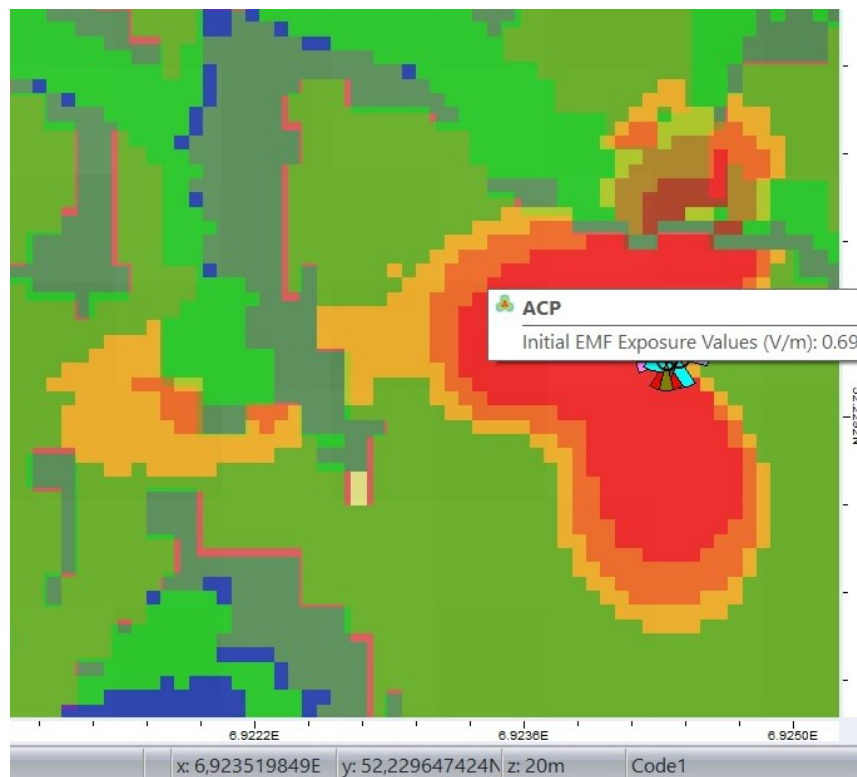


Figure 58. Sample 8 for measurement location 1.

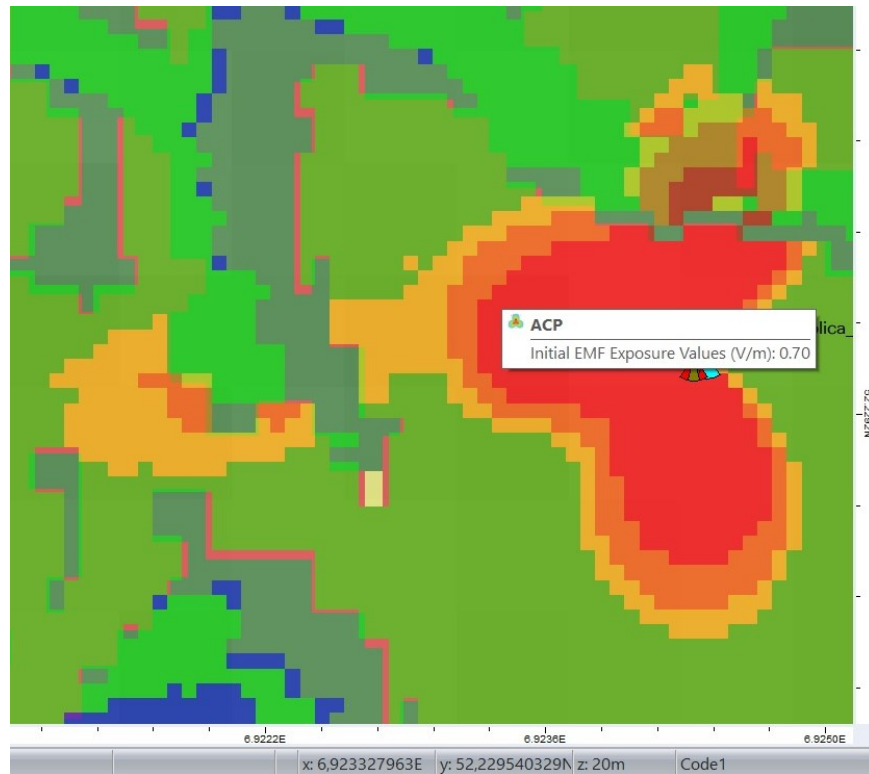


Figure 59. Sample 9 for measurement location 1.

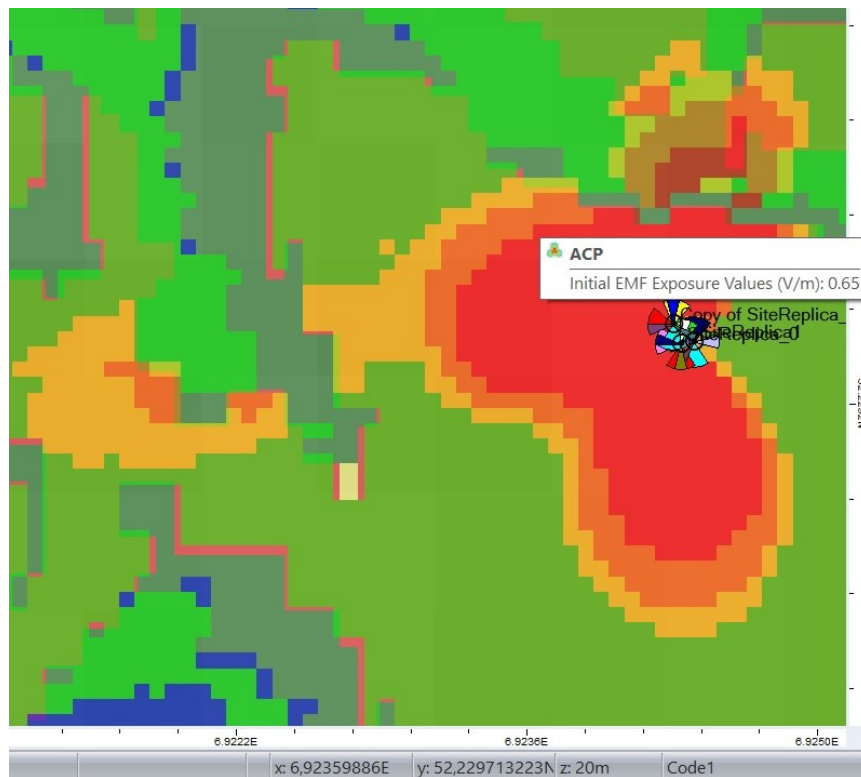


Figure 60. Sample 10 for measurement location 1.

Annex Q: LTE and GSM simulations from section 4.3

The following figures correspond to LTE and GSM simulations in section 4.3. Snapshots were generated at the time of the realization of these simulations, where the main focus was the collection of data. Some figures may have green colored artifacts which are displayed in Monte Carlo simulations to represent users. Those users are not part of simulations in section 4.3.

Data presented on the following figures correspond with the data collected in Tables present in Annex G for the calculation and discussion realized in section 4.3.

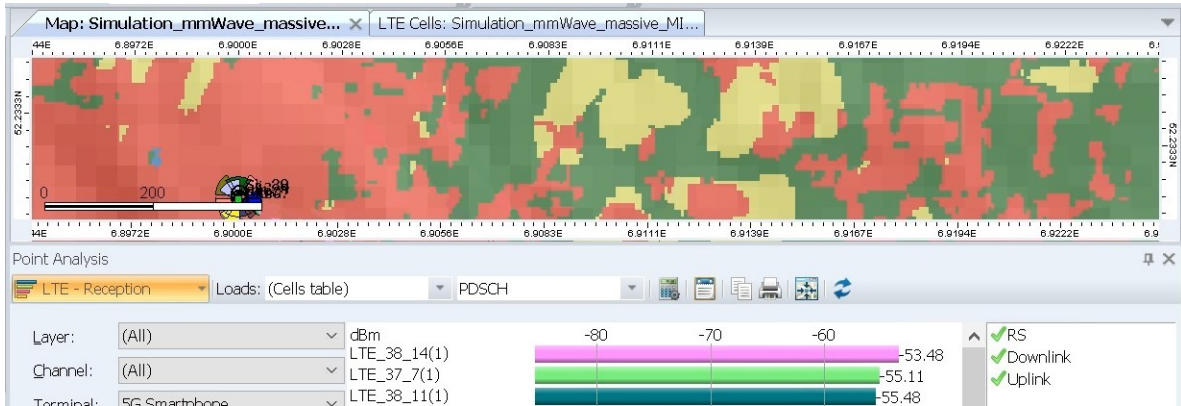


Figure 61. LTE Simulation data location 1.

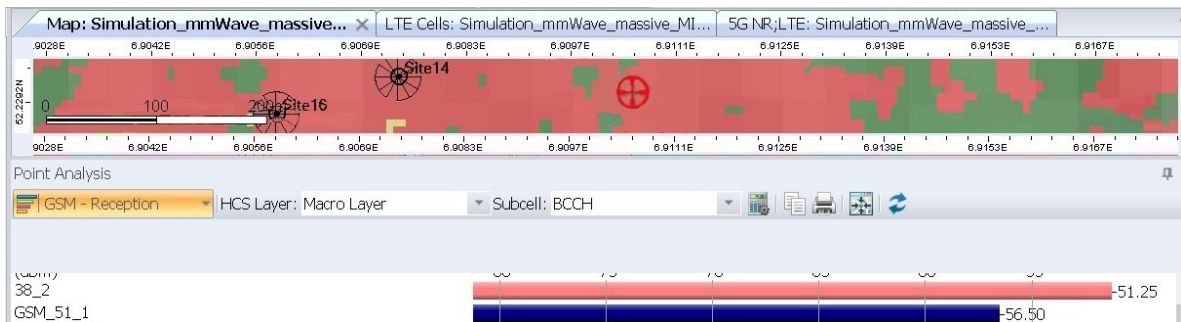


Figure 62. GSM Simulation data location 1.



Figure 63. LTE Simulation data location 2.

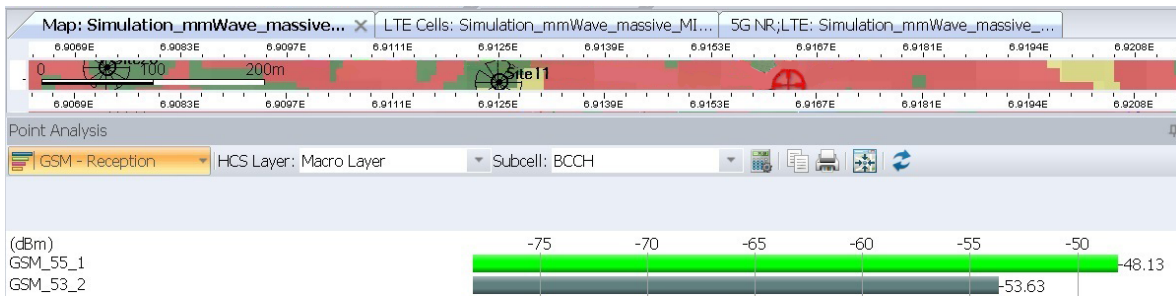


Figure 64. GSM Simulation data location 2.

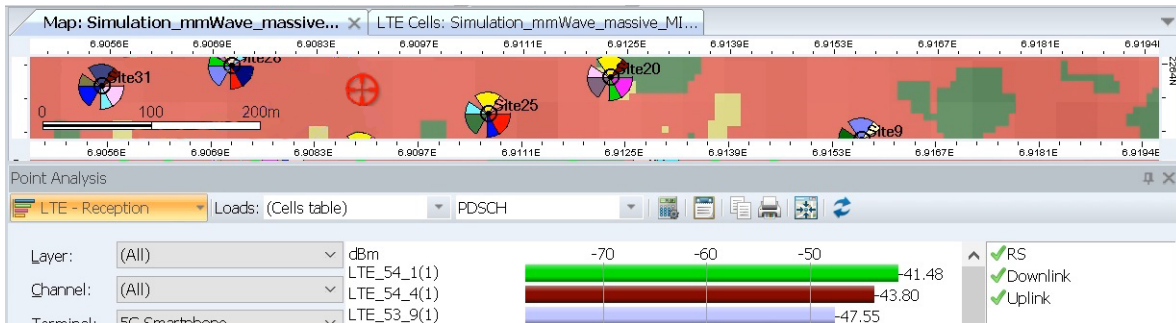


Figure 65. LTE Simulation data location 3.

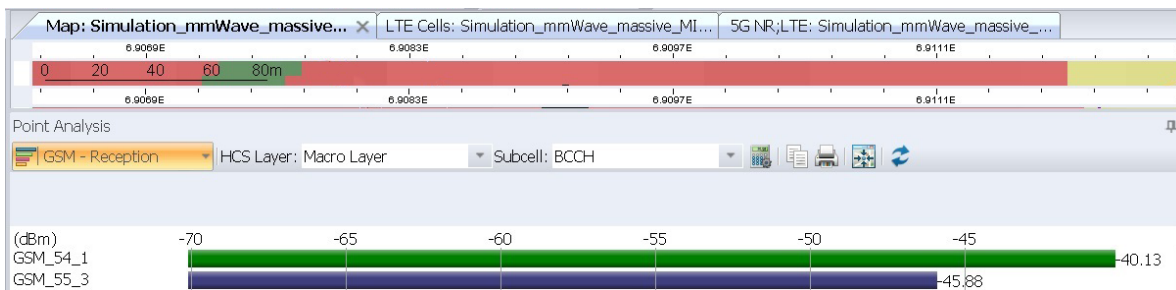


Figure 66. GSM Simulation data location 3.

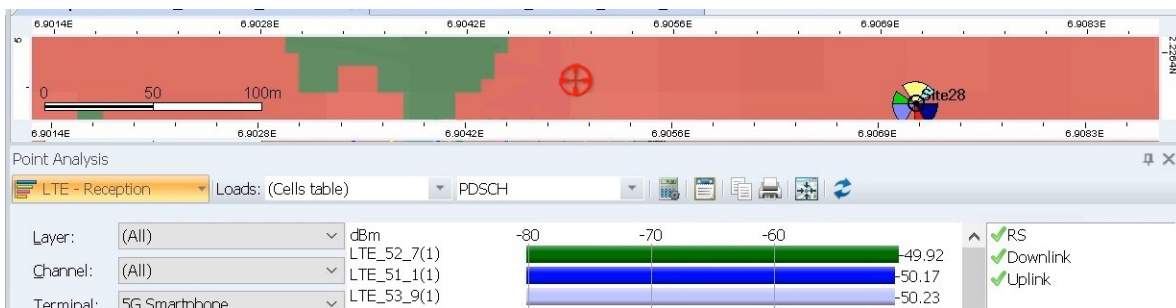


Figure 67. LTE Simulation data location 4.

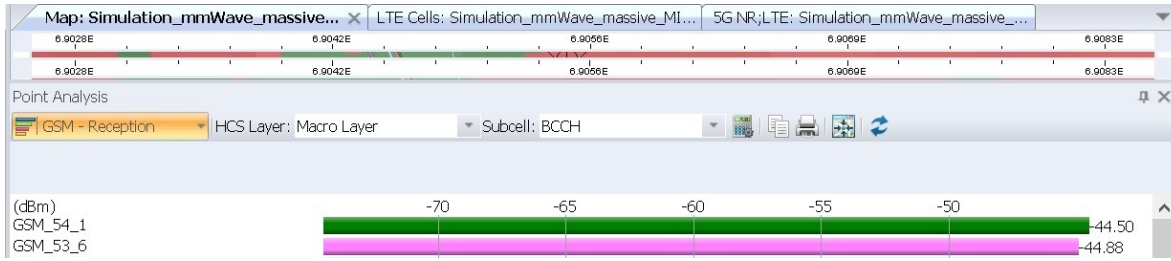


Figure 68. GSM Simulation data location 4.

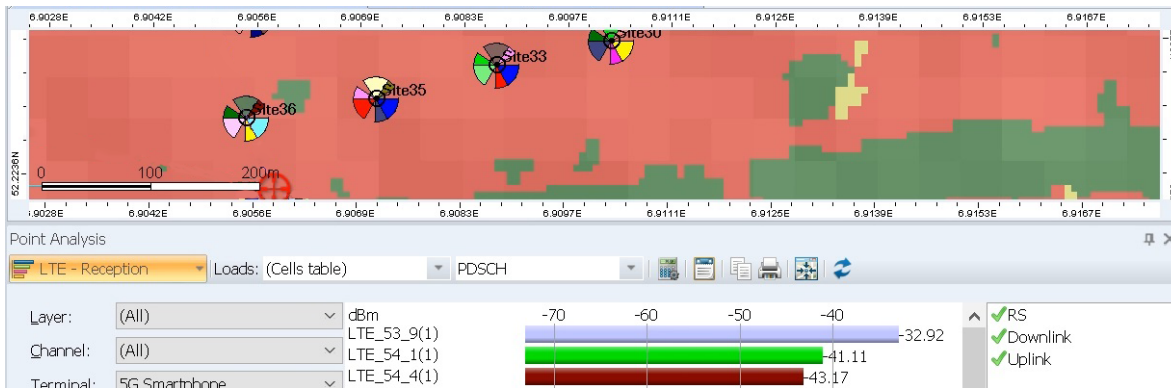


Figure 69. LTE Simulation data location 4.

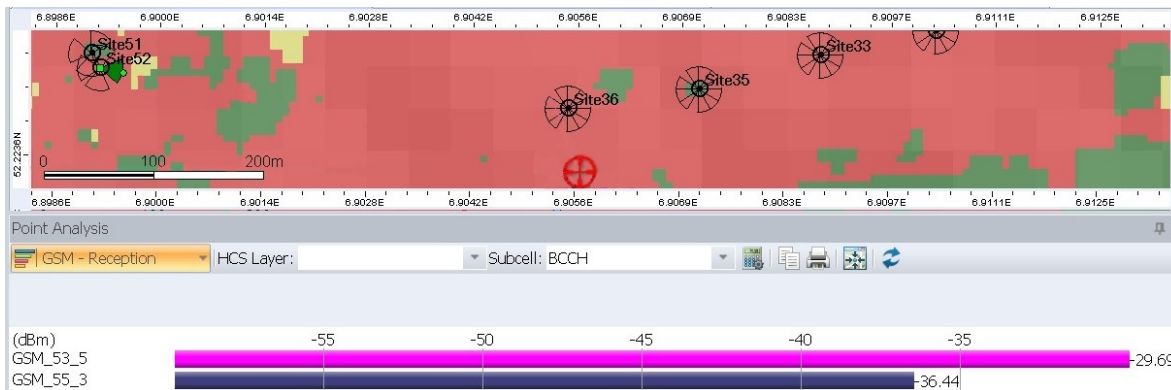


Figure 70. GSM Simulation data location 5.

Annex R: Uncalibrated Atoll EMF report example

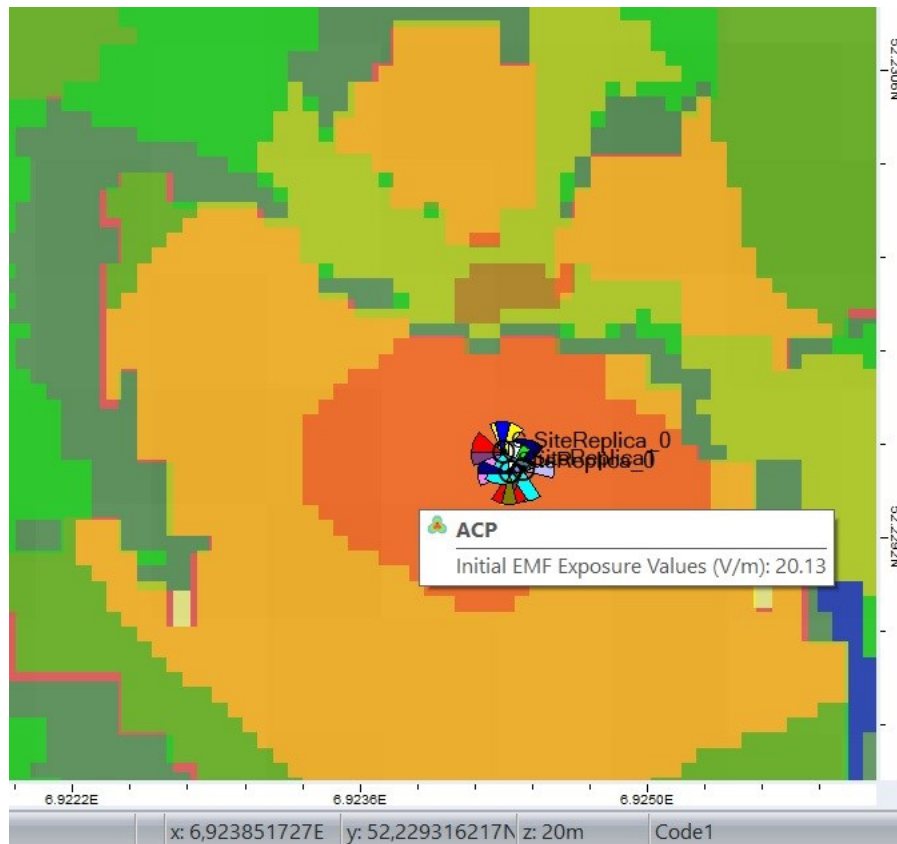


Figure 71. Uncalibrated Atoll EMF report example.

Annex S: BLER and RSRQ simulation plots

Figures in this Annex provide individual plots of simulations considered in 4.5. These plots are related to section 4.4.1, where for all simulations the following configurations are used: 240 [kHz] SCS, 400 [MHz] Channel BW, Topology 2.

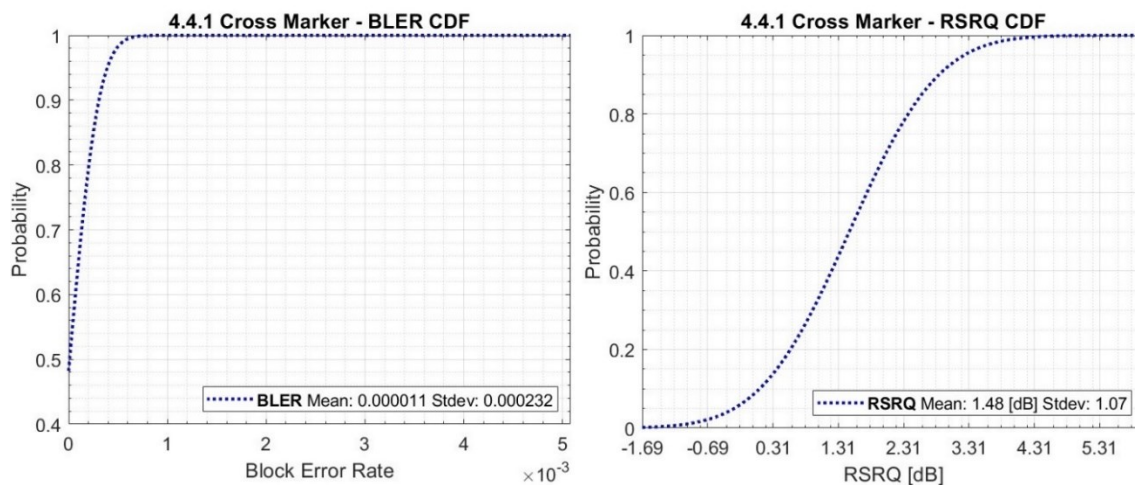


Figure 72. BLER & RSRQ CDF for the Cross Marker simulation from 4.4.1 (128x128, 60 dBm, Dense Urban).

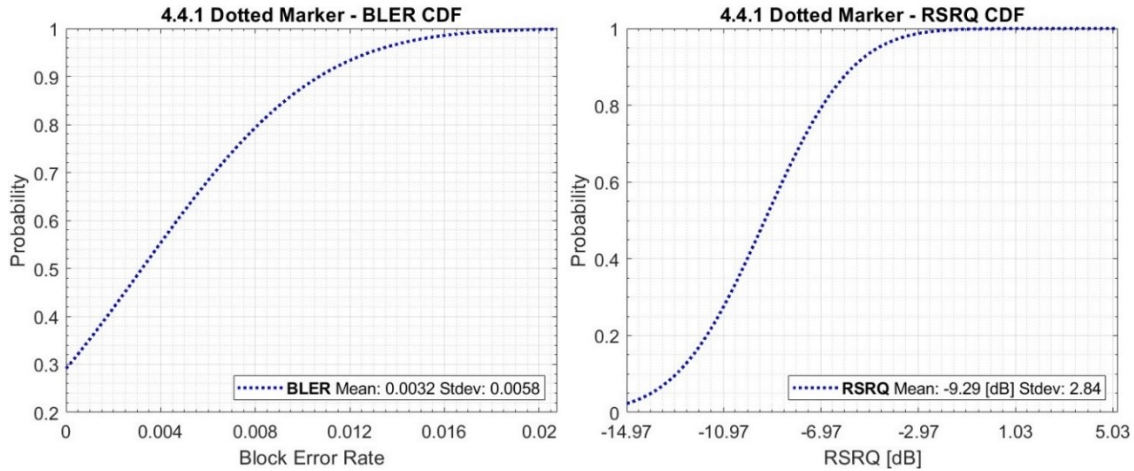


Figure 73. BLER & RSRQ CDF for the Dotted Marker simulation from 4.4.1 (4x4, 60 dBm, Dense Urban).

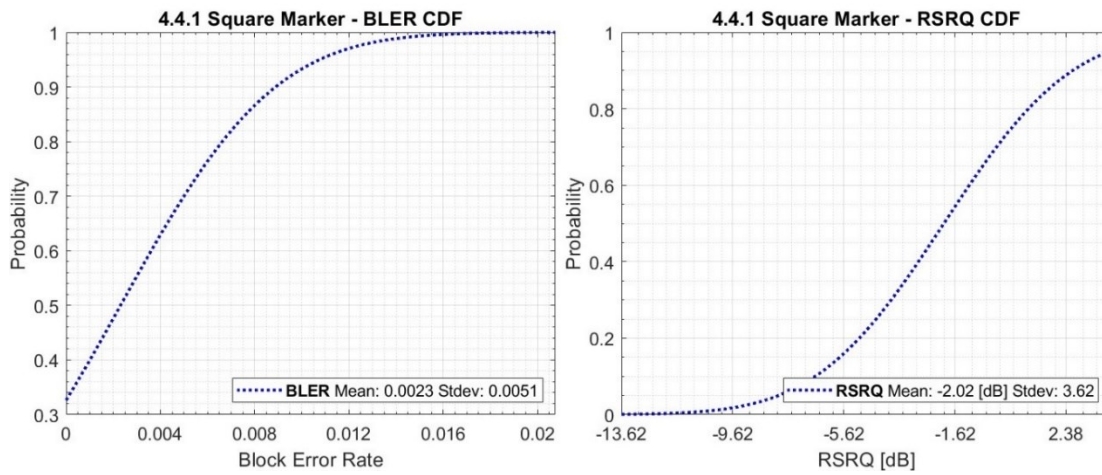


Figure 74. BLER & RSRQ CDF for the Square Marker simulation from 4.4.1 (128x128, 40 dBm, Dense Urban).

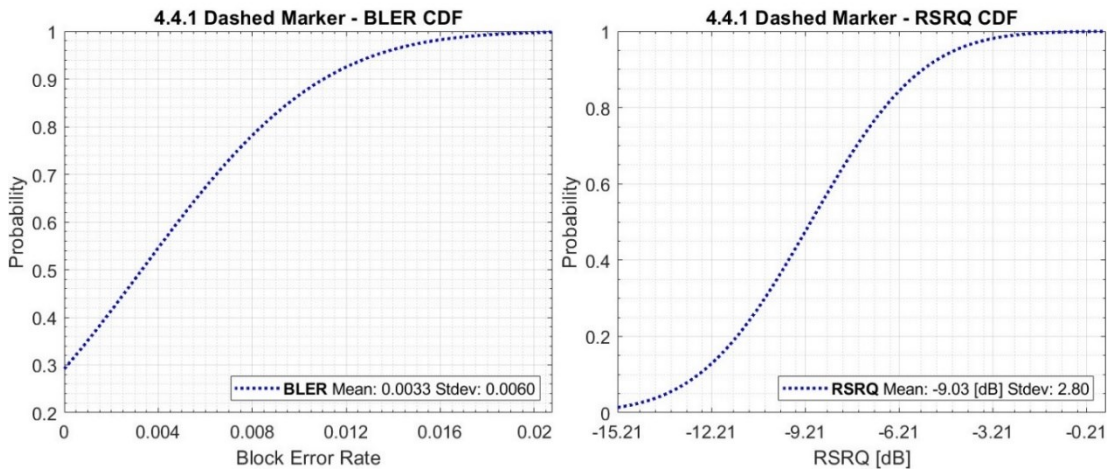


Figure 75. BLER & RSRQ CDF for the Dashed Marker simulation from 4.4.1 (4x4, 40 dBm, Dense Urban).

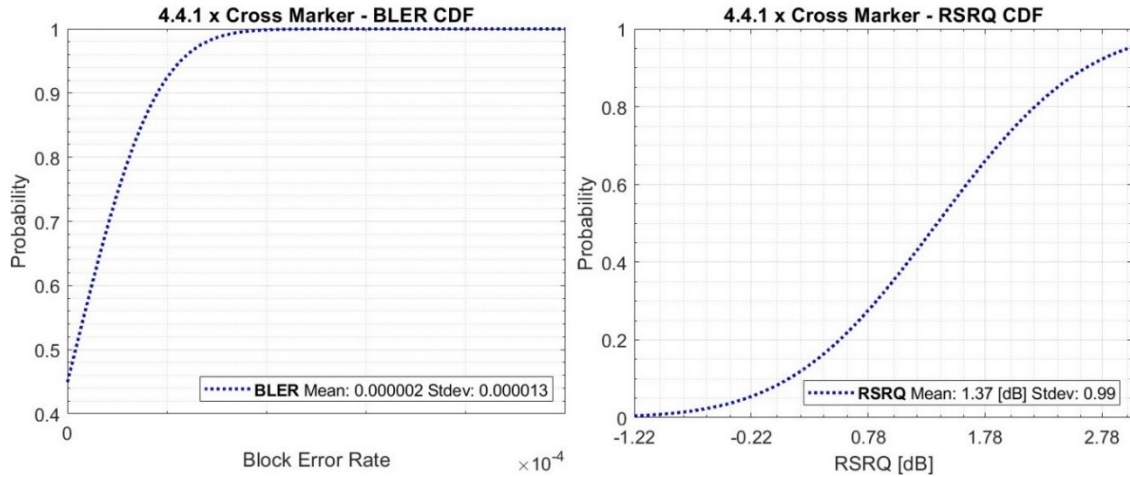


Figure 76. BLER & RSRQ CDF for the “x” Cross Marker simulation from 4.4.1 (128x128, 60 dBm, Urban).

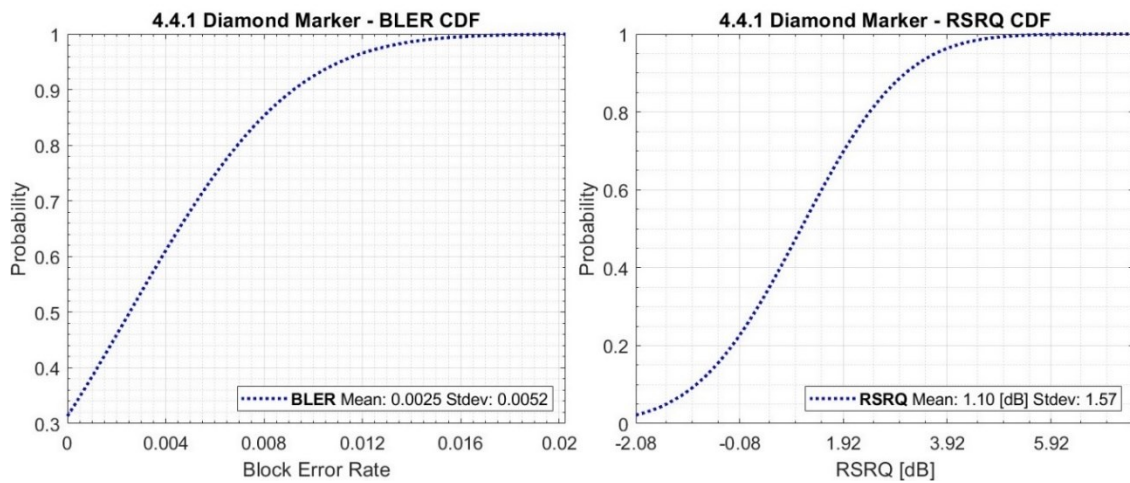


Figure 77. BLER & RSRQ CDF for the Diamond Marker simulation from 4.4.1 (4x4, 60 dBm, Urban).

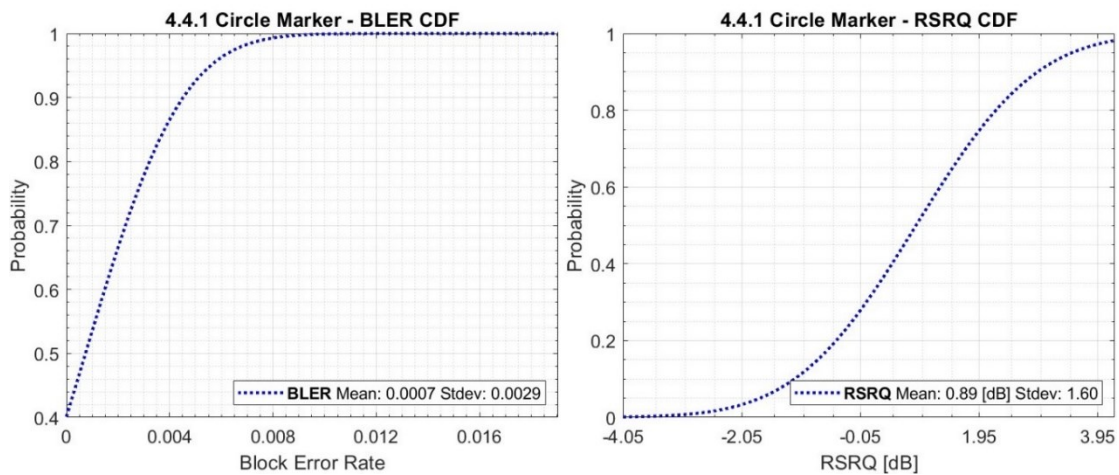


Figure 78. BLER & RSRQ CDF for the Circle Marker simulation from 4.4.1 (128x128, 40 dBm, Urban).

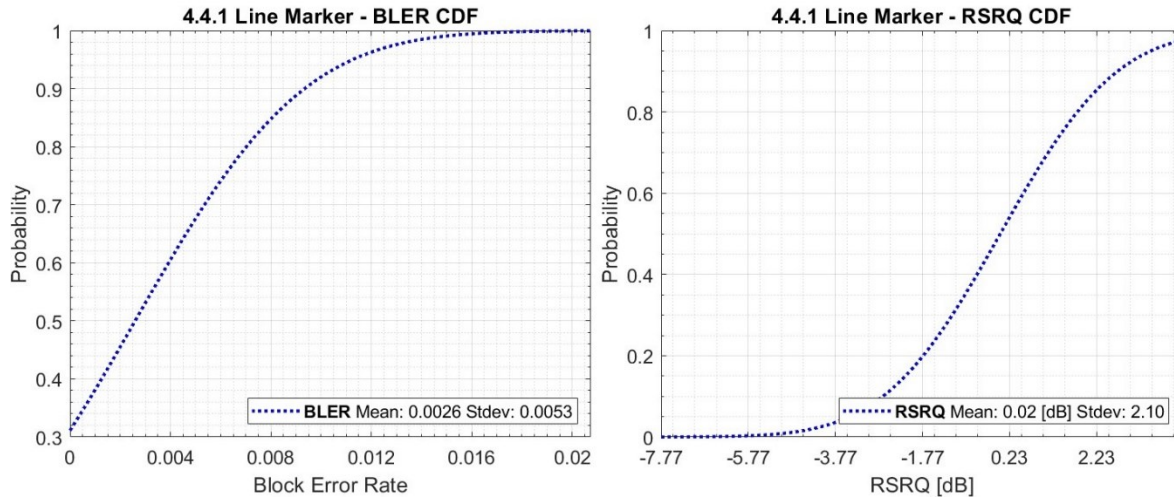


Figure 79. BLER & RSRQ CDF for the Line Marker simulation from 4.4.1 (4x4, 40 dBm, Urban).

Annex T: Statistical simulation summary example

Figure 80 shows an example of a Monte Carlo simulation summary where only 0,1% of the users was rejected. However this is usually result of a simulation glitch, where a user is placed just outside the considered computational zone, resulting in a “no coverage” status.

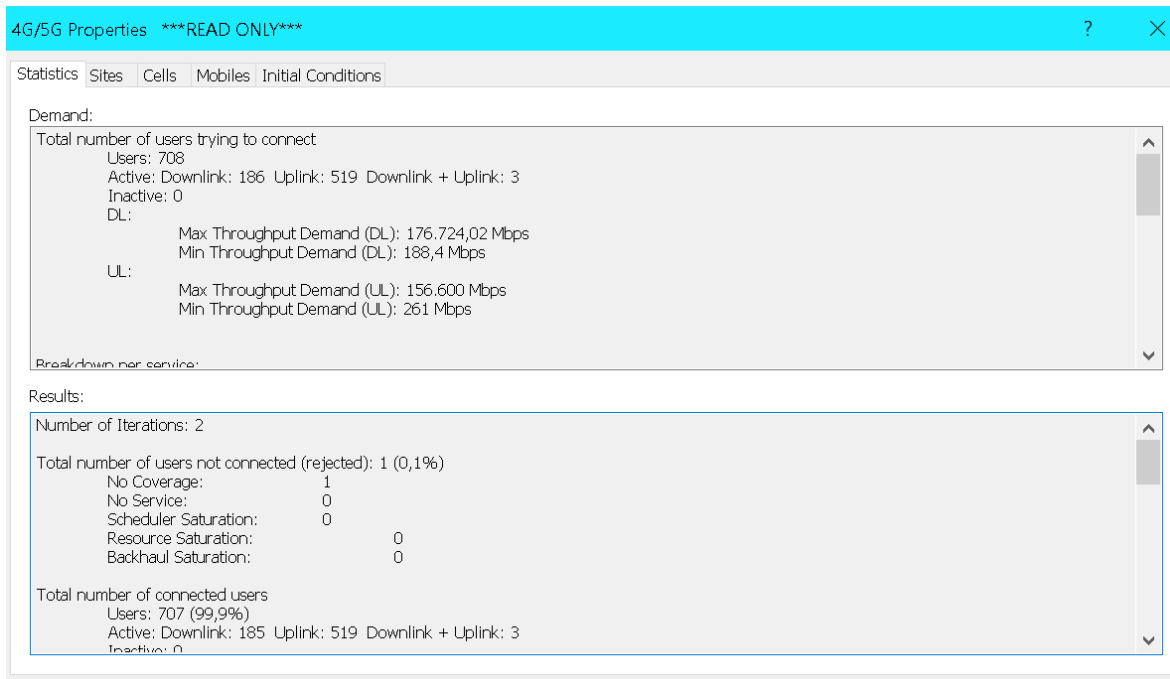


Figure 80. Statistical simulation summary example.